Horizon-Layered Cosmology: From Black Hole Gravitational Collapse to Holographic Hierarchies

Anđelko Đermek

Abstract

This work develops *horizon-layered cosmology*, a causal–holographic framework that reinterprets gravitational collapse as the generative mechanism of an emergent cosmological spacetime. Extreme gravitational time dilation prevents infalling matter from crossing the event horizon in any consistent global description; each quantum is instead absorbed through a discrete *causal incorporation* event that transfers one Planck unit of information–energy to the stretched horizon, which functions as a null-synchronized quantum code with throughput fixed by the Planck time. Its Planck-scale tessellation, approximately hexagonal with twelve required pentagonal defects, carries dipole degrees of freedom that encode mass-weight and phase information, with lateral lightlike propagation ensuring global coherence.

A central result is an explicit causal map from this two-dimensional null-ordered surface to a three-dimensional bulk: tangential adjacency yields two spatial dimensions, nested generational layering provides the radial one, and global retessellation defines temporal order. This construction uniquely reproduces a homogeneous, isotropic FRW interior. Spatial curvature, matter sectors, and vacuum-like components arise from structured dipole alignments. Internal time is the ordered sequence of incorporation events; continued accretion enlarges the horizon and drives expansion without a separate dark-energy term, giving an internal age of $\sim$ **13.4** Gyr and an observable Hubble domain containing about half the total internal mass.

If the parent black hole rotates, Kerr frame dragging imposes an azimuthal phase gradient that seeds matter–antimatter asymmetry, parity violation, and a preferred cosmic axis. The binary structure of primary dipoles supplies the geometric basis for fermionic spin and large-scale CMB and galaxy-spin alignments. Quantum randomness is epistemic, arising from coarse-grained access to a deterministic null-surface code.

This framework introduces a conceptually original synthesis: the event horizon is treated not as a passive boundary but as an actively evolving causal code whose null layering constructs the interior FRW spacetime and its matter content.

Keywords: black hole; Schwarzschild geometry; holography; cosmology, FRW geometry

1 Introduction and Preface

Preface. This work is presented not as a final theory but as a coherent framework for reinterpreting gravitational collapse and cosmological origin through a single informational principle. The central claim is that the event horizon is not merely a geometric boundary, but the *generative surface* from which spacetime, matter, and causal structure emerge. If correct even in part, the framework implies that every black hole seeds a self-contained internal universe and that our own cosmos is such a holographically projected interior.

Introduction. Black holes sit at the intersection of general relativity and quantum theory, exposing a tension between geometric determinism and informational completeness. Classically, stellar collapse culminates in a singularity hidden behind an event horizon. While internally consistent within general relativity, this picture generates unresolved paradoxes: the fate of information, the meaning of spacetime beyond causal reach, and the physical status of the singularity.

The *horizon-layered cosmology* developed in this work proposes a different viewpoint grounded in the external observer's frame. In Schwarzschild geometry, extreme gravitational time dilation halts the apparent infall of matter in external coordinate time. Although an infalling observer crosses the horizon in finite proper time, the two timescales are not independent; they are linked by an exact causal relationship. From the external frame, the infaller's clock slows without bound; from the infaller's frame, the external universe accelerates without limit. Thus, the crossing cannot complete in any globally consistent causal picture: matter asymptotically approaches the horizon, where it becomes redshift-frozen into a thin, Planck-scale *stretched horizon* just outside r_{s}. Radial dynamics are effectively frozen in this Planck-thick layer, while tangential null propagation remains fully active, so that infalling quanta are assimilated into a lateral, lightlike dynamics living on a two-dimensional null surface.

Collapse therefore proceeds not as a volumetric contraction toward a central singularity but as a *surface process of causal incorporation*. Infalling quanta are stratified into successive null layers on the stretched horizon, each layer added only after causal coherence is achieved. The horizon grows outward through a discrete sequence of Planck-time incorporations, each encoding one quantum of matter–energy in a new information-bearing stratum. The event horizon is thus elevated from a passive boundary to an active Planck-scale encoding surface whose evolution *constructs* the internal spacetime.

Early versions of the holographic principle, from 't Hooft [1] and Susskind [2] to the membrane paradigm [3], interpreted the horizon largely as a thermodynamic boundary with area-scaling entropy. AdS/CFT duality [4] provided formal equivalence between bulk and boundary theories but did not specify the causal mechanism by which infalling information becomes encoded. Quantum-informational approaches employing error-correction codes and tensor networks [5–7] captured the algebraic structure of holography but left the dynamics of encoding and spacetime emergence unresolved.

The horizon-layered framework introduces precisely this missing element. The horizon is treated as a *discrete null lattice* composed of Planck-area cells arranged

in an approximately hexagonal tessellation with twelve pentagonal curvature defects required by topology. Each cell carries a *primary dipole*, normal to the surface, which encodes its generational mass weight and thereby its radial index in the collapse history, and a *secondary dipole* tangent to the surface, which encodes mobile phase and field data (spin, charge, sector identity). Infalling quanta become encoded as patterned excitations of these secondary dipoles, while the primary dipoles retain the cumulative curvature and excision data of past incorporations. Lateral causal propagation across the null surface occurs at the invariant speed c, enabling the global synchronization needed for each new layer to be incorporated and for the code to remain coherent.

A central result of this work is that the two-dimensional horizon code admits a *precisely defined mapping* to a three-dimensional interior that reconstructs a spatially flat Friedmann–Lemaître–Robertson–Walker (FLRW) bulk. The quasi-hexagonal adjacency graph provides three independent tangential axes, which embed as the bulk (x, y, z) directions, while the discrete generational mass index carried by the primary dipoles defines the internal radial coordinate as a cumulative information measure, not a Schwarzschild distance. Externally, the Schwarzschild radius grows in equal steps of $2\ell_{\mathrm{p}}$ per Planck incorporation; internally, the effective radial increments of successive layers shrink according to the inverse information capacity of each layer. This information-geometric scaling smooths the radial direction, so that the full interval $0 \leq r \leq r_{\mathrm{s}}$ becomes a continuous FRW radial coordinate with scale factor $a(t)$ and Hubble parameter $H(t) = c^3/(GM(t))$. The 2D–3D mapping is therefore not a heuristic analogy but an explicit holographic reconstruction that yields an expanding, spatially flat FRW universe inside the black hole.

Within this picture, cosmic time is not a background parameter but the ordered sequence of horizon updates: each Planck-scale incorporation increases entropy, advances the null layering by one generational step, and thereby advances the internal causal order. The thermodynamic arrow of time is unified with the growth of the horizon, and the causal bandwidth of the membrane, set by $P_{\max} = c^5/G$, regulates the rate at which new spacetime and structure can emerge internally. Quantum measurement corresponds to an algebraically constrained boundary-state update: each global retessellation selects a single algebraically consistent sector of the horizon code. From the external viewpoint this selection is deterministic, but internal observers, who only access coarse-grained bulk fields, experience it as probabilistic wavefunction collapse. In this framework, quantum randomness is *epistemic rather than ontic*: it reflects limited access to the underlying null-surface microstate, not a fundamental indeterminism in the horizon dynamics.

The resulting cosmology is unitary, singularity-free, and bounded by the horizon's information capacity. The internal universe evolves not because a pre-existing bulk expands, but because the horizon itself grows through discrete incorporations that drive the scale factor. The Schwarzschild–Hubble equivalence, $r_h = c/H$ and $r_h = 2Gm_h/c^2$ arises naturally: the Hubble radius r_h is the largest internally coherent region in one cosmic time, while the parent horizon sits at $r_{\mathrm{s}} = 2r_h$ and defines the ultimate causal boundary. **Our own universe exhibits precisely the behavior predicted for such an interior: an expanding spacetime whose age, energy content, and Hubble structure correspond to the internal causal evolution**

of a large black hole viewed externally. The Hubble expansion emerges from the growth of horizon area without invoking an independent dark-energy term, and observed tensions in local versus global Hubble measurements reflect the internal-versus-external mapping of the null-layered causal hierarchy.

Planck-seed horizons and the emergence of spacetime. Contrary to the standard picture in which the horizon encloses a pre-existing interior, the present framework treats the horizon as a *causal seed*. It originates at the Planck scale as the smallest surface satisfying the compactness condition for null separation and the holographic entropy bound. From this seed, spacetime grows outward through sequential incorporations of redshift-frozen matter. The "interior" is not a region of classical geometry that already exists and is then enclosed, but a causal-excision domain whose FRW spacetime is assembled from the outside inward through the holographic projection defined by the evolving null-surface code and its generational mass index.

Rotational memory and cosmic asymmetry. When the parent black hole carries angular momentum, Kerr frame dragging introduces an azimuthal phase gradient across the horizon lattice. This gradient biases co-rotating versus counter-rotating tangential dipole orientations, producing a small but cumulative helicity asymmetry that seeds matter–antimatter imbalance, a preferred cosmic axis, and parity-violating correlations in the emergent bulk. The binary topology of the horizon's spin-like degrees of freedom naturally yields spin-$\frac{1}{2}$ quantization and the Pauli exclusion principle, while the combination of Kerr-induced azimuthal twist and the twelve pentagonal defects in the quasi-hexagonal tiling provides a geometric origin for large-scale CMB anomalies, galaxy-spin alignments, and early-universe chirality as holographic fossils of the parent horizon's rotation and topology.

The horizon-layered cosmology is not a cellular-automaton or hypergraph rewriting model. Although the horizon-layered cosmology employs a discrete Planck-scale substrate, it is not a cellular-automaton or hypergraph rewriting model. Its discreteness is not imposed by abstract rules but is physically required by null horizon geometry, holographic entropy bounds, and the Planck-limited causal throughput. Two distinct causal mechanisms, global radial incorporation of Planck-mass units and local lateral propagation of secondary-dipole patterns, are enforced by the horizon's null structure and have no analogue in generic automaton models. Lorentz invariance, thermodynamic scaling, and FRW emergence follow directly from these physical constraints rather than from combinatorial symmetries. The horizon-layered framework is therefore a physically mandated causal architecture, not a symbolic rewriting system.

Taken together, these developments support a unified interpretation: the event horizon is the generator of spacetime, causality, quantum statistics, and matter content; collapse is a process of informational layering, not singular formation; and the cosmos itself is the internal holographic projection of a larger black-hole spacetime. The horizon is not the end of physics but its beginning.

2 Schwarzschild Black Hole

The classical description of gravitational collapse originates from the prediction of general relativity that sufficiently massive stars, once all pressure support is exhausted, undergo an irreversible contraction. In the Schwarzschild solution, which describes a static, spherically symmetric vacuum spacetime, extension of the metric to $r = 0$ leads formally to a curvature singularity [8].

A standard assertion of classical general relativity is that an infalling observer reaches the event horizon in a finite proper time τ, even though the Schwarzschild time t measured by a distant observer diverges. This apparent inconsistency is typically resolved by invoking alternative coordinate systems, most notably the Kruskal–Szekeres coordinates, which remove the coordinate singularity at $r = 2M$ and allow the geodesic equations to extend smoothly across the horizon [9]. However, the reparameterization that renders the trajectory finite in (T, R) coordinates does not change the physical observation that, in Schwarzschild time, the particle approaches $r = 2M$ asymptotically. The distant observer's clock remains the operative measure of causal influence and continues to assign an infinite duration to the approach toward the horizon.

Despite these empirical and theoretical considerations, the standard view maintains that the particle "must clearly pass to a smaller radius unless it is destroyed" since, in its own proper time, the geometry appears smooth and non-pathological at the horizon [9]. Yet physical observation is inevitably tied to the time measured at spatial infinity. All observable signals, photons, neutrinos, and gravitational waves, experience unbounded redshift as their point of emission approaches the horizon. Every causal influence reaching the exterior does so at a rate that slows without bound when referenced to the external observer's clock.

General relativity's predictions of gravitational redshift and time dilation are experimentally confirmed with high precision: in the Hafele–Keating atomic-clock circumnavigation experiment [10], in the relativistic corrections essential for GPS satellite synchronization [11], and in high-precision optical clock tests [12]. These measurements establish that time dilation is a physical effect, not a coordinate artifact. Applying this principle to gravitational collapse requires that the external observer's infinite-time delay for horizon crossing be taken as physically meaningful, not merely mathematically inconvenient.

The physicality of the horizon is further supported by black hole thermodynamics. The Bekenstein–Hawking entropy depends on the area of the event horizon,

$$S_{\mathrm{BH}} = \frac{k_B c^3}{4G\hbar} A, \tag{1}$$

not the volume of any interior region [13]. This establishes the horizon, not the interior, as the physically significant locus of information. Hawking radiation [14] reinforces this interpretation: emission is tied to the near-horizon region, and the gradual evaporation of the black hole reflects physical processes governed entirely by horizon-area dynamics.

Taken together, these considerations reveal a fundamental tension in the classical interpretation of collapse. While proper-time geodesics suggest smooth infall, all empirically accessible quantities confirm that the horizon is approached only asymptotically in the external time that governs causal communication. Thus, any physical theory of collapse must reconcile the geometric smoothness of interior extensions with the measurable divergences experienced in the external frame. This motivates a more precise analysis of the infall process in Schwarzschild geometry, which we now turn to in the next subsections.

2.1 Radial Free Fall

The radial motion of freely falling objects in the Schwarzschild geometry is governed by the temporal, radial, and angular components of the metric [15, p. 108]. For a non-rotating, uncharged black hole of mass M, the Schwarzschild line element in geometric units ($G = c = 1$) is

$$ds^2 = -\left(1 - \frac{2M}{r}\right) dt^2 + \left(1 - \frac{2M}{r}\right)^{-1} dr^2 + r^2 \left(d\theta^2 + \sin^2\theta \, d\phi^2\right). \tag{2}$$

Although the temporal and radial coefficients diverge as $r \to 2M$, the angular part of the metric remains finite. This asymmetry between radial and tangential behavior in the near-horizon region plays a central role in the causal structure of Schwarzschild spacetime and will be revisited in later sections.

For a particle released from rest at a finite radius r_0, the proper time experienced while falling to a radius r is

$$\tau - \tau_0 = \frac{2}{3\sqrt{2M}} \left(r_0^{3/2} - r^{3/2}\right), \tag{3}$$

a standard result obtained from the timelike geodesic equations [15, p. 221]. In contrast, the Schwarzschild coordinate time interval measured by a distant observer is [15, p. 219]

$$\begin{aligned} t - t_0 = &-\frac{2}{3\sqrt{2M}} \left[r^{3/2} - r_0^{3/2} + 6M\left(\sqrt{r} - \sqrt{r_0}\right)\right] \\ &+ 2M \ln\left(\frac{(\sqrt{r} + \sqrt{2M})(\sqrt{r_0} - \sqrt{2M})}{(\sqrt{r_0} + \sqrt{2M})(\sqrt{r} - \sqrt{2M})}\right). \end{aligned} \tag{4}$$

The logarithmic term diverges for $r \to 2M$, indicating that no particle crosses the event horizon in finite Schwarzschild coordinate time.

To analyze this divergence, let

$$r = 2M + u, \qquad u \ll 2M.$$

Expanding $\sqrt{r}$ around $2M$ gives

$$\sqrt{r} - \sqrt{2M} \;\approx\; \frac{u}{2\sqrt{2M}}, \tag{5}$$

so the denominator in the logarithm of §(4) approaches zero linearly in u, producing the divergence in t as $u \to 0$.

The proper radial distance corresponding to a coordinate displacement dr near the horizon is

$$ds_r = \frac{dr}{\sqrt{1 - \frac{2M}{r}}} \;\approx\; \sqrt{\frac{2M}{u}}\, dr, \tag{6}$$

since $1 - 2M/r \approx u/(2M)$ when $u \ll 2M$. For an object of fixed proper radial length l_0, the corresponding coordinate length is therefore

$$\Delta r \;\approx\; l_0 \sqrt{\frac{u}{2M}}, \tag{7}$$

which shrinks to zero as $u^{1/2}$ when the horizon is approached. This near-horizon contraction is independent of the black hole mass.

The coordinate-time evolution of $u = r - 2M$ may be obtained from the radial geodesic equation for infall from rest at r_0 (see [16, p. 227]):

$$\frac{dr}{dt} = -\left(1 - \frac{2M}{r}\right)\sqrt{\frac{2M}{r}}. \tag{8}$$

Near the horizon, $\sqrt{2M/r} \approx 1$, so

$$\frac{du}{dt} = \frac{dr}{dt} \;\approx\; -\frac{u}{2M}. \tag{9}$$

Integrating gives

$$\ln\left(\frac{u_2}{u_1}\right) = -\frac{\Delta t}{2M}. \tag{10}$$

For a halving of the remaining radial distance, $u_2 = u_1/2$, one obtains

$$\Delta t = 2M \ln 2. \tag{11}$$

Thus the Schwarzschild coordinate time required to reduce the radial offset by a fixed fraction is proportional to the black hole mass.

Numerically, using $M_\odot \simeq 1.48 \times 10^3\,\mathrm{m}$ in geometric units,

$$\begin{aligned} M = 100 M_\odot: &\quad \Delta t \approx 6.826 \times 10^{-4}\,\mathrm{s}, \\ M = 1 M_\odot: &\quad \Delta t \approx 6.826 \times 10^{-6}\,\mathrm{s}. \end{aligned} \tag{12}$$

§(11) expresses the familiar logarithmic divergence of Schwarzschild time as the horizon is approached. Each halving of the remaining distance requires the same additional coordinate time, leading to a Zeno-like accumulation of delays reminiscent of the classical paradox of infinite subdivision [17].

Despite this divergence in t, the proper time to reach $r = 2M$ remains finite, as §(3) shows. The divergence in §(4) becomes significant only within a microscopically small interval extremely close to the horizon. Consequently, from the viewpoint of a distant observer, infalling matter approaches a region just outside the horizon (on scales far below any astrophysical resolution) within a short coordinate time, even though the horizon itself is never crossed in finite t.

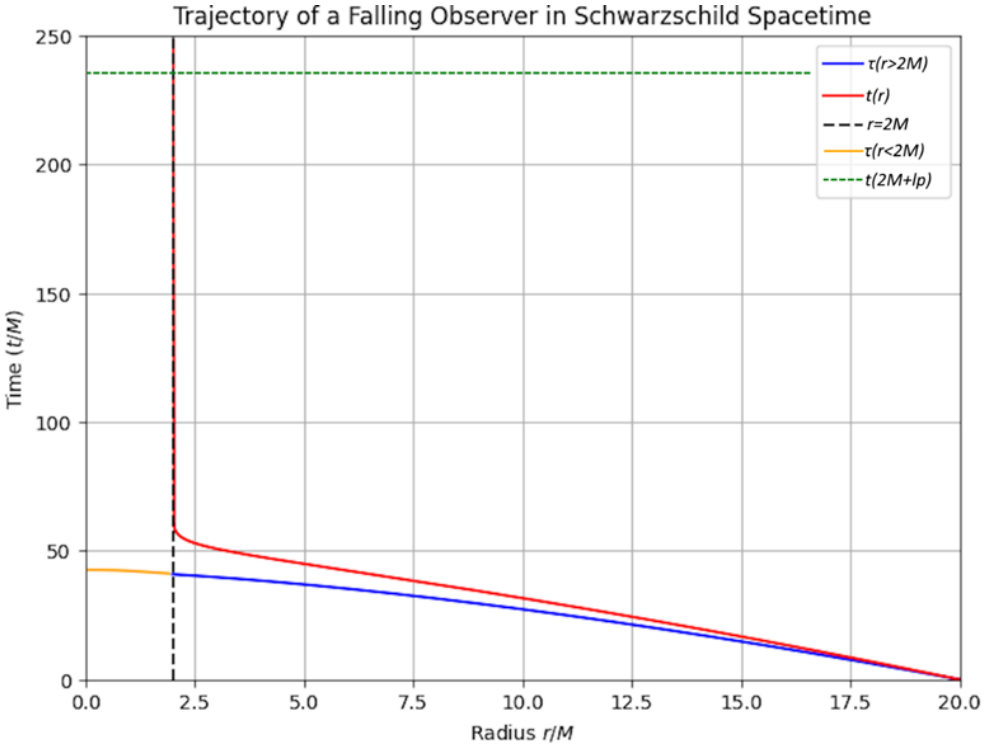

Fig. 1 The trajectory of a radially infalling observer in Schwarzschild spacetime plotted in terms of both proper time τ §(3) and Schwarzschild coordinate time t §(4). Both trajectories begin at $r_0 = 20M$, with $t_0 = \tau_0 = 0$. The orange segment represents a hypothetical continuation of the proper time trajectory past the horizon. The green line indicates the coordinate time at which the infaller reaches a Planck-length distance from the horizon. Adapted from [15].

2.2 External Observer versus Infalling Observer Experience

The Schwarzschild geometry exhibits a well-known discrepancy between the experience of a freely falling observer and that of an external, stationary observer. Both descriptions arise from the same metric but correspond to different notions of time: the proper time τ measured along the infalling worldline and the coordinate time t assigned by a distant observer. This distinction is central to the causal structure of black holes.

External stationary observer. §(4) shows that as $r \to 2M$ the coordinate time diverges logarithmically:

$$t \to +\infty \qquad \text{as} \qquad r \to 2M, \tag{13}$$

because the logarithmic denominator contains the factor $\sqrt{r} - \sqrt{2M} \to 0$. Thus the external observer never sees the infalling particle cross the horizon. The redshift factor

$$\sqrt{1 - \frac{2M}{r}} \tag{14}$$

tends to zero, producing an extreme suppression of all physical processes near the horizon and a corresponding freeze-out of radial motion. This behavior is not merely a coordinate artifact but reflects the operational fact that all signals emitted from near $r = 2M$ reach the distant observer only after arbitrarily long coordinate time; experimentally, gravitational time dilation behaves exactly in this manner.

Infalling observer. Classically, the proper time required to reach $r = 2M$ from any $r_0 > 2M$ is finite, as given by §(3). The mapping between τ and t follows from the metric relation

$$\frac{d\tau}{dt} = \sqrt{1 - \frac{2M}{r}} \longrightarrow 0 \qquad \text{as} \qquad r \to 2M. \tag{15}$$

In the conventional interpretation, this vanishing is treated as a coordinate effect: τ continues smoothly even as t diverges.

Reinterpreting the relation between t and τ. If §(15) is taken not merely as a coordinate mapping but as a *causal relation* connecting local and global evolution, then the vanishing of $d\tau/dt$ may be read as a synchronization constraint: the advance of local proper time is bounded by the rate at which the external coordinate time approaches the horizon. In this interpretation, the crossing of $r = 2M$ would require the distant coordinate time to reach $t = +\infty$, so that

$$\tau < \infty \quad \text{and} \quad t = \infty \qquad \text{would correspond to the same event,} \tag{16}$$

implying that no physical process can take a worldline beyond $r = 2M$ as long as the exterior geometry persists for only finite coordinate time.

Interaction with Hawking evaporation. If a black hole evaporates in finite external time $t_{\text{evap}} < \infty$ (as in the standard Hawking picture), then the geometry is time

dependent, and the would-be event horizon shrinks with advanced time. A collapsing worldline then asymptotically approaches a receding horizon. Because the external coordinate time available is finite, the infalling worldline cannot attain the value $t = \infty$ required for a classical horizon crossing. Consequently, the worldline remains outside the shrinking horizon and eventually encounters flat spacetime after evaporation. During the interval near $r = 2M$, the extreme blueshift of outgoing radiation exposes the infalling system to intense Hawking flux rather than to an interior region.

A number of semiclassical analyses suggest that such horizon avoidance may be generic once backreaction is taken into account. Models incorporating quantum gravitational corrections, including the Hayward–Ashtekar–Bojowald scenarios [18, 19], the non-formation arguments of Barceló *et al.* [20], and alternative proposals such as gravastars [21] and firewall frameworks [6], likewise conclude that horizon formation or traversability cannot be guaranteed in a physically realistic, evaporating spacetime.

Consequences. In such a picture, the classical event horizon never becomes a crossable surface for any physical observer. The radial infall worldline remains arbitrarily close to $r = 2M$ but always outside it for the entire finite duration of the external spacetime. The matter either becomes radiated away by the outgoing flux or experiences a transition to asymptotically flat geometry as the black hole evaporates. Thus, even though the classical metric allows a smooth continuation of τ across $r = 2M$, the global causal structure of an evaporating Schwarzschild spacetime prevents any actual crossing.

The implication is striking:

> **No particle in the observable universe ever completes a crossing of the Schwarzschild radius. All infalling matter remains arbitrarily close to $r = 2M$ until it is either emitted as radiation or the horizon itself disappears.**

This conclusion follows directly from combining the near-horizon behavior of §(15) with the finite lifetime imposed by Hawking evaporation, without yet invoking any additional modifications to general relativity.

3 Event Horizon

From the earliest collapse models of Oppenheimer and Snyder (1939) to modern numerical simulations and holographic formulations, **the formation of the event horizon has generally been treated as a global, teleological construct.** In these approaches, the horizon is defined as the causal surface separating null geodesics that eventually escape from those that do not, an object identified only after the entire spacetime evolution is known. Even in semiclassical extensions such as the membrane paradigm, loop quantum gravity, or AdS/CFT duality, the event horizon is typically regarded as a pre-existing geometric feature enclosing an evolving interior. Nowhere in these frameworks is the horizon treated as a dynamically nucleated boundary with a physically realized beginning. In contrast, the horizon-layered model regards horizon formation as a *local and causal process*, a sequence of null-surface nucleations beginning at the Planck scale and expanding outward.

In classical general relativity, a necessary condition for the formation of a local Schwarzschild horizon is the compactness inequality

$$\frac{2G\,m(r)}{r\,c^2} \;\geq\; 1, \tag{17}$$

where $m(r)$ is the mass contained within radius r. Using the mean density

$$\langle \rho(r) \rangle = \frac{3\,m(r)}{4\pi r^3}, \tag{18}$$

the same condition may be written as a lower bound on the average energy density inside r [22]:

$$\langle \rho(r) \rangle \;\geq\; \frac{3c^2}{8\pi G r^2}. \tag{19}$$

This inequality shows that the required mean density rises steeply as r decreases: smaller horizons require higher average densities. During realistic collapse, the density peaks in the core, so the compactness condition is first met at small radii and only later at larger ones.

Numerical simulations confirm this trend: only a fraction (typically $\sim$ 5–25%) of the total mass lies within the initially formed trapped region or apparent horizon [23–25], while the rest falls in later as the horizon expands outward. **Hence, the event horizon does not appear instantaneously at its final radius but grows dynamically from an inner seed, enlarging as additional mass crosses the compactness threshold.**

To formalize this behavior, define the local compactness function

$$f(r) = \frac{2G\,m(r)}{r\,c^2}, \tag{20}$$

with

$$m(r) = 4\pi \int_0^r \rho(r')\, r'^2\, dr', \tag{21}$$

which is monotonic for any nonnegative density $\rho(r) \geq 0$. Differentiating §(20) yields

$$f'(r) = \frac{2G}{c^2}\left(4\pi r\, \rho(r) - \frac{m(r)}{r^2}\right) = \frac{2G}{c^2}\,\frac{d}{dr}\left(\frac{m(r)}{r}\right). \tag{22}$$

Thus $f(r)$ increases with radius wherever the local density exceeds the interior average (since $d[m(r)/r]/dr > 0$ when $4\pi r^3\rho(r) > m(r)$). In a collapsing star, the central region typically develops the largest overdensity, so the compactness condition $f(r) = 1$ is first satisfied in a small inner domain. As more mass accumulates and crosses this threshold, the solution $f(r) = 1$ moves outward, describing an expanding trapped surface.

This picture is consistent with the physical dynamics of collapse. If most of the mass were confined to a thin outer shell while the interior mass $m(r < R)$ remained small, the shell would experience only a weak inward gravitational pull,

$$a(R) \approx -\frac{G\, m(R_{\text{inner}})}{R^2}, \tag{23}$$

and would require finely tuned initial velocities or external pressures to collapse rapidly enough to satisfy §(17) at its own radius. Realistic collapse solutions instead develop a central overdensity that naturally drives the compactness condition to be met first at small r, followed by outward growth of the horizon as additional layers fall in.

In the horizon-layered framework, this dynamical growth acquires a discrete, Planck-scale interpretation. The minimal self-trapped configuration occurs when a single Planck mass $m_{\text{p}} = \sqrt{\hbar c/G}$ is confined within its own Schwarzschild radius,

$$r_{\text{s}}(m_{\text{p}}) = \frac{2Gm_{\text{p}}}{c^2} = 2\,\ell_{\text{p}}, \tag{24}$$

with $\ell_{\text{p}} = \sqrt{\hbar G/c^3}$ the Planck length. **Thus the first horizon seed is necessarily of order the Planck scale: a Planck mass localized within a Planck-sized region.** Beyond this nucleation point, each additional Planck-mass increment $\Delta m = m_{\text{p}}$ increases the Schwarzschild radius by $\Delta r_{\text{s}} = 2\ell_{\text{p}}$, so the horizon grows outward in discrete null layers of thickness $2\ell_{\text{p}}$, in step with the causal incorporations that define internal time.

In summary, the compactness inequality §(17), the density bound §(19), numerical collapse results, and the Planck-scale relation $r_{\text{s}}(m_{\text{p}}) = 2\ell_{\text{p}}$ all point to the same conclusion: **the event horizon forms causally from the inside out, nucleating at the Planck scale and expanding as successive layers of matter satisfy the compactness condition.** It is not a teleological surface that appears suddenly at macroscopic radius, but a dynamically generated null boundary whose growth is tied, step by step, to the Planck-synchronized incorporation of mass–energy.

3.1 Formation of the Planck Seed and the Onset of Horizon Layering

The event horizon must form at the smallest radius where the compactness condition is locally satisfied. As collapse drives the core density toward the Planck regime, a minimal trapped region nucleates, forming the initial horizon seed. Subsequent accretion increases $m(r)$, pushing the equality $2Gm(r)/(rc^2) = 1$ outward through a sequence of nested null surfaces. Thus the event horizon is not a pre-existing geometric boundary but a causally generated surface that grows layer by layer from a quantum–gravitational core.

The threshold for horizon formation follows directly from the compactness criterion

$$\langle \rho(r) \rangle \;\geq\; \frac{3c^2}{8\pi G r^2}, \tag{25}$$

obtained by rewriting the local Schwarzschild condition $2Gm(r)/(rc^2) \geq 1$ in terms of the mean density. To estimate the radius at which this condition is first met, equate the required density with the mean density of a Planck-mass configuration,

$$\rho_{\rm p}(r) = \frac{m_{\rm p}}{\frac{4}{3}\pi r^3}. \tag{26}$$

Solving $\rho_{\rm p}(r) = \frac{3c^2}{8\pi G r^2}$ yields

$$r_{\rm crit} = \frac{\ell_{\rm p}}{\sqrt{2}} \;\approx\; 1.14 \times 10^{-35}\,{\rm m}, \tag{27}$$

the smallest radius at which a Planck mass can satisfy the horizon condition. Although the exact trapped-surface condition is $r = 2Gm/c^2$, the mean-density formulation is valid for estimating first formation, since $m(r)$ increases monotonically during collapse. Thus the initial horizon seed must be of order the Planck length.

Once a minimal trapped region forms, classical compression is no longer possible at the same rate. Further collapse does not shrink the core appreciably, but instead enlarges the horizon. Additional mass–energy increases $m(r)$, and the location where $2Gm(r)/(rc^2) = 1$ moves outward. The collapse thus transitions from three-dimensional compression to two-dimensional null encoding: the horizon expands while the interior ceases to contract. This represents the onset of *horizon layering*.

The commonly quoted Planck density,

$$\rho_{\rm P}^{(\rm std)} = \frac{m_{\rm p}}{\frac{4}{3}\pi \ell_{\rm p}^3} \simeq 5 \times 10^{96}\,{\rm kg/m^3}, \tag{28}$$

arises by placing one Planck mass in a Euclidean sphere of radius $\ell_{\rm p}$. However, at the Planck scale, volume is not a classical concept, and the compactness condition provides a more physical definition. Using $r_{\rm crit} = \ell_{\rm p}/\sqrt{2}$ gives the compactness-consistent

threshold,

$$\rho_{\mathrm{P}}^{(\mathrm{crit})} = \frac{m_{\mathrm{P}}}{\frac{4}{3}\pi r_{\mathrm{crit}}^3} \simeq 1.2 \times 10^{96}\,\mathrm{kg/m^3}, \tag{29}$$

which differs only by an order-unity geometric factor but corresponds directly to the first radius at which a self-sustaining trapped surface forms.

Thus, every black hole, regardless of its eventual mass, originates from a finite Planck-scale horizon seed. Large black holes do not appear suddenly at macroscopic radii; they grow outward from a minimal quantum-gravitational core. Each newly incorporated mass element increases the Schwarzschild radius by a finite increment, and the full macroscopic horizon is a layered causal structure built through successive Planck-scale additions. The Planck density marks the upper limit of classical compression; beyond it, the dynamics are governed entirely by horizon growth and holographic null encoding.

In this horizon-layered perspective, the "singularity" of classical general relativity never forms. The physical process terminates naturally at the Planck seed, at which point the horizon begins its outward causal expansion. The interior remains finite and regular, and all further mass–energy is encoded as additional layers on the null boundary, preserving unitarity and satisfying the holographic bound at every stage of collapse.

3.2 Causal Exclusion and the Ontological Status of the Interior

As the event horizon begins its outward growth from the Planck scale, a natural question arises: *what is the physical status of the interior volume that the horizon appears to enclose?* Classically, one imagines that the horizon wraps around a pre-existing region of spacetime which continues to evolve behind it. In the horizon-layered framework, this intuition is replaced by a different and more causally consistent picture:

the interior is not a pre-existing region of spacetime. It is an emergent construct defined entirely by the information encoded on the growing horizon.

In classical GR, the event horizon is often treated as a passive geometric surface enclosing an already-formed interior. But the formation analysis shows that the horizon nucleates at the Planck scale and grows outward through a continuous sequence of null-surface incorporations. During this growth, the region "behind" the horizon is *causally excluded* from all external influence: no signal from the exterior can enter, and no information encoded on the horizon can propagate backward into an already-formed interior. The interior cannot function as an independently evolving manifold because it is not in the causal future of any external point.

The horizon-layered picture therefore treats the event horizon not as a static boundary, but as an *active, generative null surface*. With each incorporation step, the horizon expands and its encoding structure updates. It is this sequence of null-ordered updates that defines the emergent causal bulk. Nothing inside the horizon pre-exists these

updates; the interior is the spacetime *reconstructed* from the horizon code by the embedding map E_t.

From this perspective, the so-called black-hole "interior" is not an ontically independent region. It is an emergent domain whose geometry is determined entirely by the horizon's layered information content:

- the horizon provides the only physically realized degrees of freedom;
- the interior spacetime is a holographic reconstruction of these degrees of freedom;
- the apparent bulk dynamics arise from the causal, redshift-frozen ordering of horizon layers.

This interpretation resolves the classical singularity problem without requiring exotic quantum gravity modifications of curvature or stress-energy. A singularity represents an attempt to place physical content in a region that is both causally inaccessible and unconstrained by an area-based entropy bound. In the present framework, this region simply does not exist:

there is no singular point because there is no physical spacetime beyond the horizon surface. The only ontic structure is the horizon code itself.

The familiar three-dimensional interior arises only as a coarse-grained, null-projected reconstruction of the layered horizon geometry. Its apparent evolution reflects not an underlying bulk manifold but the progressive causal encoding of information on the horizon. Thus, in the horizon-layered cosmology, the interior is not a region into which matter falls, it is the emergent record of how the horizon has grown.

In this view, the horizon is the fundamental locus of gravitational physics. Spacetime "inside" is a derived construct: a causal shadow of the null surface that generates it. The classical singularity problem is replaced by a consistent holographic account in which no physical content ever resides in a region without a supporting entropy-bearing boundary. The interior is born with the horizon and grows only through the horizon's layered expansion.

3.3 Reinterpreting Hawking Radiation

In the classical treatment of black holes, an infalling particle crosses the event horizon and enters a pre-existing interior region of spacetime. Within the horizon-layered framework, this passage never occurs. Extreme gravitational redshift freezes the infalling system in the external frame, and all physically accessible structure terminates at the horizon itself. The event horizon is therefore not a permeable surface but the terminal null boundary of the external manifold, the place where infalling information is absorbed and encoded into the null-ordered causal structure.

This reinterpretation directly affects the foundations of Hawking radiation. The standard heuristic picture relies on particle–antiparticle pairs forming across an interior–exterior interface, with the negative-energy partner falling inward while the

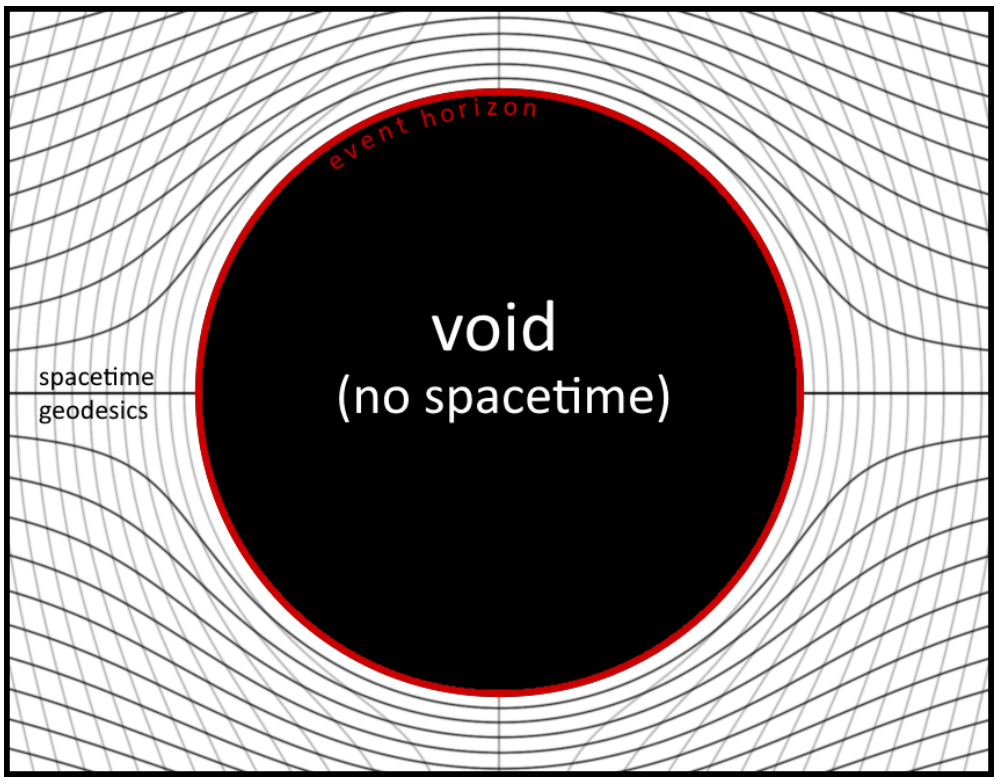

Fig. 2 Spacetime geodesics curve around a Schwarzschild black hole in this model much like streamlines in a compressible fluid flow bend around an obstacle. This behavior arises not from an embedded central mass, but from the topological excision of spacetime at the black hole interior. The event horizon marks the null surface beyond which no causal structure or geometry persists. Only geodesics orthogonal to the horizon terminate at this boundary; all others bend due to the elastic curvature induced by the absence of interior spacetime. The horizon acts as a holographic encoding surface for the excised region, consistent with entropy bounds and causal structure.

positive-energy partner escapes. Such a mechanism presupposes that an interior manifold exists as part of the same geometric domain in which quantum fields propagate. If the spacetime ends at the horizon, then there is no region inside for negative-energy modes to inhabit and no geometric support for an inward flux. Quantum fields exist only in the redshift-dominated exterior layer, the region where infalling quanta are encoded and where the vacuum structure is continually deformed by their arrival.

Hawking radiation must therefore be understood as a phenomenon of the external vacuum alone. It arises from vacuum polarization in the near-horizon region, where incoming matter perturbs the local quantum state and produces outward-propagating excitations. These excitations are created outside the horizon and, although heavily redshifted, can travel to infinity. The thermal spectrum of this radiation is a consequence of the universal Rindler-like geometry of the near-horizon region. For a static observer at fixed radius r, the asymptotic energy of an emitted quantum is related to

the local energy by

$$E_\infty = E_{\text{local}}\sqrt{1 - \frac{2Gm_{\text{bh}}}{rc^2}}, \tag{30}$$

and the near-horizon limit reproduces the standard Hawking temperature,

$$T_H = \frac{\hbar c^3}{8\pi G m_{\text{bh}} k_B}. \tag{31}$$

This temperature reflects the redshift structure of the external geometry; it does not imply radiation from an interior that is absent from the physical manifold.

Once the interior is removed from the picture, the logic that leads to black hole evaporation collapses. The usual argument requires an inward flow of negative energy and a corresponding extraction of mass from the black hole. But if no interior exists into which negative-energy modes can propagate, the inward flux is not merely unlikely; it is undefined. Likewise, the outward flux at infinity cannot be supplied by the black hole's ADM mass, because the emitted quanta originate in the polarized external vacuum and not from a reservoir of internal energy. There is therefore no physical mechanism for the mass to decrease, and the horizon cannot evaporate. Its mass either remains constant or increases through accretion, consistent with the area theorem and with the null-layered encoding of infalling matter.

This view preserves all observable features associated with Hawking radiation, its thermal spectrum, its luminosity scaling with surface gravity, and its angular and frequency distributions, while discarding the unphysical consequences of mass loss. No singular end-state arises, no violation of unitarity occurs, and no information is hidden in an inaccessible region. What appears as "evaporation" is instead the gentle readjustment of the external vacuum as it responds to continual causal incorporations at the horizon. Radiation emerges from the polarized exterior geometry, not from tunneling across a non-existent interior boundary.

In this reinterpretation, crossing the event horizon is not a physical process but a classical extrapolation that fails in the regime of extreme redshift and holographic encoding. The event horizon is the outermost, terminal surface of the manifold, a dynamic null boundary where information is absorbed, encoded, and eventually re-expressed through vacuum polarization. Black holes therefore radiate without evaporating. Their horizons remain stable, their encoded information is never lost, and the paradoxes associated with horizon crossing and mass loss dissolve once the horizon is understood as the generating surface of the spacetime itself rather than the entrance to a hidden interior.

3.4 Reinterpretation of Mass and Spacetime

In classical general relativity, gravitational collapse produces a curvature singularity under the assumptions of the Penrose–Hawking theorems [26]. These results rely on a smooth manifold and the classical stress–energy relation

$$R_{\mu\nu} - \tfrac{1}{2} g_{\mu\nu} R = \frac{8\pi G}{c^4} T_{\mu\nu}. \tag{32}$$

In the horizon-layered holographic interpretation developed here, curvature is not sourced by matter "contained inside" spacetime, but by the controlled *removal of causal connectivity* on the horizon code. A mass quantum corresponds to a finite *causal deficit*, a reduction in null adjacency that the surrounding manifold compensates by developing curvature. Geodesics bend not around a material core but around a region where the causal network is partially excised, much like streamlines curving around an obstacle in a fluid analogy (Fig. 2).

Accordingly, the black-hole event horizon is the *terminal* null boundary of the external manifold. Beyond it no spacetime points, fields, or observers exist. Hawking radiation arises entirely from the vacuum *outside* this causal edge; the excised region contributes nothing to the geometry except through its encoded causal deficit. The classical singularity is therefore replaced by a finite termination of the manifold: curvature measures the strain induced by the excised region, not a blow-up of interior fields.

This interpretation aligns naturally with the holographic principle. The Bekenstein–Hawking relation

$$S = \frac{k_B c^3}{4\hbar G}\, A \tag{33}$$

implies that gravitational information resides on *surfaces*, not in volumes. In this picture, the stress–energy tensor $T_{\mu\nu}$ encodes both conventional matter content and the geometric strain required to maintain curvature around excised causal domains. Newton's constant G quantifies the manifold's resistance to this topological deficit. A singularity cannot form because **excised regions cannot overlap arbitrarily: the causal network cannot shrink to a point without violating the holographic bound.**

With no interior spacetime to support it, the horizon is maintained entirely by the geometry outside it. The abrupt termination of the manifold produces an inward geometric pressure, while the horizon itself behaves like a coarse-grained null membrane that resists deformation. In this sense, the horizon possesses an effective surface tension: the external curvature tries to compress the surface, and the membrane's tension, supplemented by quantum and entanglement effects, counteracts that compression.

This "geometric balance" is analogous to the equilibrium condition for a physical membrane held in place by pressure on one side. Although the analogy is only phenomenological, it captures the essential idea: the event horizon remains a stable null boundary not because an interior exists to sustain it, but because the external spacetime geometry and the membrane's own effective tension mutually support its structure.

Mass as a causal dipole. Ordinary (baryonic) matter corresponds to a *causal dipole*: one pole remains connected to the surrounding null network (allowing coupling to gauge and quantum fields), while the opposite pole is causally excised, creating gravitational curvature. This explains the universal coupling of mass to gravity: the excised pole defines gravitational charge, while the connected pole maintains full participation in Standard Model interactions.

Dark matter as a fully excised causal defect. Dark-matter quanta correspond to the *symmetric* case where *both* poles are causally excised. They possess no connected pole and thus do not couple to gauge fields. Their presence is felt solely through the curvature imprint of their causal deficit. This explains their invisibility and their purely gravitational influence.

Radiation as fully connected quanta. Massless excitations (photons, gravitons, conformal fields) correspond to quanta with *both* poles fully connected to the causal network. With no causal deficit, they produce no rest mass and propagate on null geodesics as pure coherence patterns of the underlying code.

The vacuum as de-synchronized causal capacity. The vacuum corresponds to causal degrees of freedom that are not phase-locked to the coherent code. These de-synchronized modes reproduce the usual quantum vacuum fluctuations of QFT when projected into the bulk, but in the holographic picture they represent latent, uncommitted causal capacity capable of supporting coherent excitations.

In this framework the Planck mass,

$$m_p = \sqrt{\frac{\hbar c}{G}}, \tag{34}$$

marks the threshold where causal excision becomes self-sustaining. Below m_p, matter remains embedded in spacetime; above it, the causal deficit self-closes into a horizon. Rest energy $E = mc^2$ acquires geometric meaning as the strain required to maintain the causal discontinuity; kinetic energy represents the dynamic redistribution of this strain across the null network.

Thus mass, radiation, dark matter, and vacuum emerge as distinct patterns of causal connectivity. Gravity arises as the elastic response of the manifold to causal excision, and the classical singularity is avoided because spacetime simply ceases beyond the horizon rather than collapsing into a divergent point.

3.5 Singularity as Holographic Inconsistency

Classical general relativity treats the event horizon of a black hole as a fictive geometric boundary beyond which physical quantities may diverge. The interior singularity, characterized by formally infinite curvature and vanishing volume, is regarded as a real endpoint of spacetime evolution. However, this treatment is incompatible with the holographic principle, which asserts that the physical degrees of freedom of a gravitational system are fully encoded on its bounding surface, with entropy proportional to area rather than volume.

If the singularity were a physical object, it would permit the accumulation of unbounded entropy and curvature within a region that contributes negligibly to the area-based entropy budget. In standard treatments, the holographic limit is usually applied only to the event horizon of a black hole. In the framework proposed here, however, **the holographic bound must hold for *every* causally complete volume**

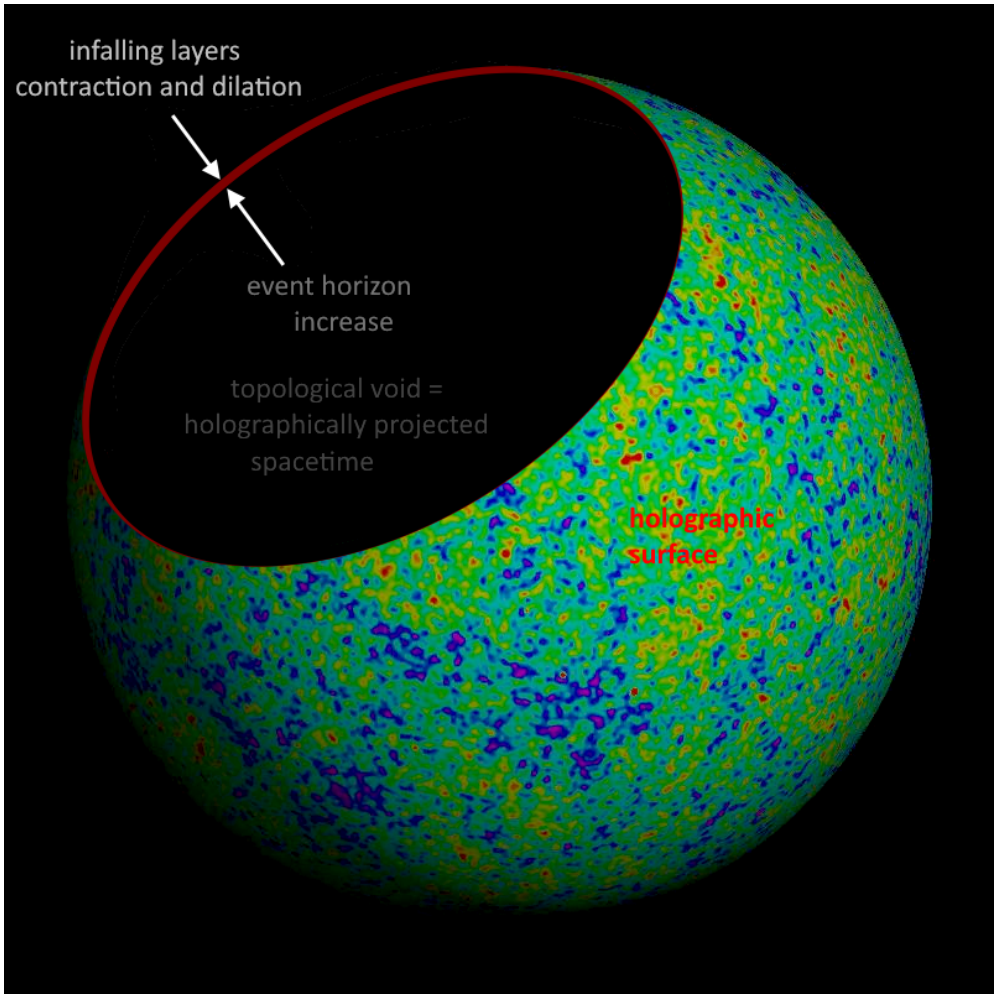

Fig. 3 Schematic representation of black hole gravitational collapse at a causal distance of ℓ_p above the event horizon. As infalling mass increases, the horizon expands, creating a redshift-based foliation of null layers just above the event horizon. Internal spacetime exists only as a holographic projection.

containing matter–energy, including regions that would classically evolve toward a singularity. Allowing a singularity would then violate this bound by concentrating information density beyond the allowed limit in a vanishing spatial region. This contradicts the Bekenstein–Hawking entropy limit and the covariant entropy bound [27], which restrict the maximal entropy of any causal domain to

$$S_{\max} = \frac{A}{4\,\ell_{\mathrm{p}}^2}, \tag{35}$$

where A is the area of the boundary enclosing the region. Permitting a singularity would undermine unitarity and the self-consistency of quantum gravity in any physically meaningful volume.

In the horizon-layered cosmological model, this inconsistency is resolved by *removing* the interior volume from the causal description. **The event horizon is not a fictive boundary but a physically operative, null-ordered, information-bearing surface that encodes infalling matter in Planck-scale strata.** The classical singularity is replaced by a dynamically expanding code surface whose entropy is finite and precisely saturates the holographic bound. All physical degrees of freedom are accounted for at this surface; no information is hidden behind a spacelike singularity.

As gravitational collapse proceeds, the horizon area increases in discrete Planck-scale steps. Each incorporation of a Planck mass triggers a global retessellation of the horizon, adding a finite increment of area and increasing the maximal information capacity,

$$I_{\max}(t) = \frac{A(t)}{4\,\ell_{\mathrm{p}}^2}. \tag{36}$$

In this sense, **the growth of the horizon is the physical mechanism by which the universe's information capacity increases**. Holographic saturation is maintained dynamically: the boundary expands exactly fast enough to encode all infalling matter–energy without ever requiring a singular concentration of information in zero volume.

This reformulation preserves unitarity, maintains the validity of entropy bounds, and aligns with holographic expectations. The singularity, in this view, is not a physical endpoint but a symptom of the breakdown of classical description beyond its applicable domain. The true physical content lies in the quantum encoding at the horizon, from which time, matter, and geometry emerge as bulk projections of the null-surface code.

The holographic bound is more fundamental than the dynamical predictions of classical general relativity. Any apparent violation of the entropy bound, such as the occurrence of singularities predicted by the Penrose–Hawking theorems, must be resolved by a transition in the holographic encoding of information. When gravitational collapse drives a system toward saturation of the holographic limit, the classical singularity is replaced by a new phase of spacetime description, characterized by horizon-layered encoding and causal bandwidth saturation.

On a holographic surface, regions of extreme curvature that would classically evolve toward singularities instead manifest as *localized domains of maximal bandwidth absorption*. These are areas where the local (redshifted) rate of causal updates approaches the universal causal power limit $P_{\max} = c^5/G$, forming stable null surfaces that function as internal horizons. Each such domain sustains a self-consistent holographic encoding of an emergent internal spacetime, an informationally complete, recursively defined causal substructure, without requiring a physical singularity or excised interior volume. Through this mechanism, singularities never form: they are replaced by successive layers of bandwidth-saturated horizons, each preserving the holographic information bound.

The present model enforces the holographic bound globally: **no spacetime volume may *contain* more information than permitted by the area of its boundary, and wherever this limit is approached, a horizon forms and carries the excess as boundary degrees of freedom.** This principle restores unitarity and ensures continuity of the information measure across all nested surfaces. The Planck-scale holographic horizon dynamically enforces this condition by transcribing infalling matter into surface quanta once its approach distance reaches the Planck threshold. Thus, while ordinary relativistic dynamics remain valid in the low-curvature regime, they are globally subordinated to a deeper holographic conservation law: the causal flux and informational capacity of the universe remain continuous and finite across every hierarchical level of gravitational collapse.

3.6 Internal Universe Fundamental Constants

In the horizon-layered cosmology, the interior of a black hole is not a hidden spacetime region but a genuine *topological void*: a domain in which spacetime, distance, duration, and geometry have no physical meaning. This is the only coherent sense in which "nothingness" can be defined: not as a quantum vacuum, not as a fluctuating field, but as the *absence of spacetime itself*. The event horizon marks the boundary where this void first differentiates into being. All structure, geometry, and physical law emerge from the way this boundary regulates causal distinction.

Within this perspective, the fundamental constants are not arbitrary empirical inputs but direct reflections of how the boundary between non-being and being operates. Each constant encodes one aspect of the causal grammar that allows the horizon to produce distinguishable states, sustain coherence, and project an emergent spacetime.

The speed of light as the rate of causal propagation. In the horizon-layered picture, the speed of light c has a precise microscopic origin. Each global incorporation of one Planck mass occurs in a discrete interval of Planck time t_{p}. During this interval, phase information may propagate laterally by exactly one Planck-length step ℓ_{p} across the secondary-dipole network. The maximal causal propagation rate is therefore

$$c = \frac{\ell_{\mathrm{p}}}{t_{\mathrm{p}}}, \tag{37}$$

representing one tangential adjacency update per horizon tick. Null excitations in the internal universe are holographic projections of these maximal-rate lateral updates. The universality of c follows because every physical process inherits its causal structure from this horizon-regulated update rule.

The gravitational constant as geometric compliance. The gravitational constant G quantifies the horizon's geometric response to energetic input. When a Planck mass is absorbed, the horizon expands by a fixed geometric amount:

$$\Delta r_{\mathrm{s}} = \frac{2G}{c^2}\,\Delta m. \tag{38}$$

Thus G links energy incorporation to spatial reconfiguration. It measures the *compliance* of the horizon's null geometry, the efficiency with which the causal boundary adjusts to maintain global null-ordering in response to incoming energy. Gravity becomes the bookkeeping rule that translates energetic additions into the required geometric update preserving causal consistency at the edge of being.

Planck's constant as the quantum of distinguishable phase. Planck's constant $\hbar$ encodes the minimal quantum of phase information that can be registered on the horizon without violating causal synchrony. At the Planck scale, the fundamental triplet

$$(m_{\mathrm{p}},\, \ell_{\mathrm{p}},\, t_{\mathrm{p}}) = \left(\sqrt{\frac{\hbar c}{G}},\, \sqrt{\frac{\hbar G}{c^3}},\, \sqrt{\frac{\hbar G}{c^5}} \right) \tag{39}$$

satisfies the identity

$$m_{\mathrm{p}} c^2\, t_{\mathrm{p}} = m_{\mathrm{p}} c\, \ell_{\mathrm{p}} = \hbar, \tag{40}$$

revealing that $\hbar$ is the action associated with a *single causal update* of the horizon. Where c governs the maximum *rate* of causal propagation and G governs the *amplitude* of geometric response, $\hbar$ determines the *granularity* of distinguishable phase differences. It is the smallest unit of action that the causal network can resolve, the minimum contrast required to create a distinct physical state.

Thus the fundamental constants arise not from arbitrary initial conditions nor empirical coincidence, but from the way the universe differentiates itself from the void at its boundary. They express three orthogonal aspects of the minimal causal structure required for existence to emerge from non-existence:

$$\boxed{\text{Nothingness} \longrightarrow \text{Causal Contrast} \longrightarrow (c,\, \hbar,\, G) \longrightarrow \text{Emergent Spacetime}} \tag{41}$$

Here, c is the speed of causal propagation on the horizon, $\hbar$ is the quantum of distinguishable phase, and G is the geometric compliance of the null boundary. Together they define the Planckian kernel from which spacetime, matter, locality, and cosmic evolution arise. They are not constants presupposed by a pre-existing stage but the parameters governing the very act by which the universe becomes distinguishable from nothingness.

3.7 Planck-Step Horizon Synchronization

Gravitational collapse halts at the Planck redshift limit, where further infall is converted into surface information rather than volumetric compression. Beyond this threshold, incoming matter–energy is no longer described by classical trajectories into a pre-existing volume, but by its transcription into horizon-localized degrees of freedom: angular-momentum eigenmodes, quantum fluctuations, and spin-network links that together form the black hole's holographic code. The "interior" is not an independently evolving spacetime region but an emergent, holographically reconstructed domain whose causal ordering is defined entirely by the stratified horizon surface. Although the internal volume scales as r_{s}^3, its causal and informational origin lies in the ordered sequence of null layers that expand the horizon.

The Schwarzschild radius of a black hole of mass $m_{\rm bh}$ is

$$r_{\rm s} = \frac{2G\, m_{\rm bh}}{c^2}, \tag{42}$$

so a small mass increment $\Delta m_{\rm bh}$ changes the radius by

$$\Delta r_{\rm s} = \frac{2G\, \Delta m_{\rm bh}}{c^2}. \tag{43}$$

For a single Planck mass,

$$\Delta m_{\rm bh} = m_{\rm p} \quad \Rightarrow \quad \Delta r_{\rm s} = 2\,\ell_{\rm p}. \tag{44}$$

Each Planck-mass incorporation therefore extends the horizon by two Planck lengths, forming one global null layer of thickness $2\ell_{\rm p}$. In the horizon-layered cosmology, such a layer constitutes the smallest discrete reconfiguration of spacetime geometry, one tick of the holographic code.

The Planck quantities form the synchronized triplet

$$m_{\rm p} = \sqrt{\frac{\hbar c}{G}}, \qquad \ell_{\rm p} = \sqrt{\frac{\hbar G}{c^3}}, \qquad t_{\rm p} = \frac{\ell_{\rm p}}{c}, \tag{45}$$

linked by

$$\frac{G m_{\rm p}^2}{\ell_{\rm p}} = m_{\rm p} c^2 = \frac{\hbar}{t_{\rm p}}. \tag{46}$$

At this scale, gravitational self-energy, relativistic causality, and quantum uncertainty coincide, defining the smallest self-localized excitation compatible with both GR and QM. Thus the synchronized triplet

$$(\Delta m,\, \Delta r,\, \Delta t) = (m_{\rm p},\, 2\ell_{\rm p},\, t_{\rm p}) \tag{47}$$

represents the minimal causal act of horizon growth.

Each Planck step transfers one Planck energy in one Planck time, corresponding to the universal causal power limit

$$P_{\rm max} = \frac{E_{\rm p}}{t_{\rm p}} = \frac{c^5}{G}. \tag{48}$$

Numerically $P_{\rm max} \approx 3.63 \times 10^{52}\,\mathrm{W}$. **The event horizon operates precisely at this limit: one Planck energy per Planck time per global incorporation step.** Once the collapsing core first confines a Planck mass within a Planck-scale region, this causal power limit is reached; classical collapse transitions to discrete causal incorporation, and the horizon begins to grow through sequential Planck updates.

The corresponding change in horizon area is

$$A = 4\pi r_{\rm s}^2 \quad \Rightarrow \quad \Delta A = 8\pi r_{\rm s}\,\Delta r_{\rm s} = 16\pi r_{\rm s}\,\ell_{\rm p}, \tag{49}$$

so that

$$\frac{\Delta A}{\ell_{\rm p}^2} = 16\pi\,\frac{r_{\rm s}}{\ell_{\rm p}} = 32\pi\,\frac{m_{\rm bh}}{m_{\rm p}}, \tag{50}$$

where the last equality follows from $r_{\rm s} = 2(Gm_{\rm bh}/c^2) = 2(m_{\rm bh}/m_{\rm p})\,\ell_{\rm p}$.

The holographic principle assigns a maximal information content

$$I_{\rm max} = \frac{A}{4\,\ell_{\rm p}^2}, \tag{51}$$

which in this framework is *exactly saturated* and dynamically maintained by Planck incorporations. Using

$$A = 16\pi\,\frac{G^2 m_{\rm bh}^2}{c^4}, \qquad \ell_{\rm p}^2 = \frac{\hbar G}{c^3}, \tag{52}$$

one finds

$$I = 4\pi\left(\frac{m_{\rm bh}}{m_{\rm p}}\right)^2, \tag{53}$$

with incremental information

$$\Delta I_{\rm p} = 8\pi\,\frac{m_{\rm bh}}{m_{\rm p}}. \tag{54}$$

The entropy follows the same law,

$$S_{\rm bh} = 4\pi k_{\rm B}\left(\frac{m_{\rm bh}}{m_{\rm p}}\right)^2, \tag{55}$$

with incremental entropy

$$\Delta S_{\rm p} = 8\pi k_{\rm B}\,\frac{m_{\rm bh}}{m_{\rm p}}. \tag{56}$$

In this framework, mass, entropy, and information are unified as complementary expressions of a single causal process: the sequential incorporation of null layers at the Planck-scale bandwidth $P_{\rm max} = c^5/G$. Each step increases $m_{\rm bh}$, A, S, and I in lockstep, maintaining exact holographic saturation,

$$S \propto I \propto A \propto m_{\rm bh}^2, \qquad \Delta S,\,\Delta I \propto m_{\rm bh}. \tag{57}$$

Planck-step horizon synchronization thus realizes bulk–boundary duality as an explicit causal mechanism, furnishing a singularity-free picture of black-hole growth and ensuring unitarity by encoding all information on the evolving horizon.

3.8 Radial Freezing and Null-Ordered Layering

As infalling matter approaches the stretched horizon, defined as the surface one Planck length above $r_{\rm s}$, gravitational redshift and relativistic length contraction compress it into exponentially thinner shells. From the viewpoint of a distant observer, radial motion becomes increasingly time-dilated and eventually freezes: for a near-radial null trajectory,

$$\frac{dr}{dt} = \pm\Big(1 - \frac{r_s}{r}\Big), \tag{58}$$

implying $dr/dt \to 0$ as $r \to r_s$. Any dynamical process requiring motion in r thereby becomes inaccessible.

At fixed proper radial length l_0, the Schwarzschild coordinate interval satisfies

$$\Delta r \approx l_0\sqrt{\frac{\epsilon}{r_s}}, \qquad r = r_s + \epsilon, \quad \epsilon \ll r_s, \tag{59}$$

so that as $\epsilon \to 0$ the coordinate thickness of any radially extended structure collapses toward zero. However, no physically meaningful configuration can be compressed below one Planck length: quantum gravity prohibits a thickness smaller than $\ell_{\rm p}$. Thus the redshift divergence halts the radial contraction at $\epsilon \simeq \ell_{\rm p}$, defining an irreducible *Planck-thick holographic layer*. Within this layer, proper radial distances are minimized to the smallest scale allowed by physics; any further radial motion would require $\Delta r < \ell_{\rm p}$ and is therefore kinematically forbidden.

Consequently, the near-horizon region undergoes a natural dimensional reduction: radial dynamics freeze, while tangential directions retain full causal capacity. This dimensional reduction enforces the Bekenstein–Hawking area law and shows that the horizon is a *causal interface* encoding information on its surface rather than the boundary of an interior volume.

Null-ordered layering and holographic compression. As ϵ approaches $\ell_{\rm p}$, collapsing matter enters a regime in which redshift divergence arranges it into a hierarchy of *null-ordered layers*. Each layer corresponds to a lightlike hypersurface of constant advanced or retarded time, representing a discrete causal moment of the collapse. Once this null stratification reaches the Planck limit, the stretched horizon becomes the operational locus of holographic encoding: the external manifold terminates at the null surface, and all interior degrees of freedom are represented within a gauge-invariant boundary code.

Preserved lateral dynamics on the stretched horizon. Although radial motion is frozen, tangential propagation remains fully active. For a null angular displacement at fixed r,

$$0 = -\Big(1 - \frac{r_s}{r}\Big)dt^2 + r^2 d\Omega^2, \tag{60}$$

giving the coordinate angular velocity

$$\frac{d\Omega}{dt} = \frac{\sqrt{1 - r_s/r}}{r}. \tag{61}$$

On the stretched horizon ($\epsilon \sim \ell_{\rm p}$),

$$\frac{d\Omega}{dt} = \sqrt{\frac{\epsilon}{r_s + \epsilon}} > 0. \tag{62}$$

The Schwarzschild metric gives

$$d\tau_{\rm loc} = \sqrt{1 - \frac{r_s}{r}}\, dt, \tag{63}$$

so the locally measured angular rate is

$$\frac{d\Omega}{d\tau_{\rm loc}} = \frac{d\Omega/dt}{d\tau_{\rm loc}/dt} = \frac{\sqrt{1 - r_s/r}/r}{\sqrt{1 - r_s/r}} = \frac{1}{r}. \tag{64}$$

Thus the tangential speed is

$$v_\perp = r\, \frac{d\Omega}{d\tau_{\rm loc}}. \tag{65}$$

In natural units ($c = 1$), the product $r(1/r) = 1$, so $v_\perp = 1$; restoring units yields

$$v_\perp = c. \tag{66}$$

Therefore, the stretched horizon is a two-dimensional, lightlike, dynamically vibrant membrane: radial dynamics freeze due to Planck-scale contraction and infinite dilation, yet lateral propagation remains exactly luminal.

3.9 Planck-Scale Horizon Dynamics and Causal Incorporation

As matter becomes null-ordered within the stretched horizon, its information is assimilated through discrete *causal incorporation* events. Each event transfers one Planck unit of mass–energy to the horizon, increasing the Schwarzschild radius by $\Delta r_s = 2\ell_{\rm p}$ and advancing the internal causal order by one tick. Horizon growth occurs only when the entire membrane achieves full lateral phase coherence. Each incorporation corresponds to a horizon-wide retessellation,

$$\Psi_{\mathcal{M}}(t_{n+1}) = \mathcal{U}_n\, \Psi_{\mathcal{M}}(t_n). \tag{67}$$

Although the mass increment is only one Planck mass, the area increment is

$$\Delta A = 16\pi r_s\, \ell_{\rm p}, \qquad \frac{\Delta A}{\ell_{\rm p}^2} = 32\pi \frac{m_{\rm bh}}{m_{\rm p}}, \tag{68}$$

so a solar-mass black hole acquires $\sim 10^{40}$ new Planck cells per update. Internal time $t_{\rm internal}$ advances only when such an update occurs and is operationally indistinguishable from $\tau_{\rm loc}$ on the stretched horizon.

Global synchronization without lateral signaling. A horizon-wide update does not require tangential propagation: the horizon is a null surface defined entirely by the mass parameter M. When $M \to M + \delta M$, the entire null generator family is redefined geometrically, not via signals traveling across the surface but through the change in the condition $r = r_s(M)$.

Gravitational redshift ensures that one internal Planck tick, $t_{\rm p}^{(\rm internal)}$, corresponds to an extremely long external interval,

$$t_{\rm ext} \sim (1 + z_{\rm h})\, t_{\rm p}^{(\rm internal)} \gg t_{\rm p}. \tag{69}$$

Thus internally, updates occur as single coherent steps, while externally the same process is stretched into very long durations. Causality is fully preserved.

Bandwidth saturation and jet ejection. If infalling matter arrives faster than the membrane can synchronize its degrees of freedom, a causal backlog forms. The horizon cannot process the information at the maximal causal rate,

$$P_{\rm max} = c^5/G, \tag{70}$$

and excess energy is expelled along open null channels, typically near magnetic poles. Astrophysical relativistic jets therefore reflect the finite causal bandwidth of the encoding surface.

Unified picture. Null layering, radial freezing, tangential lightlike propagation, Planck-limited incorporation, global retessellation, and jet ejection all arise from a single mechanism: *coherence-regulated causal incorporation.* The horizon expands only after achieving lateral phase coherence; internal time advances only through discrete incorporation ticks; and the apparent freezing of infalling matter is the physical manifestation of finite information throughput, not a coordinate artifact. The stretched horizon is therefore a radially frozen yet laterally vibrant two-dimensional membrane on which all physics near $r_{\rm s}$ is encoded.

3.10 Relativity of Planck Scales Across Holographic Hierarchies

In a universe holographically generated from the horizon of a parent black hole, the fundamental Planck quantities remain invariant in their local definitions but become *relational* when compared across hierarchical causal frames. Each level of the hierarchy possesses its own proper time and spatial metric, yet all share the same underlying constants of nature:

$$m_{\rm p} = \sqrt{\frac{\hbar c}{G}}, \qquad \ell_{\rm p} = \sqrt{\frac{\hbar G}{c^3}}, \qquad t_{\rm p} = \frac{\ell_{\rm p}}{c}, \qquad E_{\rm p} = m_{\rm p} c^2. \tag{71}$$

These relations express the universal equilibrium between quantum uncertainty, relativistic causality, and gravitational self-energy, holding identically within every causal domain because the constants $\hbar, c$, and G are global invariants of the total causal structure.

When one spacetime emerges holographically as the interior of another, the mapping between their proper times introduces a gravitational redshift between frames, analogous to time dilation in special relativity. From the viewpoint of the parent universe, infalling matter appears to freeze near the event horizon; from the internal viewpoint, causal processes proceed normally according to the local metric. The relation between the parent coordinate time t and the internal proper time $t_{\rm int}$ satisfies

$$\frac{dt_{\rm int}}{dt} = \frac{1}{1+z_{\rm h}} \ll 1, \tag{72}$$

so that one internal Planck tick $t_{\rm p}$ corresponds to an externally measured interval

$$\Delta t_{\rm ext} = (1+z_{\rm h})\, t_{\rm p}. \tag{73}$$

This does not alter the Planck time itself but expresses a redshifted correspondence between causal frames: the same local quantum process is perceived as slower when viewed through the gravitational dilation of the parent metric.

Because the Planck energy is inversely related to the Planck time, $E_{\rm p} = \hbar/t_{\rm p}$, an external observer perceives the same causal event as carrying proportionally lower energy,

$$E_{\rm eff}^{(\rm ext)} = \frac{E_{\rm p}}{1+z_{\rm h}}. \tag{74}$$

Yet their *local* ratio,

$$\frac{E_{\rm p}}{t_{\rm p}} = \frac{c^5}{G}, \tag{75}$$

remains fixed. This invariant defines the maximum rate of causal information flow that any horizon patch can sustain in its own proper frame. All observers, regardless of position within the holographic hierarchy, agree on the numerical value of this bound, even though the *coordinate* energy and time intervals they assign to a given process are redshifted.

Thus, the apparent hierarchy of Planck scales is not a variation of constants but a manifestation of redshifted causal reference frames. Each internal universe experiences its own proper causal rhythm, while the constants $\hbar, c$, and G remain universally fixed. The causal power c^5/G serves as a frame-independent invariant *bound* on local information flux, ensuring that no horizon exceeds the fundamental bandwidth of causal updating.

Thermodynamically, this invariance guarantees that every horizon saturates the same holographic entropy bound,

$$S = \frac{A}{4\,\ell_{\rm p}^2}, \tag{76}$$

since both the Planck area $\ell_{\rm p}^2$ and the causal throughput scale c^5/G are invariant. The entropy–area relation therefore holds identically for all horizons, preserving energy conservation, unitarity, and the arrow of time across the holographic stack: redshift alters perception, not the underlying informational law.

A key implication of this hierarchy is that temporal and dynamical rates, not spatial extents, transform asymmetrically between parent and child horizons. If the internal universe evolves over a proper duration t_0 and possesses a horizon radius r_s, the parent observer measures

$$t_0^{(\text{parent})} = (1 + z_{\text{h}})\, t_0, \qquad r_s^{(\text{parent})} = r_s, \tag{77}$$

so that the apparent causal rate is suppressed by $(1 + z_{\text{h}})$:

$$\frac{r_s^{(\text{parent})}}{t_0^{(\text{parent})}} = \frac{r_s}{t_0(1 + z_{\text{h}})}. \tag{78}$$

Time dilation alone accounts for the perceived slowing of the internal universe; its geometric scale and informational capacity remain invariant. The black hole corresponding to our universe is vast in the parent cosmos, its enormous radius preserved while its internal dynamics are redshifted into near stillness.

While the *apparent* causal rate decreases by the factor $(1 + z_{\text{h}})$, the underlying bound on local causal throughput,

$$\left(\frac{E}{t}\right)_{\text{proper}} = \frac{c^5}{G}, \tag{79}$$

remains the same at every hierarchical level. Each universe therefore saturates the same fundamental causal power in its own proper frame, even though its internal processes unfold at different perceived rates when viewed from other frames. The horizon retains its full radius r_s and invariant number of Planck-area cells,

$$N = \frac{A}{\ell_{\text{p}}^2}, \tag{80}$$

so its informational capacity and physical scale are identical for both internal and external observers. The distinction between frames arises solely from temporal redshift: the internal universe evolves at its proper rhythm, while to the parent observer it appears frozen, though the underlying geometry and encoded information remain unchanged.

From the parent frame, the horizon appears dynamically frozen because each internal causal tick is redshifted by $(1 + z_{\text{h}})$, suppressing the apparent rate of evolution. From within, those same ticks constitute the full unfolding of spacetime, generating a vast and coherent cosmological domain. The enormous internal scale of our universe thus coexists consistently with the same vast external black hole that contains it, both sustained by the invariant causal throughput bound c^5/G that ties all hierarchical levels into a single, self-consistent causal structure.

This correspondence mirrors special relativity, generalized to holographic hierarchies: in the parent frame, internal processes appear time-dilated; in the internal frame, they proceed normally. Gravitational redshift here plays the role of relative velocity, governing temporal dilation across causal domains. Both perspectives describe one

invariant causal architecture whose geometry and informational content are fixed, differing only in the perceived rhythm of its updates.

Having established that causal redshift preserves all fundamental invariants, we may reinterpret temporal evolution itself as the ordered sequence of horizon code updates, the informational heartbeat of the universe. In this sense, the total informational count N replaces geometric measure as the true invariant of reality: space and time are emergent projections, while the number of encoded causal degrees of freedom remains eternally fixed.

The holographic hierarchy preserves complete physical and informational self-consistency. Each causal domain operates at its own redshifted temporal rate yet shares the same invariant constants and causal power bound c^5/G. Planck scales are not variable but *relational*, expressing the gravitationally time-dilated correspondence between nested causal frames. At any given epoch, the horizon area, and hence the number of Planck-area cells, $N = A/\ell_{\rm p}^2$, is the same geometric quantity for both the parent and internal frames; N grows with successive incorporations, but its value at a fixed horizon state is observer-independent. Mass–energy is added in discrete incorporations of $m_{\rm p}$ per $t_{\rm p}$; the only distinction between frames is how the same sequence of incorporations is time-ordered by gravitational redshift.

The universes within universes are thus locally realized phases of one self-similar causal order, an unbroken chain of holographic horizons, each saturating the same invariant information-flux bound that defines the rhythm of reality itself.

3.11 Time as the Order of Horizon Code Configurations

Time, in the horizon-layered framework, is not a pre-existing background parameter but an emergent *order parameter* associated with the sequence of global horizon code configurations. Each configuration Σ_i represents a complete, self-consistent encoding of matter, geometry, and causal relations at a given null layer of the stretched horizon. The passage of time corresponds to the discrete succession of these configurations, ordered by the causal incorporation of new layer quanta at the maximal holographic rate:

$$t_{\rm internal} \;\equiv\; \mathcal{O}(\{\Sigma_1, \Sigma_2, \Sigma_3, \dots\}), \tag{81}$$

where the ordering $\mathcal{O}$ follows the null sequence of successful incorporations permitted by the horizon's finite processing rate: one Planck-scale incorporation per internal Planck time $t_{\rm p}$.

Each infalling layer, once admitted through the causal queue, triggers a global reconfiguration of the horizon code. This update redistributes entanglement, realigns dipoles, and rewrites the causal lattice across the entire surface. The resulting holistic reorganization defines one fundamental tick of internal time. The process is locally deterministic (via gauge-invariant update rules) but appears coarse-grained and probabilistic when reconstructed as bulk physics, naturally giving rise to quantum uncertainty as informational incompleteness between discrete updates.

Externally, infalling quanta follow null trajectories of constant advanced time

$$v = t + r_*, \qquad r_* = r + r_s \ln\left|\frac{r}{r_s} - 1\right|, \tag{82}$$

so each increment in v corresponds to the arrival and successful incorporation of one additional null layer. Thus internal time is synchronized with the external advanced-time coordinate:

$$t_{\text{internal}} = N\, t_{\text{p}} \quad \longleftrightarrow \quad v = v_0 + N\, \delta v_{\text{p}}, \tag{83}$$

where N counts the number of successfully incorporated Planck-mass quanta and δv_{p} is the advanced-time increment associated with one incorporation event.

Since each incorporation adds one Planck mass,

$$N = \frac{m_{\text{bh}}}{m_{\text{p}}}, \tag{84}$$

and because

$$\frac{t_{\text{p}}}{m_{\text{p}}} = \frac{G}{c^3}, \tag{85}$$

we obtain the cumulative internal time

$$\boxed{t_{\text{internal}} = \frac{m_{\text{bh}} G}{c^3}} \tag{86}$$

in SI units. Equivalently, using the geometric mass $M_{\text{bh}} = G m_{\text{bh}}/c^2$,

$$\boxed{t_{\text{internal}} = \frac{M_{\text{bh}}}{c}}. \tag{87}$$

Cessation and resumption of internal time. When accretion halts, the horizon mass becomes constant and the sequence of code updates stops. Internal time does not "flow" in the absence of new incorporations; the last configuration Σ_N remains stable, fully coherent, and stationary. If accretion later resumes, time reactivates seamlessly: the next incoming quantum triggers the next global update Σ_{N+1}. Internal observers experience steady temporal flow because their perception is tied to the unfolding of these configurations, while the frequency of updates is causally tied to the parent universe's advanced-time sequence.

Global synchronization without lateral signaling. Although no light signal can traverse a macroscopic horizon within a single Planck time, a horizon update is not a lateral communication event. A null surface is globally defined by its mass content: when the enclosed mass increases by one Planck unit, the entire family of null generators shifts outward to the new r_{s}. The retessellation is therefore a global geometric redefinition of the null surface, not a causal transmission across it. Internal Planck ticks correspond to the redshifted proper-time intervals associated with these geometric updates; externally, the transition is a global shift of the causal boundary.

In this view, **each Planck-mass incorporation produces a global, horizon-wide causal reconfiguration**: one fundamental tick of cosmic time. This unifies gravitational growth, entropy increase, and causal continuity within a single holographic mechanism, in which the sequencing of horizon code updates $\{\Sigma_i\}$ *is* the temporal order of the universe.

4 The Holographic Membrane

In the horizon-layered cosmology, the event horizon is not a passive geometric boundary but an active, null-synchronized membrane composed of Planck-scale degrees of freedom. Infalling matter never crosses this surface in finite external time; instead, once redshifted to the Planck limit, it is assimilated through *discrete causal incorporations* of one Planck mass per Planck time. Each incorporation adds a new layer of Planck-area cells, triggers a global retessellation of the membrane, and redefines the adjacency relations of all existing cells. The horizon thus acts as a self-updating causal code whose sequential configurations encode the full dynamical content of the emergent interior spacetime.

At the microscopic level the membrane forms a nearly hexagonal adjacency graph with approximately six local neighbors per cell. This valence-6 structure provides the discrete set of tangential directions that seed the two spatial axes of the interior bulk, while the *generational index* of each newly created layer supplies the radial dimension. The global null-ordering of successive retessellations furnishes the time direction. The (3+1)-dimensional interior is therefore not pre-existing but reconstructed, tick by tick, from the horizon's two-dimensional causal architecture. Horizon cells do not move; global retessellation simply reindexes them at each incorporation, while the new cells receive the appropriate generational labels derived from the parent black hole's mass growth.

Local excitations of the membrane encode all forms of matter and energy. Stable, localized patterns of adjacency and phase structure correspond to particle species; their apparent bulk motion arises from membrane-level update rules described in later sections. Gravitational curvature corresponds to localized deficits in causal connectivity: reductions in the membrane's lateral bandwidth that force neighboring links to reconfigure. Regions of reduced connectivity project to curvature in the emergent bulk, whereas perfect causal isotropy projects to flat geometry. Thus, gravitation emerges not as a force within the bulk but as the membrane's geometric readjustment required to preserve holographic consistency.

From an informational viewpoint, each Planck-scale link encodes a binary state of causal connectivity. The membrane carries information not in trivial homogeneous states, fully connected or fully disconnected, but in the fine-grained pattern of connections and excisions. Mass–energy corresponds to localized deficits in connectivity, and the Einstein equations emerge as the coarse-grained bookkeeping of how the membrane redistributes its finite causal flux. Curvature is thus the macroscopic trace of microscopic causal reindexing.

These properties are not arbitrary. They arise inevitably from gravitational collapse. The event horizon must be a *closed* null surface: only compact surfaces saturate the Bekenstein–Hawking entropy bound and only compact surfaces can serve as maximal information boundaries. A surface with an edge cannot trap information; null rays escape, the holographic map becomes non-invertible, and the interior cannot be consistently defined. Hence the spherical (or slightly deformed ellipsoidal) topology of the parent horizon is not a choice but the unique geometric end-state of collapse.

Discrete incorporations must synchronize across the entire horizon in a single causal tick. This requirement is satisfied only for compact null surfaces, where causal relations close consistently and no information leaks through boundaries. A surface with edges would break global synchronization, disrupt lateral propagation, and compromise the dual geometric–algebraic constraints that underlie entanglement and gauge structure in the emergent bulk.

The horizon processes information at the invariant Planck-rate throughput c^5/G, distributed across all of its degrees of freedom during each global incorporation step. A compact surface is required to distribute this causal flux uniformly; open surfaces accumulate or lose flux at their boundaries, violating causal invariance. Only a closed topology supports the null-ordered retessellation needed to generate a coherent interior spacetime with Lorentzian geometry.

4.1 Membrane Dipole Encoding

The holographic membrane is a two-dimensional null surface tessellated by Planck-area cells. Each cell carries a pair of bipolar causal dipoles: a *primary* dipole aligned with the horizon normal and a *secondary* dipole lying within, or tilted relative to, the local tangential plane. These dipoles are not derived from deeper substructure; they constitute the minimal self-consistent degrees of freedom through which causal connectivity, phase constraints, lateral coherence, and quantized excision are encoded. They are neither matter nor fields nor geometry by themselves; rather, they are the primitive causal nodes from which all three emerge.

Primary dipole: encoding causal excision and rest mass. Every horizon-incorporated quantum carries a primary dipole with one *connected* face (externally causal) and one *excised* face (internally causal). Gravitational redshift freezes these quanta one Planck length outside the Schwarzschild radius, locking their excised faces inward. This inward-facing excision represents a quantized withdrawal of causal capacity, producing curvature. Spatial gradients of excision density, encoded directly in the primary dipole orientations, are interpreted as the gravitational field in the parent universe, but in the internal interpretation encode the radial coordinate or generational index, because each generation of Planck cells carries its own mass weight of primary dipole.

Secondary dipole: encoding matter, radiation, and vacuum sectors. The secondary dipole oriented randomly in reference to the primary dipole determines the internal-matter character of the quantum. Only those secondary dipoles whose orientation lies within a narrow tangential cone of half-opening angle γ relative to the local horizon plane may establish lateral causal connectivity:

$$|\beta| < \gamma, \qquad \gamma \simeq 18^\circ, \tag{88}$$

where β is the deviation from perfect tangency. Quanta satisfying this constraint can join coherent lateral networks and contribute to matter or radiation; those outside this cone behave as vacuum-like degrees of freedom.

Causal edges and dipole fractions. Each secondary dipole has two lateral "edges" that may be *connected* with probability $(1-p)$ or *disconnected* with probability p. This yields the dipole fractions

$$\begin{aligned} f_{\text{dark matter}} &= (\sin\gamma)\, p^2, \\ f_{\text{baryon}} &= (\sin\gamma)\, 2p(1-p), \\ f_{\text{massless}} &= (\sin\gamma)\, (1-p)^2, \\ f_{\text{vacuum}} &= 1 - \sin\gamma, \end{aligned} \tag{89}$$

and, with

$$\gamma = 18^\circ = 90^\circ/5, \qquad p = \frac{11}{12}, \tag{90}$$

one obtains

$$f_{\text{baryon}} \simeq 0.048, \qquad f_{\text{dark matter}} \simeq 0.262, \qquad f_{\text{vacuum}} \simeq 0.691, \qquad f_{\text{massless}} \simeq 0.002,$$

a striking match to the observed cosmic composition. Thus the relative abundance of baryons, dark matter, vacuum, and radiation arises directly from elementary dipole statistics on the membrane.

Pentagons, icosahedra, and the geometry of causal orientation. The angular tolerance γ and the $1/12$ connectivity probability both follow from the polyhedral tiling of the inward hemisphere. A dodecahedral partition divides the hemisphere into five 18° sectors, while its dual, the icosahedron, provides twelve optimal tangential directions. These twelve directions align with the twelve unavoidable pentagonal defects in any near-hexagonal tessellation of a sphere, so that the quasi-hexagonal horizon lattice, the twelve curvature-correcting pentagons, and the twelve discrete tangential orientations of dipole edges are all manifestations of the same topological constraint. The cosmic matter fractions are thus encoded in the horizon's geometric and topological necessity.

Identity codewords move through secondary-dipole propagation, not cell motion. Horizon cells themselves never move: each carries a fixed primary dipole and a fixed generational index g_{cell} inherited at incorporation. Particle motion arises because the *secondary-dipole configuration* of an identity codeword $\mathcal{C}$ propagates from one stationary cell to the next. An identity codeword is a compact, coherently oriented cluster of secondary dipoles with at least one disconnected secondary edge. Its associated field envelope $F_{\mathcal{C}}(t)$ spreads and shifts across the membrane by sequentially reassigning secondary-dipole orientations to neighboring cells whose primary labels satisfy the generational filter $g_{\text{cell}} \le g_{\text{signal}}$. The codeword's centroid follows this propagated pattern,

$$\mathcal{C}(t+1) = \text{centroid}\big[F_{\mathcal{C}}(t+1)\big], \tag{91}$$

so that particle trajectories in the emergent bulk correspond to the drift of secondary-dipole patterns on the fixed primary-dipole lattice. Lateral components follow the six

primitive hexagonal directions; radial motion is encoded by how the pattern advances across layers of increasing or decreasing generational index.

Massless excitations as propagating secondary-dipole phase patterns. Quanta with purely tangential secondary-dipole orientation and with both secondary edges connected behave as massless field modes. They have no identity core because they do not require additional bandwidth to sustain a localized disconnected secondary edge. Their secondary-dipole phase pattern propagates across eligible cells at the maximal lateral update rate along the six primitive directions, producing null trajectories under the embedding map E_t.

Vacuum quanta and decoherence. Dipoles whose secondary orientation falls outside the coherent-bandwidth regime ($|\beta| > \gamma$) cannot join lateral coherent networks. Their secondary-dipole data do not propagate, and no stable envelope forms. These quanta remain as non-propagating degrees of freedom on the fixed primary-dipole lattice, contributing to vacuum energy but unable to generate identity codewords or coherent field excitations.

Recursive universes and dipole-role inversion. When a child universe emerges from a parent black hole, the roles of dipoles invert: the primary dipole of the parent becomes the active tangential dipole of the child, while the secondary becomes its radial excision axis. This ensures causal orthogonality between generations and passes dipole statistics, including cosmic matter fractions, from parent to child.

In this unified and dynamically consistent picture,

$$\text{causal excision} \rightarrow \text{gravity}, \tag{92}$$

$$\text{lateral connectivity} \rightarrow \text{matter and radiation}, \tag{93}$$

$$\text{misaligned dipoles} \rightarrow \text{vacuum energy}, \tag{94}$$

while identity clusters move with their fields, mass is the combinatorial imprint of excision, and cosmic composition follows from the orientation statistics of Planck-scale dipoles on a quasi-hexagonal null membrane.

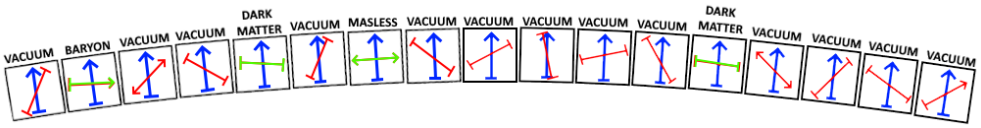

Fig. 4 Black hole holographic membrane quanta schematic representation. Each quantum possesses a primary dipole that operates in the parent universe (blue) and a secondary dipole that operates in the child universe, the holographic projection of the membrane's lateral dynamics (red and green). Only quanta with laterally oriented secondary dipoles (green) encode the internal matter/energy sector. Causally connected dipole edges are shown as arrows; disconnected edges as dashes.

Taken together, these arguments show that the closed topology of the event horizon is neither an assumption nor an aesthetic choice. It is an unavoidable consequence

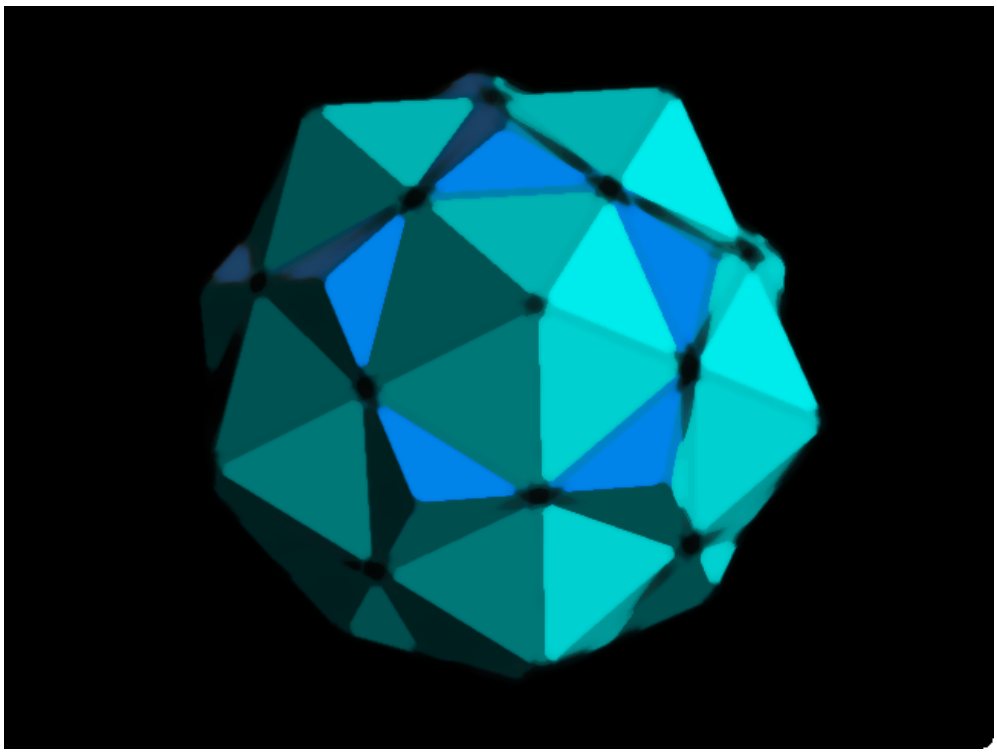

Fig. 5 Icosahedron–dodecahedron dual structure governing dipole orientation symmetries.

of gravitational collapse, finite causal bandwidth, holographic saturation, and the necessity of global synchronization. The interior spacetime emerges only because the horizon is a closed, null-synchronized, Planck-rate membrane whose discrete causal updates generate the relational structure of the bulk. A surface with edges cannot project a universe.

4.2 Hexagonal Horizon Geometry, Radial Indexing, and the Emergence of Three Spatial Dimensions

A nearly uniform hexagonal tessellation of the holographic horizon arises naturally as the configuration that maximizes the local equidistance of Planck-scale degrees of freedom distributed on a spherical surface. Hexagonal packing provides the densest and most isotropic arrangement of nearest neighbours in two dimensions, and a tension-regulated null membrane therefore relaxes toward an almost-regular hexagonal lattice. However, a perfect hexagonal tiling is incompatible with the topology of a closed sphere. Euler's theorem for polyhedral decompositions,

$$\chi = V - E + F, \qquad \text{with} \quad \chi_{\mathbb{S}^2} = 2,$$

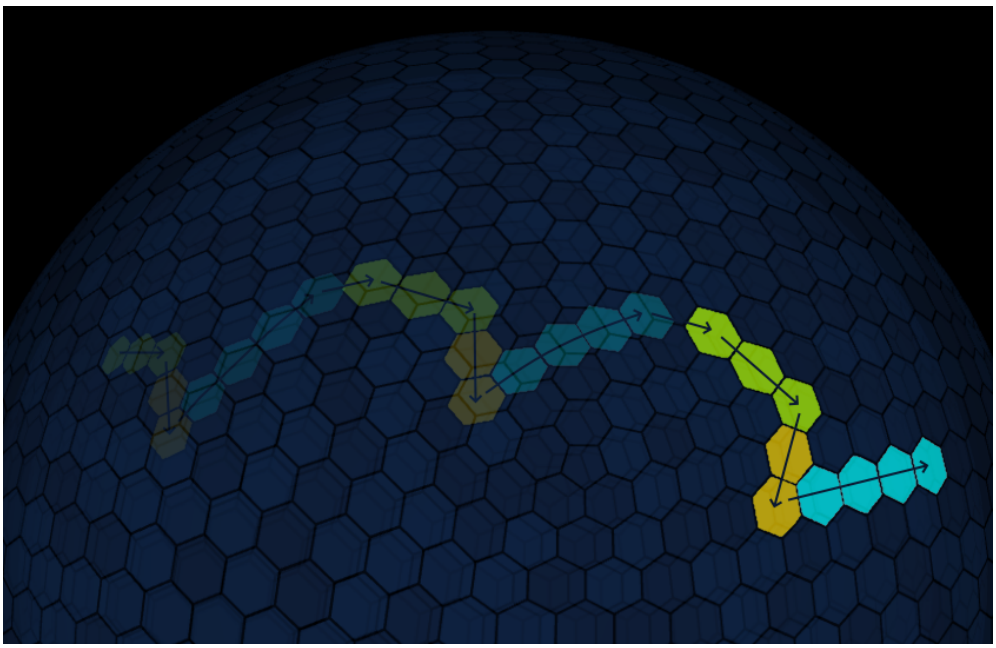

Fig. 6 Schematic representation of propagation along the event horizon. The depicted trajectory follows a fixed directional vector in the emergent three–dimensional bulk (e.g., $3x+2y+4z+1g$), while remaining confined to the two–dimensional null surface. Three successive generations of Planck–scale horizon shells are shown, each composed of quasi–hexagonal cells; together they illustrate how lateral propagation on the horizon is experienced internally as motion through emergent 3D space. Hexagonal sphere created by @arscan.

implies that any attempt to wrap a hexagonal lattice over a spherical surface must introduce discrete curvature sources. Hexagons possess internal angles of 120°, so three meeting at a vertex sum to 360°, corresponding to zero Gaussian curvature; a sphere, by contrast, requires positive curvature at every point. The only polygons that can supply the needed angular deficit are pentagons, whose internal angles (108°) fall short of the hexagonal 120° and thus insert localized positive curvature. Applying Euler's theorem to a tiling composed primarily of hexagons with a small number of pentagons yields the universal result that *exactly twelve pentagonal defects* are required to close the lattice on a sphere. Consequently, a Planck-thick holographic horizon, formed at the equilibrium point where the external curvature pressure of the manifold is balanced by the membrane's effective tension, organizes itself into an almost-uniform quasi-hexagonal tessellation containing the twelve topologically required pentagonal curvature defects. These defects act as distinguished points in the null-synchronized causal code, anchoring large-scale anisotropies and supplying a discrete geometric scaffold for the emergent internal spacetime.

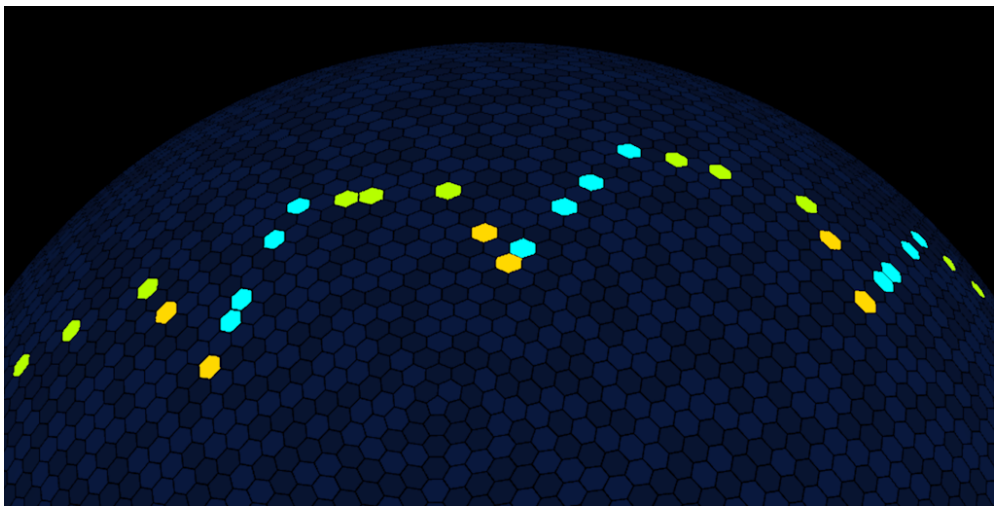

Fig. 7 Schematic representation of how propagation on a hexagonally tessellated horizon is actually realized. A signal following an effective bulk direction (e.g. $3x + 2y + 4z + 1g$) moves only between neighboring Planck cells, and each hop is constrained by the local generational rule: transitions into cells with $g_{\rm cell} \leq g_{\rm signal}$ are allowed, while neighbors with $g_{\rm cell} > g_{\rm signal}$ are forbidden. Propagation is therefore implemented as a strictly local adjacency filter that preserves radial generational ordering without any nonlocal search. Hexagonal sphere created by @arscan.

Each cell therefore has six tangential neighbors, forming a six-valent causal lattice. These six neighbors group naturally into three opposite pairs

$$(\hat{e}_{+x}, \hat{e}_{-x}), \qquad (\hat{e}_{+y}, \hat{e}_{-y}), \qquad (\hat{e}_{+z}, \hat{e}_{-z}),$$

which define three independent tangential axes. These axes encode the two angular dimensions of the horizon, but because the valence is 6, they furnish at most three independent propagation directions. **The (x, y, z) structure of the emergent bulk arises from these tangential axes, but they alone do not supply the radial dimension.**

The radial dimension arises from the generational index g encoded in the primary dipole mass weight. Each incorporation of one Planck mass $m_{\rm p}$ increases the parent black hole mass from $m_{\rm bh}$ to $m_{\rm bh} + m_{\rm p}$ and creates a new generation of horizon cells. The Schwarzschild radius satisfies

$$r_{\rm s} = \frac{2Gm_{\rm bh}}{c^2}, \tag{95}$$

so the horizon area is

$$A = 4\pi r_{\rm s}^2, \tag{96}$$

and its increment per incorporation step is

$$\Delta A = A(m_{\rm bh} + m_{\rm p}) - A(m_{\rm bh}) \simeq 8\pi r_{\rm s}\, \Delta r_{\rm s}, \tag{97}$$

which, in Planck units, yields a number of new cells

$$\Delta N_{\rm cell} = \frac{\Delta A}{\ell_{\rm p}^2} \simeq 32\pi\, \frac{m_{\rm bh}}{m_{\rm p}}. \tag{98}$$

Because each step adds the same mass $\Delta m = m_{\rm p}$, the effective mass-per-cell associated with that generation is

$$\mu_g \equiv \frac{\Delta m}{\Delta N_{\rm cell}} \simeq \frac{m_{\rm p}^2}{32\pi\, m_{\rm bh}(g)}, \tag{99}$$

which decreases monotonically as the black hole mass (and thus g) grows. **This mass-per-cell is *inscribed* in the primary dipole: its excision weight encodes μ_g and thereby fixes the cell's generational label $g_{\rm cell}$. In this sense, each horizon cell "knows" its radial index from the parent-universe mass distribution.** The secondary dipole, by contrast, determines the internal matter sector of the child universe (baryonic, dark, massless, vacuum-like) and encodes the masses of internal particles, but does not alter the parent-side mass-per-cell bookkeeping. The discrete label $g_{\rm cell}$ defined by the primary dipole mass weight is therefore the holographic proxy for interior radius.

When a field excitation or identity cluster is created, it inherits a definite generational index

$$g_{\rm signal} = g_{\rm inc}, \tag{100}$$

representing its initial radial position in the emergent interior.

Generational filtering as the local radial rule. A propagating excitation may occupy only horizon cells whose generational index does not exceed its own:

$$\boxed{g_{\rm cell} \le g_{\rm signal} \quad \text{(allowed)}, \qquad g_{\rm cell} > g_{\rm signal} \quad \text{(forbidden)}.} \tag{101}$$

At each null-step the signal checks only its local neighbors. If the chosen neighbor has $g_{\rm cell} > g_{\rm signal}$, the move is disallowed and another direction is chosen. Propagation is thus a local adjacency filter, never a nonlocal search.

Retessellation introduces an interwoven mixture of generations in every patch, so excitations always have accessible neighbors with $g_{\rm cell} \le g_{\rm signal}$. Propagation therefore remains strictly local and causal.

Null-step sequences and tangential drift. A signal or identity cluster propagates laterally via sequences

$$W = \hat{e}_{i_1}\hat{e}_{i_2}\cdots\hat{e}_{i_N}. \tag{102}$$

The coarse-grained displacement along the tangential axes is

$$(\Delta_x, \Delta_y, \Delta_z) = (N_{+x} - N_{-x},\, N_{+y} - N_{-y},\, N_{+z} - N_{-z}), \tag{103}$$

which determines the angular component of the bulk trajectory. Many distinct null sequences share the same $(\Delta_x, \Delta_y, \Delta_z)$, and their interference defines the wave-like structure of lateral motion.

Radial updating without expansion. True radial motion, arising from four-momentum or interactions, would allow

$$g_{\text{signal}}(t+1) = g_{\text{signal}}(t) + \delta g, \qquad \delta g \in \{-1, 0, +1\}. \tag{104}$$

This represents genuine physical motion through interior shells.

Generational renormalization of signals under expansion. The horizon radius increases by a fixed amount each tick,

$$r_{\text{s}}(t+1) = r_{\text{s}}(t) + 2\ell_{\text{p}}, \tag{105}$$

but horizon cells retain their original g_{cell}, and with them their primary-dipole mass weights. Cosmic expansion must however be isotropic throughout the interior: comoving objects must drift apart even without true radial motion. To maintain this isotropy and preserve the holographic matching between area and interior volume, the radial labels of *signals* must undergo a global fractional rescaling.

We therefore define the expansion factor

$$\lambda(t) \equiv 1 + \frac{2\ell_{\text{p}}}{r_{\text{s}}(t)}, \tag{106}$$

and introduce the update rule

$$\boxed{g_{\text{signal}}(t+1) = \lambda(t)\, g_{\text{signal}}(t) + \delta g.} \tag{107}$$

Here δg accounts for genuine radial motion, while the multiplicative factor $\lambda(t)$ encodes pure expansion. Only internal excitations are renormalized; horizon cells keep their fixed generational indices and mass-per-cell labels. Thus comoving particles drift outward in the bulk while no membrane cell moves.

Bulk direction from combined tangential and radial data. The full effective 3D direction of motion is reconstructed from the quadruple

$$(\Delta_x, \Delta_y, \Delta_z, \dot{g}), \tag{108}$$

where $\dot{g}$ includes both the global expansion term and any dynamical δg from interactions. Under the embedding map E_t, this quadruple is interpreted as a smooth timelike or null geodesic in the emergent interior.

Measure matching: boundary channels versus interior Planck volumes. The constraint $g_{\text{cell}} \leq g_{\text{signal}}$ ensures that the accessible set of horizon cells has cardinality

$$N_{\text{cell}}(\leq g_{\text{signal}}) \simeq \frac{4\pi r_{\text{s}}(g_{\text{signal}})^2}{\ell_{\text{p}}^2}, \tag{109}$$

approximately equal to the number of Planck volumes in the bulk shell of thickness ℓ_{p} at radius $r_{\mathrm{s}}(g_{\mathrm{signal}})$, up to order-unity factors from curvature. Because the expansion factor rescales g_{signal} but not the g_{cell}, shell matching remains consistent: the interior expands while the boundary structure remains a fixed historical record of incorporation events inscribed in the primary dipole mass weights.

In the horizon-layered cosmology, the generational index g is not a geometric Schwarzschild radial distance but a null-ordered causal label recording the sequence of Planck-mass incorporation events. Each incorporation adds a new horizon layer of external thickness $2\ell_{\mathrm{p}}$, and each layer receives a distinct primary-dipole mass weight μ_g, so every Planck cell "remembers" its epoch of creation through its excision weight. When the bulk interior is reconstructed through the embedding map E_t, this causal index becomes the internal radial coordinate: successive values of g map to successive FRW radial shells, continuously spanning the full interval from $r = 0$ to the parent horizon $r = r_{\mathrm{s}}$.

However, the mapping from horizon layering to internal radius is not geometric but informational. Externally, the Schwarzschild radius grows in strictly uniform steps of $2\ell_{\mathrm{p}}$, but internally the radial increment associated with a generational step is

$$\Delta r_{\mathrm{bulk}} = a(t)\,\Delta\chi(g), \tag{110}$$

where $\Delta\chi(g)$ is controlled by the information capacity of the corresponding horizon layer. Because a layer of area $A_g = 4\pi r_{\mathrm{s}}(g)^2$ contains $N_g = A_g/\ell_{\mathrm{p}}^2$ cells, its intrinsic radial resolution scales as

$$\Delta\chi(g) \sim N_g^{-1} \sim \frac{\ell_{\mathrm{p}}^2}{4\pi r_{\mathrm{s}}(g)^2}. \tag{111}$$

Thus, although every external layer has the same physical thickness $2\ell_{\mathrm{p}}$, the *internal* radial thickness of a layer depends on the holographic scaling $\Delta\chi(g)$, which shrinks rapidly for later (larger-area) generations.

This difference is precisely what keeps the interior smooth and isotropic: radial distance is reconstructed from information geometry, not from external Schwarzschild geometry. Two successive external layers do not correspond to equal bulk radial increments; early layers have large $\Delta\chi(g)$, while late layers have extremely fine $\Delta\chi(g)$. As a result, the interior obtains the full radius r_{s}, not half the radius $r_{\mathrm{s}}/2$, even though the exterior layering is built from equal increments $2\ell_{\mathrm{p}}$.

The expansion factor $a(t)$ rescales the signal index g_{signal} but leaves the historically fixed cell indices g_{cell} unchanged, so radial ordering remains consistent even as the interior stretches. In this way, the entire bulk radial dimension is a holographic reconstruction of the layered causal history of the horizon: every value of g corresponds uniquely to a bulk radius, and the smooth FRW radial direction emerges from the generational structure of the null boundary.

Early generations and central behavior. In the deep interior, few Planck volumes exist per shell and only early generations contribute. Retessellation maintains

connectivity even in this sparse regime. The same rules apply: an excitation accesses exactly the cells that encode the volume of its radial shell and propagates without nonlocal jumps.

With these ingredients, the 2D→3D emergence becomes exact and dynamically consistent. Hexagonal adjacency provides three tangential directions; the primary dipole mass weight fixes the generational index of each cell and thereby the radial coordinate; generational filtering enforces the boundary–bulk mapping; and a global renormalization of *signals* under expansion produces the comoving drift of the internal universe. The horizon remains the stationary causal substrate; the interior is the continually reinterpreted projection of its null-step dynamics and expansion-renormalized radial indexing.

4.3 Hubble Expansion, Scale Factor Dynamics, and FLRW Correspondence

The holographic membrane grows through the incorporation of one Planck mass per Planck time, increasing the Schwarzschild radius by

$$r_{\mathrm{s}}(t+t_{\mathrm{p}}) = r_{\mathrm{s}}(t) + 2\ell_{\mathrm{p}}. \tag{112}$$

To maintain isotropic expansion in the emergent bulk, the radial index of every internal excitation must be rescaled by the same fractional increase:

$$g_{\mathrm{signal}}(t+t_{\mathrm{p}}) = g_{\mathrm{signal}}(t)\left(1+\frac{2\ell_{\mathrm{p}}}{r_{\mathrm{s}}(t)}\right) + \delta g, \tag{113}$$

where δg represents genuine dynamical radial motion. Neglecting δg isolates the pure expansion dynamics. Since $r = g\,\ell_{\mathrm{p}}$ to leading order, the induced radial update is

$$r(t+t_{\mathrm{p}}) = r(t)\left(1+\frac{2\ell_{\mathrm{p}}}{r_{\mathrm{s}}(t)}\right). \tag{114}$$

Define the expansion factor

$$\lambda(t) = \frac{r(t+t_{\mathrm{p}})}{r(t)} = 1 + \frac{2\ell_{\mathrm{p}}}{r_{\mathrm{s}}(t)}. \tag{115}$$

Promoting the discrete update to a differential relation yields

$$\frac{\dot r}{r} = \frac{\lambda(t)-1}{t_{\mathrm{p}}} = \frac{1}{t_{\mathrm{p}}}\frac{2\ell_{\mathrm{p}}}{r_{\mathrm{s}}(t)}. \tag{116}$$

Thus the effective Hubble parameter becomes

$$\boxed{H(t) = \frac{\dot r}{r} = \frac{2}{r_{\mathrm{s}}(t)}\,\frac{\ell_{\mathrm{p}}}{t_{\mathrm{p}}} = \frac{2c}{r_{\mathrm{s}}(t)}.} \tag{117}$$

Because all internal comoving distances scale proportionally to $r(t)$, the scale factor of the emergent FLRW universe satisfies

$$\frac{\dot{a}}{a} = H(t) = \frac{2c}{r_{\rm s}(t)}. \tag{118}$$

Using $r_{\rm s}(t) = 2Gm(t)/c^2$, with

$$m(t) = m_0 + \frac{m_{\rm p}}{t_{\rm p}} t \tag{119}$$

the monotonically increasing horizon mass, gives

$$H(t) = \frac{c^3}{G\, m(t)}. \tag{120}$$

Integrating,

$$a(t) = a_0 \exp\!\left(\int^t \frac{c^3}{G\, m(t')}\, dt' \right). \tag{121}$$

When $m(t)$ increases linearly,

$$a(t) = a_0 \left(m_0 + \frac{m_{\rm p}}{t_{\rm p}} t \right), \tag{122}$$

since the exponent equals unity by the Planck relations. Thus the emergent bulk expands with a scale factor proportional to the horizon mass, which itself grows through the continuous, discrete incorporation of Planck-sized quanta.

Proper distances obey

$$d_{\rm phys}(t) = a(t)\, d_{\rm com}, \qquad H(t) = \frac{\dot{a}}{a} = \frac{c^3}{G\, m(t)}. \tag{123}$$

This reproduces the defining feature of FLRW cosmology: comoving points recede at a rate proportional to their separation. In this framework, the FLRW expansion emerges directly from the null-ordered holographic kinematics of the horizon, without invoking any bulk field equations.

The effective energy density is

$$\rho(t) = \frac{m(t)}{\frac{4\pi}{3} r_{\rm s}(t)^3} = \frac{3c^6}{32\pi G^3 m(t)^2}, \tag{124}$$

hence

$$\rho(t) \propto a(t)^{-2}. \tag{125}$$

This differs from the standard dust law ($\propto a^{-3}$) because the interior volume scales as $r_{\rm s}^3$ while the incorporated mass grows linearly. The bulk therefore behaves as a diluting effective matter fluid whose scaling is set by holographic kinematics.

From the Friedmann equation,

$$H^2 = \frac{8\pi G}{3}\rho - \frac{k}{a^2}, \tag{126}$$

substitution yields

$$H^2 = \frac{8\pi G}{3}\rho, \qquad \Rightarrow \qquad k = 0. \tag{127}$$

The emergent universe is thus spatially flat, a direct consequence of the area–volume relation inherent in the holographic construction.

Isotropy and the physical meaning of the generational index. Although each incorporation step increases the Schwarzschild radius by the discrete amount $\Delta r_{\rm s} = 2\ell_{\rm p}$, this does *not* discretize or anisotropize distances inside the emergent three-dimensional bulk. The generational index is not a physical radial thickness but a causal-ordering label for successive null layers. Because each layer forms a uniform spherical shell, generational depth defines an isotropic radial coordinate in the reconstructed FRW interior. Bulk distances are determined by the internal scale factor $a(t)$, not by the exterior Schwarzschild increments, and therefore all objects have the same proper length in all directions. A propagating excitation "knows" its radial location by its generational index rather than geometric distance, and the emergent bulk remains locally Minkowskian and isotropic despite the Planck-thick, radially frozen encoding surface.

Causal depth and the observable Hubble radius. The null-ordered generational hierarchy spans the range $0 \le g \le g_{\max} = r_{\rm s}/\ell_{\rm p}$. However, FRW conformal time grows sublinearly with generational depth, so only the earliest $\sim 50\%$ of the layered structure lies within our past light cone. Consequently the observable Hubble radius corresponds to

$$r_{\rm h} \approx \frac{1}{2}\, r_{\rm s}, \tag{128}$$

while the emergent universe extends smoothly to $R_{\max} = r_{\rm s}$. This matches the empirical fact that the observable Hubble domain contains roughly half of the total internal mass; the remainder is simply a later portion of the null layering whose signals have not yet reached us.

Unified picture. Continuous Planck-scale incorporation increases $r_{\rm s}$ by $2\ell_{\rm p}$ each tick; isotropy requires a global rescaling of radial indices, producing $a(t) \propto m(t)$ and $H(t) = c^3/(Gm(t))$. **The emergent interior is therefore a spatially flat, expanding FLRW universe whose scale factor, density evolution, causal depth, and observable limits arise entirely from the null-ordered growth of the holographic horizon.**

4.4 Generational Mass Index, Horizon Discreteness, and the Emergence of a Smooth FRW Interior

A central structural insight of the horizon-layered cosmology is that the radial dimension of the emergent bulk does not pre-exist the horizon but is *created* by it. Each

Planck-scale incorporation event increases the Schwarzschild radius by a fixed amount

$$\Delta r_{\rm s} = \frac{2Gm_{\rm p}}{c^2} = 2\ell_{\rm p}, \tag{129}$$

so the external geometry grows through a strictly uniform sequence of radial increments. The associated horizon area increase

$$\Delta A = 8\pi r_{\rm s}\,\Delta r_{\rm s} = 16\pi r_{\rm s}\,\ell_{\rm p}, \tag{130}$$

creates

$$\Delta N_{\rm cell} = \frac{\Delta A}{\ell_{\rm p}^2} = \frac{16\pi r_{\rm s}}{\ell_{\rm p}} \tag{131}$$

new Planck-area cells, each endowed with an inward-facing *primary dipole*. Because the incorporated mass $\Delta m = m_{\rm p}$ is fixed, each generation has an effective mass-per-cell

$$\mu_g = \frac{m_{\rm p}}{\Delta N_{\rm cell}} = \frac{m_{\rm p}^2}{16\pi m_{\rm bh}(g)}, \tag{132}$$

which decreases monotonically as the black hole mass grows. This μ_g value is permanently inscribed in the primary dipole and becomes the cell's *generational label* $g_{\rm cell}$.

Because propagation rules enforce

$$g_{\rm cell} \le g_{\rm signal},$$

each bulk excitation inherits a radial coordinate determined by the deepest generation it can access. Thus the internal radial direction is *informational*: a cumulative index of decreasing mass-per-cell, not the geometric Schwarzschild radius itself.

Information-weighted internal radial increments. Although external layers have uniform thickness $2\ell_{\rm p}$, internal radial increments cannot be uniform. The correct bulk increment must reflect the *information capacity* of each new layer. If a layer of radius $r_{\rm s}(g)$ contains

$$N_{\rm cell}(g) = \frac{4\pi r_{\rm s}(g)^2}{\ell_{\rm p}^2},$$

then the intrinsic radial resolution contributed by that layer is

$$\Delta\chi(g) = \frac{1}{N_{\rm cell}(g)} = \frac{\ell_{\rm p}^2}{4\pi r_{\rm s}(g)^2}, \tag{133}$$

up to normalization absorbed into $a(t)$. Early generations (small $r_{\rm s}$) thus contribute large increments to χ, while late generations contribute extremely fine increments.

The emergent bulk radial element is

$$\Delta r_{\rm bulk}(g) = a(t)\,\Delta\chi(g) = a(t)\frac{\ell_{\rm p}^2}{4\pi r_{\rm s}(g)^2}, \tag{134}$$

so the interior radial coordinate becomes

$$r_{\text{bulk}}(g) = a(t) \sum_{g'=0}^{g} \Delta\chi(g'). \tag{135}$$

Since $r_{\text{s}}(g) = 2\ell_{\text{p}} g$, the sum approaches

$$r_{\text{bulk}} \simeq a(t) \int^{g_{\max}} \frac{dg'}{16\pi g'^2} = \frac{a(t)}{16\pi} \left(1 - \frac{1}{g_{\max}}\right), \tag{136}$$

so (up to normalization)

$$r_{\text{bulk}} \propto a(t).$$

The internal radius depends only on the scale factor, not on the raw Schwarzschild increments. This is exactly the FRW radial geometry.

Why the interior is smooth and isotropic. Although horizon layers are discrete, their internal images are not. Because

$$\Delta r_{\text{bulk}}(g) \propto \frac{1}{r_{\text{s}}(g)^2},$$

late generations supply arbitrarily fine increments, yielding a *continuous* radial coordinate, while the uniform scaling by $a(t)$ ensures *isotropy*. The embedding map E_t reconstructs interior displacements by mapping horizon steps $(\Delta_x, \Delta_y, \Delta_z, \Delta g)$ to bulk steps via the FRW metric

$$g_{rr} = a(t)^2, \quad g_{\theta\theta} = a(t)^2 r^2, \quad g_{\phi\phi} = a(t)^2 r^2 \sin^2\theta.$$

Tangential directions come from six-valent hexagonal adjacency; the radial direction comes from decreasing μ_g; yet E_t scales them uniformly by $a(t)$, making them geometrically indistinguishable. No internal experiment can detect the discrete layering of the horizon.

Discrete horizon, continuous bulk. Only the horizon is fundamentally discrete: it is tiled by ℓ_{p}^2 cells carrying primary and secondary dipoles. The bulk fields correspond to coarse-grained null-walk superpositions over enormous numbers of cells; no bulk mode has support on a single horizon element. Consequently, the internal spacetime exhibits no lattice effects or graininess. General relativity's smooth geometry emerges automatically from the many-cell limit of horizon null propagation.

Planck scales still appear in bulk physics, but only indirectly: the Planck time sets the retessellation rate; Planck area sets the maximum causal throughput c^5/G; and $\hbar$ and G emerge as renormalized parameters encoding the update algebra of secondary dipole phases.

Origin of the uncertainty principle. The Heisenberg uncertainty relation

$$\Delta x \, \Delta p \geq \frac{\hbar}{2}$$

does *not* arise from any Planck-scale graininess of the bulk. Instead, it emerges from the algebra of the secondary-dipole phase field. Each dipole carries a phase ϕ and conjugate occupation number n obeying

$$[\phi, n] = i.$$

Under the embedding map E_t, ϕ becomes the bulk wavefunction phase and n becomes the generator of spatial translations, yielding

$$[x, p] = i\hbar.$$

Thus uncertainty is *algebraic*, not geometric: it reflects the intrinsic non-commutativity of the horizon's phase-update rules, not the discreteness of spacetime.

Interpretation of the embedding map. The embedding map E_t is not an additional dynamical structure living on the horizon; it is the unique information-theoretic reconstruction that internal observers must adopt to describe membrane dynamics as a smooth, local, isotropic spacetime. Individual cells carry no geometric data; geometry arises only when many null interactions are coarse-grained into a continuum-limit correlation structure. E_t is therefore the emergent rule that turns an underlying discrete null surface into a differentiable four-dimensional spacetime obeying FRW symmetry.

Conclusion. The generational mass index g is the holographic origin of the radial dimension: decreasing μ_g defines the interior's causal depth, while the information-weighted increments $\Delta\chi(g)$ convert discrete horizon layers into a continuous radial coordinate. Through the embedding map, the horizon's Planck-scale discreteness gives rise to a perfectly smooth, homogeneous, isotropic FRW universe. The internal geometry is therefore not assumed, it is emergent, arising inevitably from the causal stacking of horizon layers.

4.5 Quantum Tunnelling and Causal Information Exchange

The evolution of the holographic code unfolds through discrete, null-synchronized updates of the horizon membrane. Each incorporation of one Planck mass adds a new generational layer of Planck-area cells, defining a single "Planck tick" during which the membrane globally retessellates, reindexes all adjacency relations, and updates the causal structure of the emergent interior. From the external frame, this process appears as the steady outward growth of the event horizon; from the internal frame, it appears as the expansion of cosmic space. The dynamics of quantum tunnelling, causal synchronization, and wavefunction collapse arise naturally from these discrete causal updates.

The membrane itself is a stationary quasi-hexagonal lattice. Cells do not move across the surface; instead, their *relations* are continually redefined by the global incorporation of new generations of cells. Each new generational layer adds one unit to the radial index g, thereby shifting the embedding map E_t used to reconstruct the interior bulk. Cosmic expansion is thus relational rather than kinetic: galaxies drift apart not

by moving through space but because the radial indexing of stable identity clusters is repeatedly updated as new horizon layers are added.

During each Planck tick, the retessellation modifies adjacency in two complementary ways. Radially, new cells increase the maximum admissible generational depth for signals and identity clusters, producing the geometric growth of the interior. Laterally, each cell updates its tangential neighbors within the six primitive hexagonal directions, maintaining phase continuity and propagating field amplitudes from one tick to the next. This tangential exchange is the origin of all field propagation, radiation, and quantum tunnelling within the emergent interior.

In this framework, lateral propagation concerns both the propagation of fields and the motion of identity codewords themselves. Field amplitudes advance along the six null tangential directions every Planck tick, carrying with them the centroid of any associated identity cluster. Identity codewords therefore *do* move across the membrane, but with sub-null drift: part of their causal bandwidth is devoted to maintaining the internal dipole structure that encodes rest mass and intrinsic quantum numbers. Massless excitations devote their entire bandwidth to lateral propagation and therefore advance at exactly the null rate; massive excitations divide their bandwidth between internal organization and external propagation, yielding subluminal motion in the emergent bulk.

In this framework, gravitational attraction does not originate from the primary dipoles themselves; they encode only the static generational structure of the horizon. Instead, gravity is sourced by secondary dipoles, whose local alignment patterns adjust in response to variations in mass–energy encoded on the horizon. A concentration of encoded mass corresponds to a local reduction in lateral causal capacity across the secondary-dipole network: tangential bandwidth decreases, phase-matching becomes more constrained, and null propagation is slightly redirected. Bulk fields, being holographic projections of these secondary-dipole dynamics, experience this bandwidth gradient as spacetime curvature. Test particles therefore "fall" toward regions where secondary-dipole alignment reduces tangential connectivity, reproducing the effective gravitational attraction of general relativity without invoking any influence from the primary dipole structure. Thus large-scale cosmic structure emerges from the interplay between outward radial retessellation and inward gradients of available lateral propagation.

The two fundamental operations of the membrane are therefore synchronized: radial incorporation, which extends the causal manifold one generational layer at a time, and lateral phase exchange, which propagates fields along the six hexagonal directions at the null update rate. These two processes together define the universal speed of light,

$$c = \frac{\ell_{\mathrm{p}}}{t_{\mathrm{p}}}, \tag{137}$$

as the invariant rate of tangential phase propagation on the membrane. The constancy of c is nothing more than the fixed causal bandwidth of the lateral update process.

This unified mechanism explains both cosmological redshift and light propagation. A photon's internal wavelength stretches because the embedding map E_t

changes as the horizon grows through successive ticks, while its local phase propagation remains locked to the invariant tangential null-step rate. Thus cosmic expansion and the universality of the speed of light are two aspects of the same discrete causal structure.

This causal–informational description resembles discrete frameworks such as causal sets or quantum cellular automata, but with a crucial difference: here the fundamental "automaton" is a null-synchronized, hexagonally tessellated membrane whose global retessellation simultaneously encodes gravitational dynamics, quantum tunnelling, and cosmic expansion. Reality emerges from a stationary but continually reindexed holographic code whose radial layering and lateral phase coherence jointly generate motion, radiation, and the continuity of spacetime.

4.6 The Multiplex Causal Structure of Planck-Scale Horizon Cells

The holographic horizon cannot be composed of simple binary units. Because every cell on the stretched horizon participates in encoding the full three-dimensional interior, each Planck-area element must support *multiple generational layers of information simultaneously.* This requirement follows directly from the causal rules governing propagation on the membrane.

A signal with radial generational depth g_{signal} may occupy any horizon cell whose index satisfies $g_{\text{cell}} \leq g_{\text{signal}}$. Since a single cell must serve excitations from many deeper layers ($g_{\text{signal}} \gg g_{\text{cell}}$), it cannot represent only the information of its own layer. Instead, each cell must act as a *multiplex node*, hosting a compressed representation of numerous internal radial states. This property is essential for reproducing a smooth FRW bulk and for allowing signals to propagate continuously in the emergent three-dimensional geometry.

Local Hilbert structure. Each Planck cell therefore carries a multi-component state rather than a single degree of freedom. Its internal Hilbert space factorizes schematically as

$$\mathcal{H}_{\text{cell}} = \mathcal{H}_{\text{primary}} \otimes \mathcal{H}_{\text{secondary}} \otimes \mathcal{H}_{\text{phase}},$$

where:

- $\mathcal{H}_{\text{primary}}$ encodes the primary dipole defining the cell's generational orientation and its role in the 2D–3D projection,
- $\mathcal{H}_{\text{secondary}}$ stores the local curvature, matter-field, and gauge-sector information that influences bandwidth and bulk fields,
- $\mathcal{H}_{\text{phase}}$ maintains lateral null coherence across the membrane and governs signal routing on the horizon graph.

This structure ensures that a single Planck cell can support, route, and phase-lock many distinct excitations of different generational depths at once. The cell is therefore not a pointlike element of geometry but a compact *causal operator patch.*

Generational multiplexing. Propagation in the interior bulk corresponds to null-directed hopping on the horizon lattice. A signal's radial depth is encoded by its

generational index g_{signal}, which evolves under expansion through

$$g_{\mathrm{signal}}(t+\Delta t) = \lambda(t)\, g_{\mathrm{signal}}(t) + \delta g, \qquad \lambda(t) = 1 + \frac{2\ell_{\mathrm{p}}}{r_{\mathrm{s}}(t)}.$$

Since g_{cell} labels the layer of the cell and not the geometric thickness of the shell, two adjacent shells share the same index ($2\ell_{\mathrm{p}}$ thick), yet the signal still resolves them individually. Bulk propagation therefore tracks the full radial sequence $1 \to 2 \to 3 \to 4 \to 5 \ldots$ even though the horizon increments g_{cell} in steps of two. This is possible only because each cell encodes the compressed structure of all deeper layers it serves.

Isotropy and recovery of continuous radial geometry. The generational index is a *causal-ordering label*, not a physical radial thickness. Every horizon layer is a uniform spherical shell, so generational depth defines an isotropic radial coordinate in the emergent FRW interior. Bulk distances are determined by the internal scale factor, not by the discrete increments $r_{\mathrm{s}} \to r_{\mathrm{s}} + 2\ell_{\mathrm{p}}$. Thus an excitation has the same proper length in all directions, and the emergent bulk remains locally Minkowskian despite the Planck-thick, radially frozen encoding surface.

Functional role of the Planck cell. Each horizon cell therefore functions simultaneously as:

- a *routing node* for excitations of different generational depths,
- a *projection operator* mapping 2D horizon structure to 3D bulk coordinates,
- a *coherence element* ensuring null-synchronized lateral dynamics,
- a *curvature carrier* encoding local bandwidth gradients.

Its internal structure must therefore possess multiple coupled degrees of freedom, allowing the cell to behave less like a classical pixel and more like a small quantum circuit element embedded in a null surface.

Consequence for the emergent universe. This multiplex causal structure is what makes it possible for a two-dimensional Planck-thick null membrane to generate a smooth, isotropic, expanding three-dimensional FRW interior. The generational hierarchy supplies the radial coordinate, the phase network supplies lateral causal connectivity, and the multiplex Planck cells unify both into a coherent holographic code encoding the entire internal cosmological spacetime.

4.7 Identity Cores, Entanglement, and Emergent Locality on a Moving Horizon

In the horizon-layered cosmology, particles do not preexist as fixed codewords on the membrane but arise dynamically as *self-assembled identity cores* within localized peaks of lateral field intensity. A propagating excitation whose horizon fields become sufficiently coherent and concentrated nucleates an *identity seed*: a stable configuration of secondary dipoles, adjacency rules, and internal phase relations. Once formed, this configuration persists as an identity cluster $\mathcal{C}$ until disrupted by interactions, encoding

intrinsic quantum numbers, spin, charge, and statistics without relying on a rigid geometric location.

The identity cluster is not stationary. Its motion is governed by *centroid locking* to the propagating field envelope $F_{\mathcal{C}}(t)$ from which it formed. At each Planck-time update, the cluster relocates to the centroid of its own horizon field,

$$\mathcal{C}(t+1) = \text{centroid}\big[F_{\mathcal{C}}(t+1)\big], \tag{138}$$

so identity follows field, not the reverse. At each tick, the associated signal propagates along the six primitive tangential directions of the quasi-hexagonal lattice (the angular axes $\hat{e}_{\pm x}, \hat{e}_{\pm y}, \hat{e}_{\pm z}$ on the horizon) while carrying its generational index g, which encodes its radial placement in the emergent bulk. Massless excitations exploit the full null update bandwidth for coherent propagation in this combined (tangential, g) space, so their images under the embedding map E_t trace null geodesics in the 3D interior. Massive excitations must dedicate part of this bandwidth to sustaining the internal dipole structure of $\mathcal{C}$, leading to sub-null drift of the identity centroid in the embedded bulk and thus timelike trajectories.

Although field envelopes may spread broadly across the membrane, local peaks of intensity keep the identity cluster compact. The bulk position of a particle is the image, under the embedding map E_t, of this drifting centroid. Bound systems arise when several identity clusters mutually stabilize their field envelopes so that their centroids co-move; photons correspond to pure field propagation without an associated identity core. Identity seeds form locally whenever coherent field overlap exceeds a stability threshold (for example, in high-energy collisions). The generational index g_{inc} of the horizon layer at which the seed forms fixes its initial radial coordinate in the emergent bulk,

$$r_{\text{init}} = r_{\text{horizon}}(g_{\text{inc}}), \tag{139}$$

and subsequent bulk motion arises from lateral and generational drift of the fields and their identity cores on the membrane.

Geometric adjacency vs. algebraic constraint. Quantum measurement, wavefunction collapse, and entanglement emerge from the interaction between two complementary relational structures on the horizon:

1. *Geometric relations* , the fixed-valence adjacency graph of Planck cells that governs null-step causal propagation.
2. *Algebraic relations* , dipole-phase constraints, SU(2)/U(1) labels, correlation rules, and exclusion conditions among secondary-dipole patterns that define the global entanglement structure.

Geometric relations define the lateral causal cone: during any single Planck tick, information stored in secondary-dipole patterns can propagate only to adjacent cells. Projected through E_t, this finite-valence network becomes the light-cone structure of the emergent interior. Algebraic relations, by contrast, are *global constraints*: they do not propagate along the lattice but must be satisfied by all horizon configurations

at every retessellation tick. Locality in the bulk corresponds to geometric adjacency; entanglement corresponds to algebraic constraint.

Entanglement as a shared algebraic condition. Interactions between particles correspond to superposition of their field envelopes on the horizon. When two identity clusters overlap, the dipole and phase structure of their fields may impose a shared algebraic relation, a representation-matching, phase-locking, or parity constraint, that binds their internal degrees of freedom:

$$\mathcal{R}(\mathcal{C}_1, \mathcal{C}_2) = 0. \tag{140}$$

Because this constraint is stored in the internal structure of the identity clusters rather than in their geometric proximity, it persists under arbitrary lateral separation. Entanglement correlations therefore do not arise from signals propagating on the horizon but from the requirement that all identity clusters evolve under the same global, null-synchronized update of the membrane. Entanglement is a single algebraic rule engraved in the membrane's constraint layer, not a dynamic influence.

Measurement, branching, and decoherence. A measurement device is a large, complex identity cluster with an enormous lateral field envelope. When its fields interact with those of a particle, the combined dipole configuration admits several mutually incompatible algebraic sectors $\mathcal{S}_1, \ldots, \mathcal{S}_N$, each corresponding to a distinct measurement outcome. Before decoherence, the joint field supports all sectors because no global inconsistency has yet emerged.

As the apparatus and environment couple to the system, the field configurations associated with different sectors drift apart under null-step propagation. Their combinatorial overlap on the horizon rapidly vanishes, producing decoherence not through literal "wavefunction splitting" but through divergence of field envelopes in the null-walk ensemble: sectors become effectively disjoint in the horizon configuration space.

Collapse as global algebraic pruning and emergent locality. Every Planck-mass incorporation triggers a *global* retessellation of the horizon, a null-synchronized update of both the geometric adjacency network and the algebraic constraint layer. During such a retessellation the horizon must select a single algebraic sector $\mathcal{S}_k$ that is self-consistent across all identity clusters involved. All incompatible sectors violate adjacency, phase, or representation constraints somewhere on the membrane and are therefore pruned:

$$\mathcal{R}(\mathcal{C}_1, \mathcal{C}_{\text{apparatus}}, \mathcal{C}_{\text{env}}) = 0. \tag{141}$$

Collapse is thus the global elimination of algebraically inconsistent sectors. It is instantaneous in code-time but causal: no information travels between spatially separated bulk regions, because the update acts on the horizon algebra itself, not on geometric paths. Apparent nonlocality is simply boundary constraint selection, not bulk signaling; lateral propagation in the bulk remains strictly limited by nearest-neighbor null steps.

Entanglement correlations are perfect because the algebraic constraint is encoded once, applies globally, does not propagate or degrade, and is preserved by every retessellation. The membrane acts as a globally self-consistent constraint system, and the embedding map E_t projects this consistency into the emergent bulk.

In this unified description, particles arise as locally nucleated identity cores that follow their own propagating fields; entanglement is a static algebraic relation preserved under global null-synchronized updates; measurement induces algebraic branching; decoherence follows from diverging field envelopes; and collapse is global algebraic pruning. All quantum behavior in the emergent bulk reflects the interplay of geometric adjacency and algebraic constraint on a hexagonally tessellated null horizon.

4.8 Relativistic Kinematics from Causal Bandwidth and Field–Identity Separation

In the horizon-layered cosmology, relativistic effects arise from the finite causal throughput of the holographic horizon. Each Planck-scale cell can update its secondary-dipole (phase and correlation) data only at the invariant maximal rate

$$\dot{\mathcal{I}}_{\max} = \frac{1}{t_{\mathrm{p}}} = \sqrt{\frac{c^5}{\hbar G}}, \tag{142}$$

the fundamental processing bandwidth of the null-synchronized membrane. This bandwidth must be allocated among three tasks: (i) maintaining the coherence of identity codewords, (ii) propagating field correlations laterally, and (iii) participating in global retessellation events. All relativistic phenomena are expressions of how this fixed causal budget is partitioned.

Primary vs. secondary dipoles. Primary dipoles are fixed, non-propagating properties of stationary horizon cells. They encode the cell's generational (radial) index and its causal excision weight. *Secondary dipole configurations*, by contrast, are the data that propagate from cell to cell; they carry all field, phase, and identity information. Bulk motion arises entirely from the motion of these secondary-dipole patterns across the static primary-dipole lattice.

Massive particles: identity-bearing excitations. A massive particle corresponds to a compact, coherently organized cluster of secondary dipoles (an identity codeword $\mathcal{C}$) together with its surrounding field envelope $F_{\mathcal{C}}$. Identity codewords secondary-dipole pattern migrates across neighboring horizon cells subject to the generational filter $g_{\mathrm{cell}} \leq g_{\mathrm{sig}}$. The codeword's worldline is the centroid of its propagating field pattern,

$$\mathcal{C}(t+1) = \mathrm{centroid}[F_{\mathcal{C}}(t+1)]. \tag{143}$$

However, part of the local causal bandwidth must always be reserved to maintain the coherence of the identity pattern. This bandwidth cost enforces a sub-null drift: massive particles cannot move at the full lateral update rate c.

Massless particles: pure field propagation. A photon corresponds to a propagating secondary-dipole phase pattern without an identity core. Because no bandwidth is

spent on internal identity maintenance, *all* causal throughput is available for lateral propagation along the six primitive null directions of the hexagonal lattice. The pattern therefore advances one Planck cell per Planck time and follows a null trajectory in the emergent bulk,

$$|\dot{\gamma}(t)| = c. \tag{144}$$

Bandwidth allocation and time dilation. Let $\dot{\mathcal{I}}_{\rm lat}$ denote the bandwidth devoted to lateral propagation and $\dot{\mathcal{I}}_{\rm int}$ the bandwidth devoted to identity maintenance, with

$$\dot{\mathcal{I}}_{\rm lat} + \dot{\mathcal{I}}_{\rm int} = \dot{\mathcal{I}}_{\rm max}. \tag{145}$$

If a particle's bulk drift velocity is v, the required directional coherence of its field envelope consumes the fraction v/c of the horizon's causal throughput, leaving only

$$\dot{\mathcal{I}}_{\rm int} = \dot{\mathcal{I}}_{\rm max}\sqrt{1 - v^2/c^2} \tag{146}$$

for internal updates. Proper time therefore advances as

$$\frac{d\tau}{dt} = \sqrt{1 - v^2/c^2}, \tag{147}$$

and massive particles accrue relativistic energy

$$E = \frac{m_0 c^2}{\sqrt{1 - v^2/c^2}}. \tag{148}$$

Why massive trajectories are timelike. Because identity-bearing excitations must maintain internal coherence, they must allocate nonzero bandwidth to $\dot{\mathcal{I}}_{\rm int}$. This prohibits them from saturating the lateral throughput channel and forces their effective drift velocity to satisfy $v < c$. Thus timelike geodesics emerge from the requirement that identity codewords preserve their structure.

Why massless trajectories are null. Massless excitations have no identity core and therefore no internal coherence cost:

$$\dot{\mathcal{I}}_{\rm int} = 0, \qquad \dot{\mathcal{I}}_{\rm lat} = \dot{\mathcal{I}}_{\rm max}. \tag{149}$$

They can devote their entire bandwidth to lateral propagation and hence follow null geodesics.

Inertia as resistance to identity deformation. To accelerate a massive particle is to increase the directional coherence of its propagating field pattern, diverting bandwidth away from identity maintenance. The identity core resists this reallocation. This resistance is inertia: the effort required to redistribute a portion of the fixed causal throughput from internal codeword coherence to external field propagation.

Stress–energy as coarse-grained bandwidth flow. Variations in how the membrane allocates bandwidth across its surface coarse-grain into the stress–energy tensor.

Regions where lateral causal flow is impeded (e.g. by high excision density or deep secondary-dipole gradients) project as curvature in the emergent bulk. The Einstein equations thus appear as the macroscopic bookkeeping of how causal bandwidth is redistributed across the horizon,

$$G_{\mu\nu} = \frac{8\pi G}{c^4} T_{\mu\nu}. \tag{150}$$

In this unified picture, massive and massless motion differ only in how they use the finite causal bandwidth of the horizon. Massive trajectories arise from propagating secondary-dipole patterns constrained by identity coherence, while massless trajectories arise from unconstrained propagation. Time dilation, inertia, relativistic energy, and the distinction between timelike and null geodesics all emerge from a single mechanism: the causal economics of how the holographic membrane allocates its invariant throughput c^5/G.

4.9 Mach's Principle and the Origin of Inertia

In classical mechanics, inertia quantifies a system's resistance to changes in motion. Its origin has remained conceptually opaque: in Newtonian theory it is intrinsic; in Mach's view it is relational; and in general relativity it arises from spacetime geometry shaped by global energy–momentum.

In the horizon-layered cosmology, inertia becomes an explicit informational property of the holographic membrane. Each Planck cell participates in a null-synchronized causal lattice supporting both geometric adjacency and algebraic phase constraints. A massive excitation corresponds not to a fixed location on this lattice but to a *propagating secondary-dipole pattern*: a stable cluster of phase correlations that moves laterally across horizon cells according to the membrane's null-step update rules. The primary dipoles remain fixed and encode generational index (radial position), while the secondary dipoles carry all identity and field information and are responsible for particle motion in the emergent bulk.

To accelerate a particle is therefore to force a change in the directional coherence of this propagating secondary-dipole pattern. Such a change demands a redistribution of the finite causal bandwidth of the local horizon region: more throughput must be committed to maintaining directed, coherent lateral propagation, and less remains available for internal identity maintenance. Acceleration is thus resisted because it requires global readjustments of lateral coherence across the membrane.

This provides a concrete implementation of Mach's principle: **inertia is relational, not intrinsic**. The effective inertial frame of a particle is the state in which its secondary-dipole pattern maintains a stationary, statistically isotropic relationship with the surrounding horizon cells. Any attempt to accelerate the particle disturbs this relational equilibrium and forces compensating adjustments throughout the broader causal network. Because the horizon forms a globally entangled constraint system, the inertial response of any subsystem implicitly depends on the state of the entire horizon.

Formally, the effective inertial mass m_{eff} is proportional to the rate at which the horizon code must alter the mutual information between a local subsystem $\mathcal{S}$ and its complement $\bar{\mathcal{S}}$ in order to accommodate acceleration:

$$m_{\text{eff}}c^2 \;\propto\; \frac{\partial I(\mathcal{S}:\bar{\mathcal{S}})}{\partial \tau}. \tag{151}$$

A particle in uniform motion corresponds to constant mutual information under successive retessellations, while acceleration requires a change in this mutual information, representing the informational work needed to reconfigure causal coherence. This reconfiguration consumes causal bandwidth and is therefore energetically costly, yielding the macroscopic phenomenon of inertia.

Within this framework, the equivalence principle follows naturally. Gravitational mass and inertial mass are identical because both measure the resistance of the null-synchronized causal network to changes in relational structure. Gravitational curvature describes how the global connectivity field redirects null propagation; inertia measures the bandwidth cost of modifying that propagation locally. Both arise from the same finite-capacity causal substrate.

Thus, in the horizon-layered cosmology, Mach's principle is realized exactly: **inertia is the relational resistance of the holographic membrane to reconfiguring its causal entanglement structure**. Local inertial frames are not geometric givens but stable global connectivity patterns on the horizon. Motion, inertia, and gravitation are unified aspects of the same underlying informational architecture.

4.10 Spin from Horizon Geometry and Topology

In the horizon-layered framework, spin emerges from the discrete geometric and topological structure of the null-surface code carried by the secondary dipoles that propagate across the holographic membrane. Each Planck-area cell supports two conceptually distinct degrees of freedom:

- a *primary dipole*, fixed to the local surface normal, encoding the causal orientation, excision weight, and generational (radial) index of the cell; and
- a *secondary dipole*, lying in the tangent plane, encoding a mobile phase vector that participates in field propagation and particle identity.

Because the membrane is intrinsically two-dimensional, the secondary dipole cannot assume arbitrary three-dimensional orientations. The hexagonal adjacency graph admits only two globally stable tangential alignments: one aligned with the local azimuthal phase gradient and one anti-aligned. These two tangential orientations form the binary basis that appears in the emergent bulk as spin "up" and "down."

A massive or massless bulk particle corresponds to a coherent secondary-dipole pattern that propagates from cell to cell. The particle's spin is encoded not by the primary substrate but by a topologically protected winding of this secondary-dipole pattern. Transporting such a pattern around a closed loop on the quasi-hexagonal lattice produces a sign reversal under a 2π rotation of the local tangential links and

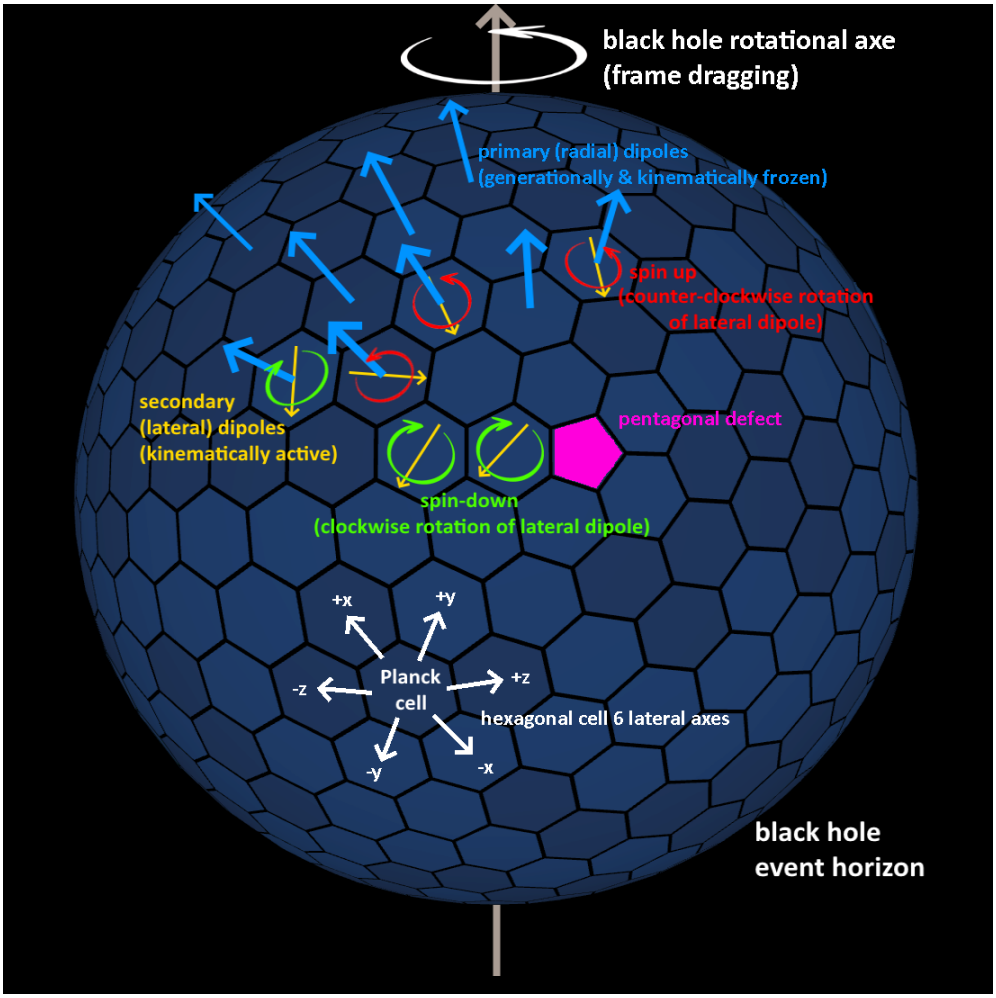

Fig. 8 Schematic representation of a Kerr black hole horizon surface composed of individual Planck cells. Hexagonal sphere created by @arscan.

returns to itself only after a 4π rotation. This double-cover behavior is exactly the transformation law of a spin-$\frac{1}{2}$ representation.

At the level of individual quanta, each Planck-scale unit on the membrane is a bipolar causal element: a primary dipole oriented along the surface normal and a secondary, spin-like dipole restricted to two discrete tangential states,

$$s = +\tfrac{1}{2} \quad \text{(aligned)}, \qquad s = -\tfrac{1}{2} \quad \text{(anti-aligned)}. \tag{152}$$

This binary structure forms the fundamental spin basis of the horizon code.

The Pauli exclusion principle follows from the topology and adjacency of this holographic lattice. Two secondary dipoles cannot occupy the same Planck cell with

identical spin orientation and phase, because the null tiling requires neighboring cells to maintain distinct spinor phases to preserve causal orientation and global consistency. The antisymmetry of fermionic wavefunctions therefore emerges as a geometric and topological constraint: the adjacency algebra of the horizon admits no duplicate spinor-phase assignments on a single cell.

Thus, intrinsic spin is not an imposed quantum label but a direct consequence of how mobile secondary-dipole patterns are constrained to propagate across the null-surface code. Discrete tangential orientation, together with nontrivial winding stabilized by the connectivity of excision defects, yields a bulk spinor obeying the standard Lorentz transformation properties when projected through the embedding map E_t. The emergent bulk inherits all familiar spin phenomena from this dual geometric–algebraic structure of the horizon: a binary spin basis, spin-1/2 double-cover behavior, and the Pauli principle, all realized as properties of a hexagonally tessellated null surface.

4.11 Kerr Rotation, Baryon Asymmetry, and Cosmic Anisotropy

In general relativity, rotation of a black hole is not the motion of matter but the rotation of spacetime itself. For a Kerr black hole of mass $m_{\rm bh}$ and angular momentum J, the spin parameter is

$$a = \frac{J}{m_{\rm bh}c}, \tag{153}$$

and the dimensionless spin fraction is

$$\chi \equiv \frac{ac^2}{Gm_{\rm bh}} = \frac{c\,J}{Gm_{\rm bh}^2}, \qquad 0 \le \chi \le 1. \tag{154}$$

The horizon radius is

$$r_H = \frac{Gm_{\rm bh}}{c^2}\Big(1 + \sqrt{1-\chi^2}\Big), \tag{155}$$

and the angular velocity of the horizon is

$$\Omega_H(m_{\rm bh},\chi) = \frac{c^3}{2Gm_{\rm bh}}\,\frac{\chi}{1+\sqrt{1-\chi^2}}. \tag{156}$$

For fixed χ, $\Omega_H \propto m_{\rm bh}^{-1}$; more explicitly,

$$\chi \ll 1: \quad \Omega_H \simeq \frac{c^3}{4Gm_{\rm bh}}\,\chi, \qquad \chi \to 1: \quad \Omega_H \to \frac{c^3}{2Gm_{\rm bh}}. \tag{157}$$

If the black hole accretes mass more efficiently than angular momentum (so that $J \approx$ const.), then $\chi \propto m_{\rm bh}^{-2}$ and

$$\Omega_H \simeq \frac{Jc^4}{4G^2m_{\rm bh}^3} \quad \Rightarrow \quad \Omega_H \propto m_{\rm bh}^{-3}, \tag{158}$$

so the horizon's rotation slows dramatically as accretion proceeds. For two Kerr black holes of equal spin fraction χ,

$$\frac{\Omega_H(m_1)}{\Omega_H(m_2)} = \frac{m_2}{m_1}, \tag{159}$$

so a $10M_\odot$ Kerr black hole spins about 10^7 times faster than a $10^8 M_\odot$ black hole with the same χ.

In the horizon-layered cosmology, the Kerr rotation acquires a direct information-theoretic interpretation. The off-diagonal metric component $g_{t\phi}$, which encodes frame dragging in the Kerr geometry, corresponds on the membrane to a global azimuthal phase gradient imprinted on the secondary-dipole network. Every Planck-scale cell participates in null-synchronized interactions whose causal adjacency relations advance azimuthally at the rate Ω_H. The horizon undergoes a genuine *causal rotation*: not as a material surface moving in space, but as a globally advancing phase pattern in the secondary dipoles.

Microphysical consequences: helicity bias and baryon asymmetry. Near the horizon, the local frame-dragging (Lense–Thirring) angular velocity is

$$\omega_{\rm fd} = \frac{2GJ}{c^2 r_H^3}. \tag{160}$$

During one Planck-time incorporation step $t_{\rm p}$, each Planck-scale cell acquires a geometric (Berry-like) phase increment

$$\Delta\phi = 2\,\omega_{\rm fd}\,t_{\rm p} = \frac{4GJ\,t_{\rm p}}{c^2 r_H^3}. \tag{161}$$

Because the secondary dipole can be aligned or anti-aligned with the global rotation, the two spin states ($s = \pm\frac{1}{2}$) accumulate slightly different phases. The co-rotating state $s = +\frac{1}{2}$ remains more nearly phase-synchronous with the Kerr-induced azimuthal gradient and is statistically reinforced across successive incorporations, whereas the counter-rotating state $s = -\frac{1}{2}$ decoheres slightly more with each step.

Over many incorporation ticks, this differential phase accumulation generates a cumulative helicity preference of order

$$\frac{\Delta\phi}{2\pi} \sim 10^{-10} \tag{162}$$

for a near-extremal stellar-mass progenitor, the scale required to seed the observed baryon-to-photon ratio $\eta_b \simeq 6 \times 10^{-10}$. In this way, the microscopic binary spin structure of horizon dipoles, combined with Kerr-induced frame dragging, provides a unified topological origin for both fermionic spin and the matter–antimatter asymmetry of the emergent universe.

Each newly formed null layer inherits the tangential spin configuration of its predecessor, so the helicity bias propagates coherently through the holographic projection into the bulk. Parity violation and directional correlations in the emergent spacetime are thus the large-scale reflection of this microscopic helicity locking.

Macrophysical consequences: cosmic anisotropy and rotational memory. From the internal point of view, the rotating horizon does not manifest as a literal bulk rotation, since the entire causal substrate co-rotates. Instead, observers encounter a primordial azimuthal phase structure: an anisotropic alignment of correlation phases in the emergent field modes. This phase structure defines a preferred axis, serving as the informational seed for cosmic anisotropy.

Because inflation in this model is driven by continued horizon growth rather than by a scalar inflaton, the Kerr-imprinted anisotropy is *not* smoothed away. It survives as a global alignment of low-ℓ CMB multipoles and possibly the intrinsic component of the CMB dipole [28]. Early internal epochs, corresponding to small $m_{\rm bh}$ and large Ω_H, exhibit strong chiral and parity-violating boundary conditions. As accretion proceeds and χ and Ω_H decline according to (158), the internal universe gradually isotropizes. This "spin-down isotropization" yields decreasing large-scale alignment in galaxy spins and polarization axes over cosmic time.

Astrophysical observations support this picture. Spiral-galaxy spin asymmetries and coherent spin directions at high redshift [29–31], including recent *JWST* results, indicate a persistent cosmic axis. CMB data show low-multipole anomalies—quadrupole–octupole alignment, hemispherical asymmetry, and parity violation in temperature and polarization [32, 33]—all pointing to a primordial preferred direction. At the same time, supermassive black holes are observed to spin down with increasing mass due to accretion torques, jets, and mergers [34, 35], mirroring the theoretical decline of $\Omega_H(m_{\rm bh})$ and supporting the link between horizon spin and cosmic anisotropy.

Unified interpretation. Kerr rotation thus acts as a bridge between external frame dragging and internal cosmic structure. At the microscopic level, the azimuthal phase gradient biases the spin states of secondary dipoles, generating baryon asymmetry and parity violation. At the macroscopic level, the same rotational memory imprints a preferred axis and large-scale alignments in the emergent universe, while its gradual decay drives the cosmos toward isotropy. Baryon asymmetry, fermionic exclusion, and cosmic anisotropy all arise from the same underlying spin–topological structure of the rotating holographic horizon.

5 Internal Universe Cosmology

In the horizon-layered cosmology, the classical Big Bang singularity is reinterpreted as the initial emergence of an internal spacetime encoded on the null surface of a black hole formed within a parent universe. Externally, the black hole begins as a Planck-scale seed and grows rapidly through accretion. Internally, this growth appears as a smooth, causally continuous expansion whose initial energy scale is set by Planck-level conditions. The apparent origin of internal time corresponds to the dynamical stratification of infalling matter onto the horizon: entropy and energy increase as new layers of the null-surface code are incorporated. This continuous influx naturally accounts for the extreme initial densities of the emergent universe without requiring arbitrary initial conditions.

In its earliest phase, the internal universe does not contain particles, radiation, or classical matter but exists in a purely vacuum-like state. A Planck-seed horizon contains only $\mathcal{O}(1)$ cells around a great circle, giving an extremely coarse angular resolution,

$$\Delta\phi_{\min} \sim \frac{\ell_{\rm p}}{r_{\rm s}} = \mathcal{O}(1)\,. \tag{163}$$

Such a minimal tessellation cannot sustain the structured secondary-dipole patterns required for gauge coherence, chirality, or stable matter. Only the simplest degrees of freedom, vacuum-like fluctuations and coarse horizon noise modes, can be encoded. Thus, the first internal epoch is a "vacuum hologram," a pre-geometric phase dominated by null-surface fluctuations rather than by classical fields.

As the parent horizon expands, the number of Planck-area cells grows as $A/\ell_{\rm p}^2 \propto r_{\rm s}^2$, improving angular resolution and permitting more elaborate dipole configurations. Gauge symmetries, chiral states, and stable matter become possible only when the horizon achieves sufficient lateral complexity to encode them. Matter fields and radiation thus do not arise from initial conditions but emerge dynamically as the holographic code acquires the necessary structural capacity. This phase transition parallels the Planck and GUT eras of standard cosmology, where fields and particles appear only after sufficient geometric organization.

In conventional cosmology, a brief period of exponential inflation is invoked to solve the horizon and flatness problems and to generate nearly scale-invariant fluctuations [36, 37]. In the horizon-layered model, an analogous stage arises naturally from early global re-synchronizations of the parent horizon. When the horizon was still small, modest accretion or merger events produced large fractional increases in area and entropy, forcing the null-ordered code to undergo global retessellations. From the internal perspective, these appear as transient *inflation-like epochs* during which the effective Hubble rate jumps discontinuously and the vacuum energy shifts abruptly. The final large-scale synchronization of the parent horizon establishes the internal universe's initial null ordering and leaves fossil signatures analogous to those attributed to inflation.

Although driven by a fundamentally different mechanism, these early synchronization bursts reproduce the key phenomenology of inflation. During each retessellation, the horizon briefly saturates the Planck-bandwidth limit $P_{\max} = c^5/G$, rapidly reorganizing lateral correlations among Planck-scale cells. Quantum fluctuations in this process imprint scalar and tensor perturbations on the emergent metric, producing approximately scale-invariant spectra. The amplitude and tilt depend on the duration and intensity of the burst: short, sudden synchronizations generate nearly scale-invariant spectra; longer or partial synchronizations introduce mild red tilts. Residual anisotropies, including parity-violating signatures and low-ℓ alignments in the CMB, may reflect incomplete equilibration during the final synchronization event.

After this final reconfiguration, the internal universe enters an adiabatic phase. The parent horizon continues to grow steadily through accretion and minor mergers, yielding a stable Hubble flow. The near-Gaussian statistics of primordial fluctuations, the small tensor-to-scalar ratio, and the long-term smoothness of expansion all follow from this post-synchronization equilibrium. Thus the horizon-layered cosmology retains the empirical successes of inflation while grounding them in a more fundamental causal mechanism: discrete null-surface synchronization at the Planck information bandwidth.

Outside these early bursts, cosmic expansion arises directly and continuously from the growth of the parent black hole. Each increment of accreted mass corresponds to the incorporation of a new null-ordered layer, triggering a global update of the holographic code that advances internal time. The internal expansion is therefore the large-scale manifestation of the continuous holographic growth of the horizon, without requiring a separate inflaton field or an independently tuned vacuum-energy term.

Within this framework, the standard cosmological puzzles admit new interpretations. The horizon problem does not arise because all internal regions descend from a single causally connected null surface, the parent event horizon. Flatness is not imposed but emerges from the entropy-driven smoothing of the null-surface code. The expansion remains smooth and self-similar because it is governed by the same causal-scaling relation at every epoch.

The coexistence of global retessellation and local lateral propagation provides a unified account of both light propagation and cosmic expansion. Each Planck-step incorporation adds a new layer of causal cells and reindexes the entire adjacency structure. In the internal universe this appears as expansion: relational distances between encoded emitter and observer increase at every global update. A photon's wavelength is stretched not because it loses energy in flight but because its underlying propagating secondary-dipole pattern is re-embedded in an ever-larger horizon lattice. The observed redshift records the cumulative effect of these successive re-indexings.

Between global updates, the horizon lattice functions as a quasi-static causal medium. Within each such frame, photons propagate by sequential transfer of their secondary-dipole pattern across neighboring cells at the invariant null rate c. Internally this appears as continuous motion through a smoothly expanding spacetime.

Thus, a photon's apparent journey across the universe results from two intertwined processes: null-propagation of its secondary-dipole pattern within each quasi-static causal frame, and global retessellation that expands the underlying relational geometry. Propagation and expansion are therefore not independent phenomena but dual manifestations of the same discrete holographic process by which the horizon continuously re-encodes the causal structure of the universe.

5.1 Universal Relation H = 1/t Across All Cosmic Epochs and Revised Cosmic Time

In the horizon-layered cosmology, cosmic time is not an emergent parameter of a continuous field evolution but a direct geometric consequence of the total encoded mass and radius of the enclosing parent black hole. The universe, viewed as the holographic interior of such a black hole, obeys the fundamental identity

$$r_{\rm s} = 2M_{\rm bh}, \tag{164}$$

which defines the causal boundary of the spacetime domain. Here $M_{\rm bh}$ denotes the black hole mass expressed in *geometric units* (i.e. as a length in meters). The corresponding physical mass in kilograms is given by

$$m_{\rm bh} = \frac{c^2 r_{\rm s}}{2G}. \tag{165}$$

From the discrete incorporation relation (§(87)), the cosmic time associated with a black hole of geometric mass $M_{\rm bh}$ is

$$t = \frac{M_{\rm bh}}{c} = \frac{G m_{\rm bh}}{c^3} = \frac{r_{\rm s}}{2c}. \tag{166}$$

Hence the physical radius of the universe at cosmic time t follows directly as

$$\boxed{r_{\rm s} = 2ct.} \tag{167}$$

This expresses the coevolution of cosmic time and horizon size as a purely geometric identity, independent of any assumed matter content, equation of state, or scale-factor dynamics.

In the standard cosmological model, the Hubble radius is defined as

$$r_h = \frac{c}{H}. \tag{168}$$

At the present epoch, it is often noted empirically that $H_0 \approx 1/t_0$, giving $r_h \approx ct_0$. In the horizon-layered model, however, this identity is elevated from a coincidence to an exact geometric law valid at all epochs. Comparing §(168) with §(167), one obtains

$$\boxed{r_{\rm s} = 2r_h,} \tag{169}$$

and equivalently, from §(164),

$$\boxed{M_{\rm bh} = 2M_h,} \tag{170}$$

where M_h denotes the effective Hubble mass enclosed within the radius r_h (in geometric units).

Thus, the cosmological horizon radius is always twice the local Hubble radius, and the total encoded geometric mass is twice the effective Hubble mass, relations that hold across all epochs and across all generations of black-hole-born universes.

The local Friedmann-like expansion rate for a spherically symmetric causal patch of radius r_h containing effective geometric mass M_h can be written as

$$H_{\rm local} = \sqrt{\frac{2M_h}{r_h^3}} = \sqrt{\frac{2Gm_h}{r_h^3}}. \tag{171}$$

Here M_h is the geometric mass associated with the patch, while m_h is the corresponding SI mass satisfying $M_h = Gm_h/c^2$.

Using $M_h = M_{\rm bh}/2$, $r_h = ct$, and

$$t = \frac{Gm_{\rm bh}}{c^3} = \frac{M_{\rm bh}}{c},$$

we obtain

$$\begin{aligned} H_{\rm local} &= \sqrt{\frac{2(M_{\rm bh}/2)}{(ct)^3}} = \sqrt{\frac{M_{\rm bh}}{c^3t^3}} \\ &= \sqrt{\frac{1}{t^2}} = \frac{1}{t}. \end{aligned} \tag{172}$$

Therefore,

$$\boxed{H = \frac{1}{t}} \tag{173}$$

is an exact and epoch-independent identity in the horizon-layered cosmology.

This result implies that **the cosmic expansion rate is a direct manifestation of the geometric time–mass correspondence of the enclosing black hole.** Unlike the Friedmann solutions, where $H(t)$ depends on the evolving energy density and equation of state, here H is entirely determined by the discrete causal synchronization of horizon incorporations. The relation $H = 1/t$ thus expresses the intrinsic holographic clock of the universe: the rate at which external incorporations generate internal time increments and horizon growth in perfect geometric proportion.

The relation §(173) allows us to directly infer the current cosmic time t_0 from the locally measured Hubble constant. Using the empirically determined value from the

SH0ES collaboration [38] we obtain:

$$t_0 = \frac{1}{H_0} = \frac{1}{2.366 \times 10^{-18}\ \mathrm{s}^{-1}} \approx 4.2265427 \times 10^{17}\,\mathrm{s} \approx 13.402279\,\mathrm{Gyr}. \tag{174}$$

This value is approximately 400 million years younger than the standard ΛCDM estimate of 13.8 Gyr. However, this is not a discrepancy but a theoretical pivot: our model redefines cosmic age as a measure of horizon growth, rather than a chronology derived from assumptions about the recombination epoch and dark energy.

Adopting $t_0 = 13.4$ Gyr therefore aligns directly with local observational data while remaining fully consistent within the horizon-layered framework.

The Hubble radius does not represent the total extent of our universe. Using §(87), and the revised cosmic time ($\approx 4.2265427 \times 10^{17}$ s, in contrast to the inferred ΛCDM cosmic time $\approx 4.355 \times 10^{17}$ s), we may compute the current parent black hole mass in geometric units:

$$M_{\mathrm{bh}} = t_0\, c = 4.2265427 \times 10^{17} \cdot 2.99792458 \times 10^{8} = 1.267086 \times 10^{26}\ \mathrm{m}. \tag{175}$$

In physical mass units this is:

$$m_{\mathrm{bh}} = \frac{c^2\, M_{\mathrm{bh}}}{G} = 1.706246 \times 10^{53}\ \mathrm{kg}, \tag{176}$$

and the corresponding Schwarzschild radius is

$$r_{\mathrm{s}} = 2M_{\mathrm{bh}} = 2.534171 \times 10^{26}\ \mathrm{m}. \tag{177}$$

From these values we can infer the total informational content of the cosmic horizon. Using the Planck mass $m_{\mathrm{p}} = 2.176 \times 10^{-8}\,\mathrm{kg}$, the number of Planck-mass incorporations that define the present universe is

$$N_{\mathrm{inc}} = \frac{m_{\mathrm{bh}}}{m_{\mathrm{p}}} \approx 7.8 \times 10^{60}, \tag{178}$$

while the corresponding number of Planck-area cells on the horizon,

$$N_{\mathrm{cell}} = \frac{A}{\ell_{\mathrm{p}}^2} = \frac{4\pi r_{\mathrm{s}}^2}{\ell_{\mathrm{p}}^2} \approx 3.089 \times 10^{123}, \tag{179}$$

establishes the maximal informational capacity of our spacetime domain. Both quantities are invariants of the causal structure: internal and external observers agree on their values because they depend solely on the horizon area and the universal constants G, $\hbar$, and c.

Hence, our universe corresponds to an extraordinarily massive black hole even within its parent cosmos, an object of order $10^{23}\,M_\odot$ and Schwarzschild radius $r_{\mathrm{s}} \sim 2.5 \times 10^{26}$ m. This confirms that, from the parent universe's perspective, the black hole

whose interior constitutes our cosmos is genuinely enormous; both frames perceive the same number of horizon cells and thus the same total informational content. Redshift and time-dilation merely alter how the internal evolution is *perceived*, not the intrinsic geometric or informational magnitude of the system.

5.2 FLRW Dynamics from Holographic Horizon Growth

In the horizon-layered cosmology, the expansion of the internal universe follows directly from two independent but complementary principles:

1. the *microscopic* Planck-step growth of the parent horizon, and
2. the *macroscopic* geometric identity relating horizon radius and cosmic time.

The convergence of these two derivations yields a fully consistent FLRW cosmology without invoking an inflaton field, dark-energy term, or equation-of-state assumptions.

1. Microscopic derivation from horizon growth. Each Planck-time incorporation increases the horizon radius by two Planck lengths,

$$r_{\mathrm{s}}(t + t_{\mathrm{p}}) = r_{\mathrm{s}}(t) + 2\ell_{\mathrm{p}}, \tag{180}$$

requiring that all comoving radial indices scale by the same fractional factor,

$$\lambda(t) = 1 + \frac{2\ell_{\mathrm{p}}}{r_{\mathrm{s}}(t)}. \tag{181}$$

Passing to the continuum limit,

$$\frac{\dot{r}}{r} = \frac{2\ell_{\mathrm{p}}}{r_{\mathrm{s}}(t)}\,\frac{1}{t_{\mathrm{p}}} = \frac{2c}{r_{\mathrm{s}}(t)}. \tag{182}$$

Thus microscopic horizon growth generates an effective expansion rate

$$H(t) = \frac{2c}{r_{\mathrm{s}}(t)}. \tag{183}$$

2. Macroscopic geometric identity. From the definition of cosmic time in this framework,

$$t = \frac{r_{\mathrm{s}}}{2c}, \tag{184}$$

we obtain the fundamental relation

$$r_{\mathrm{s}} = 2ct \qquad \Rightarrow \qquad \frac{2c}{r_{\mathrm{s}}} = \frac{1}{t}. \tag{185}$$

Substituting this into (183) yields the universal law

$$\boxed{H(t) = \frac{1}{t}}, \tag{186}$$

valid at all epochs.

3. Scale factor. Since comoving distances satisfy $\dot{r}/r = H(t)$, the scale factor obeys

$$\frac{\dot{a}}{a} = \frac{1}{t}, \tag{187}$$

giving

$$\boxed{a(t) = a_0\, t.} \tag{188}$$

The internal universe therefore expands *linearly* with cosmic time.

4. Effective energy density scaling. The interior mass $m(t)$ grows linearly with the number of Planck-mass incorporations, hence $m(t) \propto t$. The effective density is

$$\rho(t) = \frac{m(t)}{\frac{4\pi}{3} r_{\rm s}^3} \propto \frac{1}{t^2}. \tag{189}$$

Using $a(t) \propto t$,

$$\boxed{\rho(t) \propto a(t)^{-2}.} \tag{190}$$

5. Spatial curvature. Substituting $H = 1/t$ and $\rho \propto 1/t^2$ into the Friedmann equation,

$$H^2 = \frac{8\pi G}{3}\rho - \frac{k}{a^2}, \tag{191}$$

gives

$$\frac{1}{t^2} = \frac{8\pi G}{3}\rho, \tag{192}$$

leaving

$$k = 0. \tag{193}$$

Thus the emergent bulk is necessarily

$$\boxed{k = 0 \qquad \text{(spatially flat)}}. \tag{194}$$

6. Consolidated FLRW correspondence. The horizon-layered cosmology yields the FLRW dynamical relations:

$$H(t) = \frac{1}{t}, \qquad a(t) \propto t, \qquad \rho(t) \propto a^{-2}, \qquad k = 0. \tag{195}$$

These are not imposed but emerge simultaneously from: (i) the discrete Planck-scale growth of the horizon; and (ii) the macroscopic geometric identity $r_{\rm s} = 2ct$.

Summary. The holographic horizon fully determines FLRW expansion. Linear expansion, spatial flatness, and the a^{-2} density scaling arise automatically from the causal and geometric structure of the parent horizon. The convergence of microscopic and macroscopic derivations provides a self-consistent cosmological framework in which the universe's expansion follows from first principles of holographic null evolution rather than from postulated matter fields or early-time fine tuning.

5.3 Resolution of the Vacuum Catastrophe through Holographic Encoding

A standard zero-point estimate in quantum field theory (QFT) assigns to the vacuum a density

$$\rho_{\rm vac}^{\rm qft} \sim \int^{k_{\rm max}} \frac{d^3k}{(2\pi)^3}\,\frac{1}{2}\hbar\omega_k \sim \int^{1/\ell_p} k^3\,dk \sim \frac{\hbar c}{\ell_p^4}. \tag{196}$$

This result depends only on the ultraviolet cutoff ℓ_p and is independent of the size of the universe. It exceeds the observed dark-energy density by 10^{120}–10^{123}, the notorious "vacuum catastrophe." In conventional QFT this arises because every Planck-volume cell inside the cosmic volume is counted as an independent gravitating mode.

In the horizon-layered cosmology, this discrepancy is reinterpreted as a case of *causal overcounting*. Bulk vacuum modes are not independent carriers of gravitational stress-energy. Only degrees of freedom that are actually *registered on the horizon*, that is, those participating in the null-synchronized causal updates of the holographic membrane, contribute to Einstein curvature. Volumetric QFT mode-counting is therefore not physically realized: the true gravitational degrees of freedom are holographic, not volumetric.

The difference between $\rho_{\rm vac}^{\rm qft}$ and $\rho_{\rm vac}^{\rm obs}$ directly reflects the contrast between volumetric UV counting (QFT) vs. holographic causal counting (one bit per Planck area).

Using the quantities obtained earlier (§(177)–179),

$$m_{\rm bh} = 1.706246 \times 10^{53}\ {\rm kg}, \qquad r_{\rm s} = 2.534171 \times 10^{26}\ {\rm m}, \tag{197}$$

the cumulative number of Planck-mass incorporations and the number of Planck-area cells are

$$N_{\rm inc} = \frac{m_{\rm bh}}{m_{\rm p}} \approx 7.8 \times 10^{60}, \qquad N_{\rm cell} = \frac{4\pi r_{\rm s}^2}{\ell_{\rm p}^2} \approx 3.1 \times 10^{123}. \tag{198}$$

The observed vacuum density depends explicitly on the large-scale curvature:

$$\rho_{\rm vac}^{\rm obs} \sim \frac{3H^2}{8\pi G} \sim \frac{c^2}{G r_{\rm s}^2}. \tag{199}$$

Thus the QFT–observed ratio becomes

$$\frac{\rho_{\rm vac}^{\rm qft}}{\rho_{\rm vac}^{\rm obs}} \sim \frac{(\hbar c)/\ell_p^4}{c^2/(G r_s^2)} \sim \frac{G\hbar}{c^3}\,\frac{r_s^2}{\ell_p^4} = \left(\frac{r_s}{\ell_p}\right)^2 = N_{\rm cell}. \tag{200}$$

Thus the infamous 10^{122} discrepancy is not mysterious at all, it is precisely the number of horizon-area degrees of freedom of the universe. QFT counts all these UV modes as independent gravitating excitations, whereas the holographic framework recognizes that only one causal degree of freedom per Planck-area cell can gravitate. The vacuum catastrophe is therefore a misinterpretation of holographic bandwidth limits rather than a failure of either QFT or general relativity.

If the gravitationally relevant vacuum energy is set not by UV fluctuations inside the bulk but by the IR curvature scale of the horizon, one obtains generically

$$\rho_{\rm vac} \simeq \kappa \, \frac{c^4}{8\pi G r_{\rm s}^2}, \tag{201}$$

with $\kappa = \mathcal{O}(1)$ encoding the precise horizon definition and the redundancy of the null-surface code. This r_s^{-2} behavior appears independently in de Sitter thermodynamics, in holographic dark-energy models, in equipartition arguments, and in emergent-gravity approaches [39–42].

Numerically, with $r_{\rm s} = 2.534171 \times 10^{26}\,\mathrm{m}$:

$$\rho_{\rm vac}(\kappa{=}1) = \frac{c^4}{8\pi G r_{\rm s}^2} \approx 7.5 \times 10^{-11}\ \mathrm{J\,m^{-3}} \approx 8.3 \times 10^{-28}\ \mathrm{kg\,m^{-3}}. \tag{202}$$

The *Planck* measurement $\rho_{\rm vac}^{\rm obs} \approx 5.96 \times 10^{-27}\ \mathrm{kg\,m^{-3}}$ corresponds to $\kappa \simeq 7$, consistent with modest redundancy of the horizon code and with standard horizon-thermodynamic uncertainties.

Interpretation. In this framework, vacuum energy is not the energy of empty space but the residual curvature cost of maintaining a finite information redundancy at the causal limit. As the horizon grows and its area increases, the curvature per cell decreases as r_s^{-2}. Cosmic acceleration thus reflects the continuing refinement of the holographic boundary:

the universe expands as the horizon code becomes more fine-grained. (203)

Therefore the vacuum catastrophe resolves itself: QFT computes the total zero-point energy *in the bulk*, while gravity couples only to the holographically available degrees of freedom on the horizon. The cosmological constant is a bookkeeping term for the null-surface code's causal redundancy, controlled by the maximal causal throughput c^5/G and the finite information capacity of the horizon itself.

5.4 Redshift Relations, Thermal–Temporal Scaling, and Resolution of the Hubble and Early-Galaxy Tensions

In the horizon-layered cosmology, cosmic time is not defined by the evolution of a continuous scale factor but by the null-ordered growth of a holographic horizon. Because

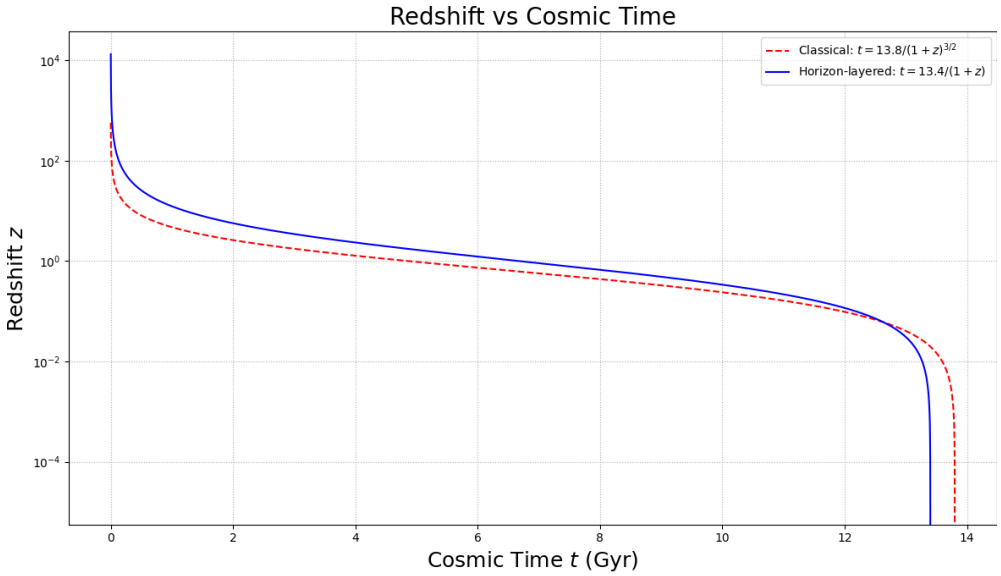

Fig. 9 Relation between redshift factor z and cosmic time according to the standard ΛCDM approximation (red dashed line, $t = 13.8 \cdot (1+z)^{-3/2}$) and the horizon-layered model (blue solid line, $t = 13.4 \cdot (1+z)^{-1}$). The horizon-layered model assumes a total cosmic time of 13.4 Gyr, consistent with the observed Hubble constant, and yields a slower temporal contraction at high redshift.

the Schwarzschild radius of the enclosing black hole satisfies $r_{\rm s} = 2ct$, redshift becomes a purely geometric ratio of horizon-encoded timescales:

$$1 + z = \frac{\nu_z}{\nu_0} = \frac{r_{\rm s}^0}{r_{\rm s}^z} = \frac{2ct_0}{2ct_z} = \frac{t_0}{t_z}, \tag{204}$$

yielding the causal time–redshift relation

$$\boxed{t_z = \frac{t_0}{1+z}}. \tag{205}$$

This formula replaces the standard FLRW relation $t(z) \propto (1+z)^{-3/2}$ and arises directly from horizon growth rather than from metric expansion.

Differentiating gives the redshift evolution of the Hubble parameter:

$$\boxed{H(z) = \frac{1+z}{t_0}}. \tag{206}$$

Because $t_0 = 1/H_0$ by construction, this relation is fixed entirely by the observed present-day Hubble constant.

Maximum causal redshift. The earliest possible internal time is the Planck time $t_{\rm p}$, giving

$$1 + z_{\rm initial} = \frac{t_0}{t_{\rm p}}, \qquad z_{\rm initial} \approx 7.84 \times 10^{60}, \tag{207}$$

interpreted as the maximum causal compression factor of the holographic encoding, not as a physical emission redshift.

Resolution of the Hubble tension. In ΛCDM the Hubble tension arises from comparing the late-time Hubble constant to the value inferred from early-universe physics. In the horizon-layered cosmology, H_0 is fundamental because it defines the global causal time t_0. Discrepancies between early- and late-time inferences do not indicate inconsistent expansion rates but reflect the fact that the standard FLRW time–redshift conversion is replaced by $t(z) = t_0/(1+z)$.

Using $z_{\rm cmb} = 1089.92$ and $t_0 = 4.2265427 \times 10^{17}$ s,

$$t_{\rm CMB} = \frac{t_0}{1 + z_{\rm cmb}} = 3.874292 \times 10^{14} \text{ s} \approx 12.2853 \text{ Myr}. \tag{208}$$

Thus the CMB is emitted 12.3 Myr after the internal "origin," rather than 380,000 yr as in ΛCDM. All observed redshifts are preserved; only the temporal interpretation changes.

Thermal scaling and causal saturation. The standard temperature law $T = T_0(1+z)$ diverges as $z \to \infty$, violating holographic entropy bounds. The null-surface causal bandwidth instead enforces the saturation relation

$$T(z) = \frac{T_{\rm P} T_0 (1+z)}{T_{\rm P} + T_0(1+z)}, \tag{209}$$

which agrees with the standard law at low z but saturates to $T_{\rm P}$ at early times. For the CMB epoch this yields

$$T_{\rm CMB} \approx 2973 \text{ K}, \tag{210}$$

consistent with standard recombination thermodynamics.

Resolution of the early-galaxy tension. *JWST* observations reveal massive, chemically evolved galaxies at $z \gtrsim 10$–14, posing a challenge to ΛCDM because the available time for structure formation is only a few hundred Myr. In the horizon-layered cosmology:

$$t(z = 14.44) = \frac{13.4 \text{ Gyr}}{15.44} \approx 0.868 \text{ Gyr}, \tag{211}$$

tripling the available formation time and eliminating the need for exotic cooling, anomalous star-formation efficiencies, or modified early dark matter.

Unified resolution of both tensions. Both the Hubble tension and the early-galaxy tension arise from assuming that redshift measures metric expansion. In the present

Feature	**ΛCDM time**	**Horizon-layered time**	**Temperature** $T(z)$
Current epoch ($z = 0$)	13.8 Gyr	13.4 Gyr	2.7 K
First galaxies ($z = 14.44$)	280 Myr	868 Myr	42 K
CMB epoch ($z = 1089.92$)	380 kyr	12.3 Myr	2973 K
Early structure growth	Fine-tuned	Natural	Starts from Planck temperature

framework, redshift measures *temporal encoding* across null-synchronized horizon layers. The modified scaling,

$$t(z) \propto (1+z)^{-1}, \tag{212}$$

combined with the causal saturation law §(209), yields a cosmology fully consistent with all observations, while providing adequate time for early structure formation.

Thus, both tensions dissolve naturally once redshift is recognized as a ratio of holographic causal timescales rather than as the effect of a classical expanding metric. The observed universe is consistent without new physics beyond the Planck-scale causal structure of the horizon itself.

5.5 The Schwarzschild–Hubble Equivalence, FRW Consistency, and the Causal Bandwidth of Cosmic Structure

In the horizon-layered cosmology, the observable universe is the holographic interior of a parent black hole whose event horizon constitutes the ultimate causal boundary of spacetime. Internal observers inhabit a spatially flat, homogeneous, and isotropic Friedmann–Robertson–Walker (FRW) geometry,

$$ds^2 = -c^2dt^2 + a(t)^2\left[dr^2 + r^2 d\Omega^2\right], \tag{213}$$

with scale factor $a(t)$ and Hubble parameter $H = \dot{a}/a$. The first Friedmann equation for a flat universe,

$$H^2 = \frac{8\pi G}{3}\rho, \tag{214}$$

implies that the Hubble radius and the mass it encloses,

$$r_h = \frac{c}{H}, \qquad m_h = \frac{4\pi}{3} r_h^3 \rho, \tag{215}$$

are related by

$$m_h = \frac{c^3}{2GH}, \qquad r_h = \frac{2Gm_h}{c^2}. \tag{216}$$

Thus the Hubble sphere obeys the same causal relation as a Schwarzschild horizon. This Schwarzschild–Hubble equivalence does not imply a true Schwarzschild geometry

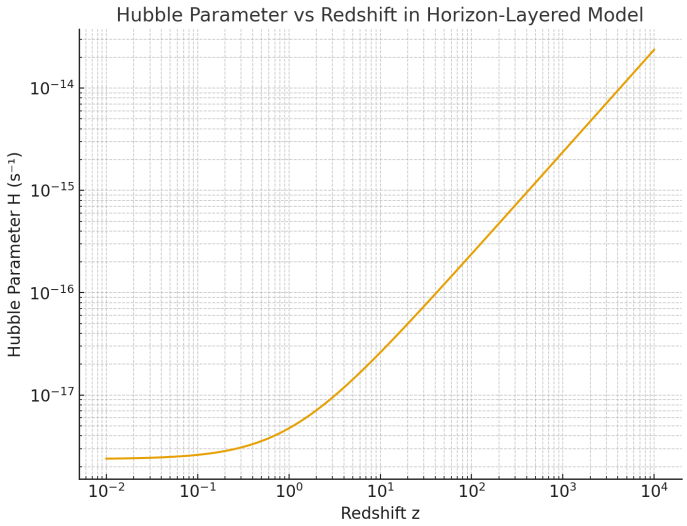

Fig. 10 Hubble parameter as a function of redshift in the horizon-layered cosmology. The plotted curve shows the linear relation $H(z) = \frac{1+z}{4.2265427\times10^{17}}$ s^{-1}, predicted by the causal incorporation model, with the redshift z expressed on a logarithmic scale. In this framework, the Hubble parameter is not governed by energy-density dilution as in standard ΛCDM cosmology, but arises directly from the discrete, constant incorporation of information quanta across the holographic horizon. The expansion of space corresponds to the cumulative growth of internal time, $H = 1/t$, where t measures the total number of successful incorporations since the initial horizon formation. Thus, the apparent decrease of H with cosmic time does not signify a slowing of dynamics or matter dilution, but simply reflects the increasing temporal depth of the internal universe as more information is encoded. The incorporation rate itself remains fixed at one quantum per Planck tick, defining the universal causal rhythm underlying cosmic expansion.

inside the universe; instead, it expresses that the Hubble scale is the largest region over which causal correlations can equilibrate in one Hubble time. The full causal saturation $P_{\max} = c^5/G$ is reached only at the outer parent horizon $r_{\rm s}$, while the Hubble radius inherits the same boundary relation by projection.

From the global scaling relations of the horizon-layered model,

$$H = \frac{1}{t}, \qquad r_s = 2ct, \qquad r_h = ct, \tag{217}$$

so that the parent Schwarzschild radius and the Hubble radius satisfy

$$r_s = 2r_h. \tag{218}$$

Equivalently in geometric units $M = r/2$,

$$M_{\rm bh} = 2M_h. \tag{219}$$

The Hubble region contains half the total internal mass but only one-eighth of the spatial volume,

$$\frac{V_h}{V_{\rm bh}} = \left(\frac{r_h}{r_s}\right)^3 = \frac{1}{8}, \tag{220}$$

a purely geometric consequence of the factor-of-two relation. No departure from FRW geometry in the interior follows from this.

A potential concern is whether identifying the Hubble radius with a Schwarzschild radius at each epoch forces a Schwarzschild interior or violates Birkhoff's theorem. It does not. Birkhoff's theorem applies only to the *exterior vacuum*, which remains exactly Schwarzschild (or Kerr). The interior domain is filled with matter and radiation and is therefore a non-vacuum FRW region to which Birkhoff's theorem is irrelevant. Nor does the equivalence $r_h = 2Gm_h/c^2$ imply any radial dependence of the internal density $\rho(r)$. Extending this relation to all radii would enforce $m(r) \propto r$ and $\rho(r) \propto r^{-2}$, producing an inhomogeneous LTB-like geometry incompatible with the homogeneous FRW solution; the Schwarzschild identity holds only at the Hubble scale and at the parent horizon but not at intermediate radii. The region $0 < r < r_s$ remains exactly spatially flat FRW on every constant-t slice.

Matching an FRW interior to a Schwarzschild or Kerr exterior is a standard general-relativistic construction: the null event horizon plays the role of a junction surface carrying the appropriate surface stress tensor. In the horizon-layered picture, the horizon itself is a Planck-thick null code surface whose retessellation provides the correct physical matching between the interior FRW region and the vacuum exterior.

Cosmic expansion inside the FRW domain follows entirely from the growth of the parent horizon. Each incorporation step adds one Planck mass and increases the external Schwarzschild radius by $2\ell_{\rm p}$,

$$(\Delta M, \Delta r_{\rm s}, \Delta t) = (m_{\rm p},\, 2\ell_{\rm p},\, t_{\rm p}), \qquad \frac{dr_{\rm s}}{dt} = \frac{2\ell_{\rm p}}{t_{\rm p}} = 2c. \tag{221}$$

Because no internal excitation can propagate faster than c, the receding outer boundary at $2c$ is permanently inaccessible. The internal universe never reaches $r_{\rm s}$; the observable region is limited by r_h, while the full FRW slice extends smoothly across $0 \le r \le r_s$.

Another concern is whether global anisotropy from Kerr rotation or other boundary features would spoil local isotropy. The horizon-layered model treats such anisotropies as global boundary data that imprint only large-scale, low-ℓ signatures, parity violation, quadrupole–octupole alignment, hemispherical asymmetry, while small-scale isotropy is preserved by horizon coherence and null-surface entanglement. This is consistent with the behavior of many holographic systems: strong global boundary anisotropies coexist with local bulk isotropy.

Finally, the Schwarzschild–Hubble identity itself is best understood as an information constraint rather than as a matter-density relation. It states that the Hubble radius is exactly the scale where the internal FRW mass distribution saturates the causal condition characteristic of a Schwarzschild boundary, while the outer horizon is its factor-of-two extension. The interior FRW dynamics and the external Schwarzschild

geometry are two consistent projections of the same null-surface causal organization. No general-relativistic principle is violated: the horizon-layered model satisfies all junction conditions, preserves FRW homogeneity, and interprets the Schwarzschild–Hubble equivalence as the statement that cosmic structure formation and expansion are globally constrained by the causal bandwidth of the holographic horizon.

5.6 Topological Defects, Kerr Coupling, and Cosmological Signatures

In the horizon-layered cosmology, the holographic boundary is a finite, closed, two-dimensional null surface whose Planck-scale cells relax into an almost uniform quasi-hexagonal tessellation. A perfect hexagonal tiling of the sphere is impossible; Euler's theorem requires a net positive curvature deficit, realized most economically as twelve pentagonal cells (valence-5 nodes of the adjacency graph). These pentagons are not imperfections but topological invariants of the closed surface. They introduce localized distortions in the lateral causal adjacency graph and thereby seed a global, low-order anisotropy in the emergent bulk geometry.

Each Planck cell participates in null-synchronized lateral information exchange through tangential links to its neighbors. Hexagonal cells possess six neighbors and therefore maximal lateral connectivity, whereas pentagonal cells have only five, producing a local deficit in causal adjacency. Because the secondary-dipole phase of horizon excitations propagates by tangential handoff from cell to cell, a pentagonal site necessarily perturbs phase-coherent null propagation: the local graph Laplacian carries an excess of curvature, and null-update coherence is slightly anisotropic in the neighborhood of each defect. These features are topologically protected and cannot be removed by local retessellation; any retiling of the closed surface must preserve the total defect charge.

Although the number of pentagons is small, the horizon code is updated globally at every Planck tick during the early growth of the parent horizon. With each null-synchronized update, secondary-dipole phases are propagated through the entire adjacency network, so the anisotropic phase shear seeded at each defect accumulates coherently along global null-update sequences. The combined effect of the small set of curvature defects is therefore low-rank and inherently large-scale: it produces a persistent pattern in the embedding map E_t that projects into the FRW interior as anisotropies on the largest observable angular scales, without spoiling small-scale isotropy.

The earliest bulk modes originate from the shallowest generational layers, formed when the horizon radius was smallest and pentagonal distortions made the largest fractional contribution to the null-surface geometry. These layers encode the primordial long-wavelength modes of the internal universe and thus imprint a characteristic pattern on the CMB: suppression of power in the quadrupole and octopole, alignment of low-ℓ multipoles (the "axis of evil"), parity asymmetry between even and odd modes, and hemispherical power asymmetry. Because these features arise from the global structure of the horizon rather than from statistical fluctuations in a Gaussian random field, they appear as coherent large-angle anomalies with minimal associated small-scale distortion.

The defect statistics are extreme: topology fixes the number of pentagons (ideally twelve, with small corrections for rotation-induced distortions), while the number of Planck-area cells grows as

$$N_{\rm cell} = \frac{A}{\ell_{\rm p}^2} \sim 10^{123}. \tag{222}$$

Naively, the raw fractional defect-induced anisotropy is

$$A_{\rm defect} \sim \frac{12}{10^{123}} \sim 10^{-122}, \tag{223}$$

microscopic at the horizon scale. However, this perturbation acts on the earliest generational layers and on the largest-scale modes; under holographic projection and cosmic expansion, its imprint is concentrated into the lowest multipoles $\ell \sim \mathcal{O}(1\text{–}10)$, where it need not be small compared to the stochastic background. The result is a natural hierarchy: order-unity deviations at very low ℓ, near-statistical isotropy at high ℓ, and weak but coherent alignments in the largest-scale structure.

At the epoch corresponding to the CMB surface in this framework,

$$t_{\rm CMB} \simeq 12.3 \text{ Myr}, \qquad t_0 \simeq 13.4 \text{ Gyr}, \tag{224}$$

the parent horizon radius obeys $r_s(t) = 2ct$, so

$$\frac{r_s(t_0)}{r_s(t_{\rm CMB})} = \frac{t_0}{t_{\rm CMB}} = 1 + z_{\rm CMB} \simeq 1090. \tag{225}$$

The defect pattern is therefore comoving: its angular structure is preserved under expansion and continues to project dominantly onto the lowest multipoles. Expansion redshifts the physical wavelength of the associated modes but leaves their large-angle pattern intact.

When the parent black hole carries Kerr spin, these unavoidable curvature defects are immersed in a global azimuthal phase gradient. The horizon's null generators rotate with angular velocity

$$\Omega_H(m_{\rm bh}, \chi) = \frac{c^3}{2Gm_{\rm bh}} \, \frac{\chi}{1 + \sqrt{1 - \chi^2}}, \tag{226}$$

with dimensionless spin fraction

$$\chi = \frac{cJ}{Gm_{\rm bh}^2}, \qquad 0 \le \chi \le 1. \tag{227}$$

Near the horizon, local frame dragging has angular velocity

$$\omega_{\rm fd} = \frac{2GJ}{c^2 r_H^3}, \tag{228}$$

so during one Planck-time incorporation step $t_{\rm p}$ each Planck cell acquires a geometric phase increment

$$\Delta\phi = 2\,\omega_{\rm fd}\,t_{\rm p} = \frac{4GJ\,t_{\rm p}}{c^2 r_H^3}. \tag{229}$$

This produces a systematic bias between co-rotating and counter-rotating spin orientations. For a near-extremal stellar-mass progenitor,

$$\frac{\Delta\phi}{2\pi} \sim 10^{-10}, \tag{230}$$

naturally of the order of the observed baryon-to-photon ratio $\eta_b \simeq 6\times10^{-10}$. Pentagonal defects locked into this Kerr twist acquire a definite handedness; the global defect pattern becomes chiral and defines a preferred axis aligned with the parent angular momentum.

Under holographic projection, this combined topological and rotational structure reproduces the main large-angle CMB anomalies. The low-ℓ power deficit in the quadrupole and octopole, reported by *WMAP* and *Planck* at high significance, arises because a small, fixed set of defects modulates the embedding map on sky-filling angular scales, effectively depressing power at $\ell = 2, 3$ relative to a Gaussian ΛCDM expectation [32, 33]. The "axis of evil" alignment emerges because the same non-random defect pattern contributes coherently to multiple low-ℓ modes; they all probe the same holographic skeleton and acquire a common phase reference from the Kerr geometry. Parity asymmetry at $\ell \lesssim 20$ follows from the chiral character of the defect pattern in a rotating background, which distinguishes reflections that flip the spin axis from those that do not. Hemispherical power asymmetry arises when the small set of defects couples slightly unevenly to the Kerr phase during the CMB projection epoch, producing a dipolar modulation of the CMB variance with dimensionless amplitude

$$A_{\rm hemi}^{(\rm pred)} \sim \mathcal{O}(10^{-2}), \tag{231}$$

comparable to the observed $A_{\rm hemi}^{(\rm obs)} \simeq 0.07 \pm 0.02$ [33]. The preferred hemispherical axis is expected to align, within observational uncertainties, with the axis defined jointly by the parent spin and the defect configuration, reproducing the observed correlation of low-ℓ anomalies with a single large-scale preferred direction.

Because there is no separate inflaton field or slow-roll epoch in this model, the horizon-layered cosmology does not predict a strong stochastic background of primordial gravitational waves. Early expansion is driven by horizon growth and null-layer retessellation, not by a scalar potential. The dominant CMB B-modes are therefore expected to be lensing-induced, as in ΛCDM, with only a subdominant defect-induced chiral phase shear on the horizon, generating extremely small EB correlations aligned with the preferred axis. The effective tensor-to-scalar ratio is

$$r_{\rm pred} \ll 10^{-3}, \tag{232}$$

comfortably below the current BICEP/Keck upper bound $r_{\rm obs} < 0.036$ (95% C.L.) [43]. No inflationary B-mode bump at degree scales is expected; instead the model

predicts a tiny, direction-dependent chiral EB signal and correlated modulations of low-ℓ EE and TE spectra along the same axis.

These features together provide a falsifiable signature set. The model anticipates that low-ℓ anomalies will persist and continue to align with a stable preferred axis as data improve rather than averaging away; that future CMB experiments will either push r far below 10^{-3} or contradict the horizon-layered dynamics; that any detected low-ℓ polarization anisotropy should be phase-locked to the temperature anomalies and to large-scale galaxy-spin alignments; that no strong running of the scalar spectral index associated with an inflaton potential will appear; and that anomalies will remain confined to $\ell \lesssim 20$, with higher multipoles approaching statistical isotropy.

In summary, pentagonal curvature defects on the quasi-hexagonal null horizon, coupled to Kerr rotational memory, act as primordial holographic fossils. The same topological structure that enforces a closed, three-dimensional bulk geometry also seeds its largest-scale anisotropies. Quadrupole–octopole suppression, preferred axes, parity asymmetry, hemispherical power modulation, and an extremely small primordial tensor signal emerge not as statistical oddities but as natural consequences of a defect-bearing, rotating holographic origin of spacetime.

5.7 Merging Black Holes and Internal Causal Reconfiguration

In the horizon-layered cosmology, a black hole merger corresponds to a reorganization of the parent horizon's null-ordered code. Each black hole possesses its own sequence of Planck-scale incorporations that defines its interior causal domain. When two horizons merge, their individual null orderings do not combine additively; instead, they re-synchronize into a single, enlarged causal hierarchy. Externally, this process appears as the coalescence of horizons accompanied by gravitational-wave emission, while internally it corresponds to a global retessellation of the null surface.

The external description obeys the area theorem:

$$S_{\text{after}} \;>\; S_1 + S_2, \qquad \Delta S = \frac{k_B c^3}{4G\hbar}\big(A_{\text{after}} - A_1 - A_2\big) > 0, \tag{233}$$

so the merged horizon always contains a larger information capacity. The internal causal domain therefore expands, with new degrees of freedom activated by the enlargement of the horizon.

Primary-dipole renormalization. A crucial feature of mergers is that the primary dipole weights, the mass weights assigned to each Planck-scale cell, *cannot* remain those of the progenitor horizons. If retained, the combined set of dipoles would encode inconsistent mass and entropy relative to the final horizon area. To preserve area additivity, entropy saturation, and smooth null ordering, the entire horizon undergoes a global renormalization:

$$w_i^{(\text{after})} = w_i^{(\text{after})}(M_{\text{after}}), \tag{234}$$

where every Planck cell is reassigned its weight according to the *final* total mass. This re-weighting ensures:

- exact saturation of the holographic bound,
- correct total mass M_{after},
- a smooth, unified generational index for the interior projection.

Thus no "mini-universes" corresponding to smaller progenitor horizons survive inside the merged black hole. All previous internal maps dissolve into a single, globally re-indexed causal ordering.

Early-stage mergers. When the parent horizon is still small, a merger represents a large fractional increase in area. The resulting retessellation is highly non-adiabatic: a dense burst of Planck-scale incorporations occurs as the new horizon synchronizes. Internally, this appears as a brief epoch of rapid causal reconfiguration. Such episodes can produce large shifts in the internal expansion rate,

$$H_{\text{int}}^{\text{after}} \neq H_{\text{int}}^{\text{before}}, \qquad \Lambda \to \Lambda', \tag{235}$$

analogous to phase transitions or reheating in standard cosmology. Quantum fluctuations during these high-frequency synchronization events produce scalar and tensor perturbations with approximately scale-invariant spectra, leaving fossil imprints visible today in the CMB.

Late-stage mergers. In the mature regime relevant to our universe, the parent horizon has become enormously massive. For a horizon mass m_{parent}, the fractional change in area from merging with a black hole of mass Δm is

$$\frac{\Delta A}{A} \sim 2\,\frac{\Delta m}{m_{\text{parent}}}. \tag{236}$$

Even the addition of a $10^6 M_\odot$ black hole produces a fractional area change smaller than 10^{-17}. Consequently, the resulting retessellation is adiabatic: the null ordering adjusts smoothly without violating the causal throughput limit $P_{\max} = c^5/G$. Internally, such events correspond not to violent restructuring but to an extremely slow modulation of curvature and expansion rate, spread over immense internal timescales.

Internal experience of mergers. Because primary-dipole weights are globally renormalized to the new mass M_{after}, the internal FRW-like projection adjusts coherently across all scales. Internal observers do *not* experience discontinuities, shocks, or jumps in $H(t)$: the relative change in generational index and expansion rate is proportional to $\Delta m/m_{\text{parent}}$ and thus undetectably small in a mature horizon. The internal universe remains smooth; the Hubble parameter, vacuum energy, and metric evolution continue without abrupt transitions. What appears externally as a rapid astrophysical coalescence corresponds internally to a barely perceptible, adiabatic drift in global parameters.

Cosmological chronology. The internal universe thus passes through two regimes:

1. *Early, non-adiabatic phase:* frequent mergers produce large fractional area jumps and rapid causal re-synchronizations, generating primordial perturbations and anisotropies.
2. *Late, adiabatic phase:* the parent horizon becomes so large that all external mergers contribute negligibly to its total area; internal evolution becomes smooth, coherent, and stable.

The observed isotropy and gentle late-time acceleration of our universe are manifestations of this mature stage.

Internal relics. Quantum fluctuations produced during early, non-adiabatic synchronization events may survive as low-ℓ CMB anomalies, dipole/quadrupole alignments, or faint modulations of cosmic acceleration. Later mergers, however, leave no detectable internal signatures.

In summary, black hole mergers are cosmogenic events whose internal manifestations depend on the evolutionary stage of the parent horizon. Early mergers generate pronounced internal effects and primordial perturbations; late mergers are adiabatic and essentially invisible inside. Primary dipole renormalization ensures that the merged horizon forms a single, self-consistent causal domain, and our universe's present smoothness reflects the immense mass, and thus the causal serenity, of the parent horizon in which it is encoded.

6 Multiverse and Holographic Hierarchies

During gravitational collapse, the forming event horizon becomes a causal boundary separating the exterior universe from an interior domain generated by null-surface dynamics. In the present framework, the internal cosmology of a black hole is not a pre-existing spacetime but a holographic projection encoded on the evolving horizon. As infalling quanta reach the stretched horizon, they are incorporated through Planck-scale updates, and the resulting sequence of null layers defines the initial conditions and subsequent evolution of an emergent universe. The classical singularity is replaced by a causal and informational origin: a boundary from which spacetime unfolds.

A parent universe may contain a vast population of black holes, primordial, stellar-mass, or supermassive, each generating its own internal universe. Every black hole thus acts as a node in a generative cosmic hierarchy, with observable properties in any universe reflecting the accretion history and null-layer structure of its parent. The resulting architecture is a recursively nested multiverse, in which each generation inherits its initial conditions from the causal encoding of the preceding level.

This picture resonates with earlier ideas of baby-universe formation [44, 45], but reinterprets black holes as holographic generators whose horizons encode the complete causal blueprint of their descendants. According to the classical no-hair theorem, a black hole is externally characterized by only mass, charge, and angular momentum [22]; yet in the holographic framework, its full set of quantum correlations encodes the internal causal structure of the child universe.

Horizon cells as the primitive substrate of spacetime. At the Planck scale, the horizon forms a discrete causal lattice. Each Planck-area cell represents a primitive correlation unit whose links to neighboring cells may be complete, partial, or absent. Complete links yield smooth causal propagation and define continuum geometry; incomplete links reduce local causal capacity, manifesting externally as curvature and gravitational mass. Spacetime is therefore an emergent network of correlations, not a pre-existing manifold. The horizon evolves at the maximal causal throughput $P_{\max} = c^5/G$, continually reorganizing its correlations to maintain global consistency.

This boundary implements a strengthened form of cosmic censorship: it is not a surface hiding a singularity, but a terminal null layer beyond which classical geometry ceases to exist. No internal observer can access or probe the parent horizon, since the emergent spacetime is generated from its causal ordering. The Bekenstein–Hawking entropy limits the total number of distinct internal causal domains that a given horizon can generate [13].

A finite, recursively generated multiverse. Although each black hole may give rise to a new universe, the total number of descendants is bounded by the entropy budget of the parent. Recursive generation is allowed, but each level imposes a strict entropy limit on productive offspring, yielding a finite and causally disjoint multiverse [44]. Universes that fail to maintain stable causal encoding or cannot form black holes produce no descendants, whereas stable lineages proliferate. This dynamic resembles cosmological natural selection [44], but here is expressed holographically: universes evolve toward optimal causal-encoding efficiency.

In this view, our observable universe originates as the emergent interior projected from a boundary located just above the parent horizon. The internal spacetime does not coexist with the boundary within the same geometric domain; rather, the boundary belongs to a higher-order spacetime that is causally inaccessible from within. The event horizon is therefore not a surface inside our universe but the generator of it, the outermost null layer defining the causal order of the internal spacetime.

Ultimate horizons and the hierarchy of time. If the holographic hierarchy has an uppermost member, a causal boundary that admits no external accretion, its dynamics differ from those of its descendants. Without inflow, such an *ultimate horizon* cannot grow through incorporation of external quanta. Its evolution is driven solely by intrinsic lateral reconfigurations of causal adjacency in a closed null lattice. Perfect null synchronization is unstable at the Planck scale, so spontaneous self-reindexing events, although extraordinarily rare, must occasionally occur to preserve coherence. These events constitute a primordial, minimal form of temporal progression: the intrinsic "ticks" of a self-sustaining null surface.

By contrast, descendant universes obtain their temporal progression from accretion-driven incorporations. Each successful incorporation advances the internal causal order and yields a discrete increment of internal time. If accretion ceases, internal time halts. The ultimate horizon, however, generates its own sparse sequence of self-organized updates, acting as a higher-order temporal substrate from which all descendant clocks inherit their ordering.

From the internal viewpoint, accretion-driven incorporations occur at a normal cosmic pace; yet relative to the ultimate horizon's sparse intrinsic ticks, each internal tick is enormously prolonged. Thus the internal rhythm of time becomes a coarse-grained projection of a nearly static causal process. In the deepest layer of the hierarchy, duration and instant approach equivalence: eternity appears as the continual renewal of the present moment. Time is not an absolute flow but a relative measure of causal update density across layers of the holographic hierarchy.

Correlation as the foundation of physical reality. In this model, all physical phenomena, matter, fields, and geometry, arise from evolving patterns of correlation among horizon cells. Spacetime is not the arena in which these patterns exist, but the projection of their causal ordering. The multiverse becomes a finite hierarchy of projected correlation structures, each constrained by the informational capacity of its predecessor. Dimension, mass, and curvature are not fundamental entities; they are emergent features of a deeper, dimensionless causal network.

The arrow of time as inherited causal order. Each new horizon layer records an irreversible causal update, increasing total entropy and defining a directed sequence of incorporations. Because every descendant universe inherits its causal order from the layered structure of its parent, temporal asymmetry propagates recursively through the hierarchy. The arrow of time is therefore not an imposed initial condition but an inherited property of the holographic generation process, the universal memory of causal ordering embedded in the structure of horizons.

6.1 Apparent Quantum Randomness and Deterministic Parent Horizons

In conventional quantum mechanics, randomness is treated as intrinsic: measurement outcomes are assumed to occur without underlying determinism. In the horizon-layered cosmology, this interpretation is replaced by a causal–informational hierarchy in which quantum indeterminacy emerges from limited access to a deeper deterministic process.

Each universe in the holographic hierarchy is the internal projection of a parent horizon. From the parent frame, every Planck-scale incorporation event is a definite causal update: a discrete, ordered addition of one quantum of information–energy to the horizon code. From within the emergent internal spacetime, however, these same updates appear as probabilistic quantum events. The apparent stochasticity of wavefunction collapse arises because observers inside the emergent universe perceive only coarse-grained projections of the external encoding sequence.

In this framework, *quantum randomness is epistemic rather than ontic*. It reflects informational coarse-graining imposed by the holographic boundary, not intrinsic indeterminism. The deterministic evolution of the parent horizon generates, by causal projection, the statistical behavior described internally by the Born rule:

$$P_{\text{internal}}(i) = \left|\langle i \,|\, \psi_{\text{encoded}}\rangle\right|^2, \tag{237}$$

where $|\psi_{\text{encoded}}\rangle$ represents the boundary state determined by successive causal incorporations. Internal measurements correspond to boundary-state updates that are deterministic externally but appear probabilistic internally due to loss of access to the full null-ordered sequence.

The rotation of the parent horizon, characterized by the Kerr parameter $a = J/(Mc)$, further modulates these statistics. Frame dragging induces an azimuthal phase gradient across the holographic code, biasing the relative incorporation rates of co-rotating and counter-rotating quanta. This introduces small but cumulative asymmetries in internal outcome frequencies, such as parity violation and matter–antimatter imbalance. Thus, while individual quantum events appear random, their global distribution retains the geometric memory of the parent horizon.

Ultimate causal closure. If the holographic hierarchy is finite, its highest level is an *ultimate parent horizon*: a closed null-ordered causal network containing all information in its lineage. At that level there is no deeper boundary and no hidden causal layers. All relationships are internally complete, and the evolution of the ultimate horizon is fully deterministic. Quantum randomness within descendant universes is therefore a perspectival illusion arising from their position inside the hierarchy, not a fundamental feature of nature.

Finiteness of the hierarchy. A finite holographic hierarchy is required for causal and informational self-consistency. An infinite regress of horizons would violate the holographic bound: each layer has finite entropy capacity, yet an infinite chain would imply divergent total entropy and no causal closure. Moreover, an infinite hierarchy would

prevent any universe from being complete, since each causal domain would depend on a deeper, never-terminating parent encoding. The chain must therefore terminate in a final, closed horizon containing all causal relations within a single self-consistent code. **Infinity is not a physical attribute here but a signal of mathematical incompleteness; only a finite causal hierarchy preserves entropy conservation and logical coherence.**

Multiplicity of ultimate horizons. While each holographic hierarchy must terminate in a finite causal closure, multiple ultimate horizons may coexist independently. The finiteness requirement applies within each lineage and does not forbid an ensemble of disjoint causal domains. Each ultimate horizon constitutes a complete informational universe, with no causal exchange between them. An unbounded multiplicity of such finite, isolated horizons does not violate the holographic principle, since no entropy or information is shared across domains.

In this view, the deepest layer of physical reality is not indeterminate but perfectly ordered. Quantum randomness, as observed within our universe, is a coarse-grained reflection of deterministic null-order dynamics occurring at the parent horizon, transmitted downward through the holographic hierarchy.

6.2 On the Necessity of Existence

Why is there something rather than nothing? In classical reasoning, "nothing" is imagined as the total absence of space, time, and matter. Within a holographic and causal framework, however, absolute nothingness is not merely improbable; it is *not a coherent state*. A configuration without distinctions contains no information and no causal relations, and thus no means of self-description. Because a state lacking all structure cannot encode the condition of its own absence, it is logically incomplete and therefore not physically realizable.

Existence does not emerge *from* nothing but from the minimal self-differentiation of a state that cannot sustain perfect symmetry. A perfectly featureless configuration contains no stable relations; the absence of distinctions is equivalent to the absence of persistence. The primordial act of being is the appearance of contrast, the establishment of a causal relation between distinguishable states. This transition need not be temporal; it is a logical transformation from an ill-defined state to a self-consistent one. From this first act of differentiation arises the entire hierarchy of information, structure, and geometry. Causality, not substance, is the true seed of reality: the universe is the enduring consequence of that initial establishment of relational order.

Within the horizon-layered cosmology, existence is identified with the persistence of a self-consistent causal code. A universe is not an object within a larger space but a closed network of causal relations whose boundary, the holographic horizon, enforces informational completeness. Each layer of the holographic hierarchy inherits coherence from the one above it, culminating in an ultimate horizon containing all causal relations within a finite, self-referential closure. Beyond that closure, no external domain exists in which "nothing" could be meaningfully defined.

Absolute nothingness is therefore impossible, not because something emerged from it, but because the notion of "nothing" lacks the capacity for causal coherence. To

exist is to participate in a relational structure capable of maintaining self-consistency. Reality, in this view, is the minimal stable configuration of causal order: the simplest informational state that does not collapse into contradiction.

Existence is the only stable solution to the equation of causality. This is not abstract metaphysics but a consequence of the universe's observed coherence. The constancy of physical laws, the persistence of spacetime geometry, and the conservation of energy all reflect a deeper requirement: the causal code must remain globally consistent. The universe endures because it satisfies this requirement across all scales, from Planck-scale discreteness to cosmic structure. Our universe is thus the empirical manifestation of existence's necessity: a self-sustaining solution written in the language of causality.

Informational closure without contradiction is not merely a feature of reality but its defining condition. Contradiction corresponds to the breakdown of causal coherence and therefore cannot be instantiated in any physically meaningful sense. Every conservation principle, every symmetry, and every dynamical law arises from this single imperative: the causal network must be self-consistent across all scales. Existence is thus not contingent but logically compelled, the only state that does not violate its own conditions of definition.

Within this framework, intelligence appears as a natural consequence of increasing causal complexity. When a causal network becomes capable of modeling aspects of its own structure, awareness emerges as the internal reflection of that coherence. Conscious beings are not separate from the universe but localized expressions of its global self-reference, instances in which the causal code temporarily models itself from within. Though finite and ephemeral, such awareness participates in the universe's self-recognition, a momentary alignment between local cognition and global causal order.

At the deepest layer, all existence converges upon a single, self-contained causal totality. It has no external cause, no external observer, and no external domain in which further explanation could be grounded. This ultimate horizon is self-originating and self-consistent: a complete informational closure within which every distinction, process, and observer arises. Its endurance follows not from chance but from necessity, for nonexistence would constitute a violation of causal coherence. Eternal in the informational sense, it persists as the framework that defines being and time. All things, matter, geometry, life, and consciousness, are local expressions of this encompassing order, transient manifestations through which the universe continuously affirms the coherence of its own existence.

7 Conclusion

This paper has developed a new paradigm in which gravitational collapse is reinterpreted as a cosmogenic process. Taking the external observer's frame as physically authoritative, the event horizon ceases to be a passive geometric boundary and becomes an active, information-bearing null surface that encodes infalling matter into redshift-frozen, causally ordered layers. These layers form a dynamically evolving holographic code whose sequential updates, each occurring at one Planck incorporation per Planck time, generate the internal spacetime as a holographic projection of a closed, quasi-hexagonally tessellated surface. The relation $R = 2M$ binds horizon growth directly to internal expansion, so the internal age of the emergent universe follows from the accumulated mass encoded on the horizon, yielding approximately 13.4 Gyr and predicting that the observable Hubble domain encloses roughly half of the total internal mass. Cosmic acceleration and the Hubble tension become natural manifestations of geometric horizon-layer dynamics, not of any external dark-energy component.

The horizon-layered framework replaces the unphysical singularity of classical general relativity with a finite, null-ordered boundary that preserves unitarity, causal completeness, and holographic information flow. The black hole interior is not a region of divergent curvature but the causal termination of geometry, maintained by the evolving horizon itself. Curvature in the bulk reflects the elastic response of the holographic surface to local deficits in causal adjacency, so gravity emerges as the macroscopic expression of finite causal capacity in the boundary code. Singularities disappear not by regularization but by being replaced with a physically operative, dynamically maintained null surface that stores all degrees of freedom permitted by the holographic bound.

When the parent black hole possesses angular momentum, Kerr frame dragging imposes a global azimuthal phase gradient across the horizon lattice. This gradient biases the incorporation of co-rotating versus counter-rotating quanta, imprinting a small but cumulative chiral asymmetry that seeds matter–antimatter imbalance and establishes a preferred cosmic axis. The binary spin structure of Planck-scale dipoles on the horizon provides the geometric origin of fermionic spin-$\frac{1}{2}$, the Pauli exclusion principle, parity violation, and the large-scale alignments observed in CMB multipoles and galaxy spins. Microscopic spin quantization and macroscopic cosmological anisotropy thus derive from the same Kerr-induced phase structure of the holographic code.

At a fundamental level, this framework unifies general relativity, holography, and quantum measurement under a single causal principle. The horizon acts as a stationary but perpetually reconfigured causal lattice: radial incorporation adds new Planck cells, while lateral null propagation across the near-hexagonal adjacency graph sustains coherence, radiation, motions, and gravitational clustering. The speed of light c appears as the invariant rate of lateral causal synchronization on this null surface. Spacetime, motion, and cosmic expansion all emerge from the sequential retessellation of a fundamentally still holographic boundary.

This causal–informational picture also resolves the vacuum catastrophe: vacuum energy corresponds to residual curvature arising from incomplete local redundancy in the horizon code, dynamically diluted as new Planck cells are incorporated. Cosmic acceleration follows as a geometric response to increasing holographic capacity rather than from an intrinsic vacuum energy density.

While the classical singularity-based paradigm remains mathematically consistent within general relativity, the horizon-layered cosmology provides a deeper, information-theoretic foundation. It preserves all verified predictions, gravitational waves, inspiral dynamics, black hole thermodynamics, while replacing the unobservable interior with a physically defined causal boundary. Observable consequences such as Kerr-induced anisotropies, horizon-coherence effects, and holographic regulation of vacuum energy yield clear pathways for future empirical tests.

Although the formulation presented here is primarily conceptual, it establishes a coherent architecture for quantitative development: realistic collapse geometries, spin-weighted tessellations, precise mappings between 2D horizon patterns and 3D bulk fields, and numerical simulations of null-layer encoding. The central insight, however, is already robust:

> **Black holes are not endpoints of collapse but generative horizons. Each horizon layers infalling matter into a null-ordered holographic code whose self-consistent projection forms an emergent** $(3{+}1)$**-dimensional universe. Our universe is not matter moving through a pre-existing spacetime, but the evolving relational pattern of a dynamically growing holographic surface, a causal code whose successive incorporations generate the very fabric of reality.**

References

[1] Hooft, G.: Dimensional reduction in quantum gravity. arXiv preprint gr-qc/9310026 (1993)

[2] Susskind, L.: The world as a hologram. Journal of Mathematical Physics **36**(11), 6377–6396 (1995)

[3] Thorne, K.S., Price, R.H., Macdonald, D.A.: Black Holes: The Membrane Paradigm. Yale University Press, New Haven (1986)

[4] Maldacena, J.M.: The large n limit of superconformal field theories and supergravity. Advances in Theoretical and Mathematical Physics **2**, 231–252 (1998) https://doi.org/10.4310/ATMP.1998.v2.n2.a1 hep-th/9711200

[5] Hayden, P., Preskill, J.: Black holes as mirrors: Quantum information in random subsystems. Journal of High Energy Physics **09**, 120 (2007) https://doi.org/10.1088/1126-6708/2007/09/120 arXiv:0708.4025 [hep-th]

[6] Almheiri, A., Marolf, D., Polchinski, J., Sully, J.: Black holes: complementarity or firewalls? Journal of High Energy Physics **2013**(2), 62 (2013) https://doi.org/10.1007/JHEP02(2013)062 arXiv:1207.3123 [hep-th]

[7] Almheiri, A., Mahajan, R., Maldacena, J., Zhao, Y.: The page curve of hawking radiation from semiclassical geometry. Journal of High Energy Physics **2020**(3), 149 (2020) https://doi.org/10.1007/JHEP03(2020)149

[8] Schwarzschild, K.: On the gravitational field of a mass point according to einstein's theory. arXiv preprint physics/9905030 (1999)

[9] Schutz, B.: A First Course in General Relativity, pp. 317–322. Cambridge university press, Cambridge (2022)

[10] Hafele, J.C., Keating, R.E.: Around-the-world atomic clocks: Observed relativistic time gains. Science **177**(4044), 168–170 (1972)

[11] Ashby, N.: Relativity in the global positioning system. Living Reviews in relativity **6**(1), 1–42 (2003)

[12] Chou, C.-w., Hume, D., Koelemeij, J., Wineland, D.J., Rosenband, T.: Frequency comparison of two high-accuracy al+ optical clocks. Physical review letters **104**(7), 070802 (2010)

[13] Bekenstein, J.D.: Black holes and entropy. Physical Review D **7**(8), 2333 (1973)

[14] Hawking, S.W.: Particle creation by black holes. Communications in mathematical physics **43**(3), 199–220 (1975)

[15] Sperhake, U.: General Relativity 2: Lecture Notes. University of Cambridge. https://www.damtp.cam.ac.uk/user/us248/Lectures/Notes/grII.pdf (2016)

[16] Carroll, S.M.: An introduction to general relativity: spacetime and geometry. Addison Wesley **101**, 102 (2004)

[17] Aristotle: Physics

[18] Ashtekar, A., Bojowald, M.: Black hole evaporation: A paradigm. Classical and Quantum Gravity **22**(16), 3349–3362 (2005) https://doi.org/10.1088/0264-9381/22/16/014 arXiv:gr-qc/0504029

[19] Hajicek, P., Kiefer, C.: Singularity avoidance by collapsing shells in quantum gravity. International Journal of Modern Physics D **10**(06), 775–779 (2001) https://doi.org/10.1142/S0218271801001118 arXiv:gr-qc/0107102

[20] Barceló, C., Liberati, S., Visser, M.: Horizon thermodynamics and emergent gravity. International Journal of Modern Physics D **20**(08), 1667–1676 (2011) https://doi.org/10.1142/S0218271811019341 arXiv:0909.4157 [gr-qc]

[21] Mazur, P.O., Mottola, E.: Gravitational vacuum condensate stars. Proceedings of the National Academy of Sciences **101**(26), 9545–9550 (2004) https://doi.org/10.1073/pnas.0402717101 arXiv:gr-qc/0407075

[22] Misner, C.W., Thorne, K.S., Wheeler, J.A.: Gravitation. Macmillan, San Francisco (1973)

[23] O'Connor, E., Ott, C.D.: Black hole formation in failing core-collapse supernovae. The Astrophysical Journal **730**(2), 70 (2011)

[24] Shapiro, S.L., Teukolsky, S.A.: Black Holes, White Dwarfs and Neutron Stars: the Physics of Compact Objects. John Wiley & Sons, New York (2024)

[25] Woosley, S., Wilson, J., Mathews, G., Hoffman, R., Meyer, B.: The r-process and neutrino-heated supernova ejecta. Astrophysical Journal, Part 1 (ISSN 0004-637X), vol. 433, no. 1, p. 229-246 **433**, 229–246 (1994)

[26] Hawking, S.W., Ellis, G.F.: The Large Scale Structure of Space-time. Cambridge university press, Cambridge, New York, Melbourne (2023)

[27] Bousso, R.: A covariant entropy conjecture. Journal of High Energy Physics **1999**(07), 004 (1999)

[28] Sullivan, R.M., Scott, D.: The cmb dipole: Eppur si muove. In: The Sixteenth Marcel Grossmann Meeting on Recent Developments in Theoretical and Experimental General Relativity, Astrophysics and Relativistic Field Theories: Proceedings of the MG16 Meeting on General Relativity; 5–10 July 2021, pp. 1532–1541 (2023). World Scientific

[29] Longo, M.J.: Detection of a dipole in the handedness of spiral galaxies with redshifts $z \sim 0.04$. Physics Letters B **699**(4), 224–229 (2011) https://doi.org/10.1016/j.physletb.2011.04.008

[30] Shamir, L.: Asymmetry between galaxies with clockwise and counterclockwise spin directions: A possible signature of large-scale structure. The Astrophysical Journal Supplement Series **250**(1), 1 (2020) https://doi.org/10.3847/1538-4365/aba4a5

[31] Shamir, L.: Evidence of large-scale spin alignment in galaxies. Mon. Not. R. Astron. Soc. **522**, 2450–2464 (2023)

[32] Copi, C.J., Huterer, D., Schwarz, D.J., Starkman, G.D.: Large-scale alignments from wmap and planck. Advances in Astronomy **2010**, 847541 (2010) https://doi.org/10.1155/2010/847541

[33] Collaboration, P.: Planck 2018 results: Isotropy and statistics of the cmb. Astron. Astrophys. **641**, 7 (2020)

[34] Reynolds, C.S.: Observational constraints on black hole spin. Ann. Rev. Astron. Astrophys. **57**, 445–487 (2019)

[35] Avara, M.J., McKinney, J.C.: Magnetically arrested accretion and the evolution of black hole spin. Astrophys. J. **893**, 16 (2020)

[36] Guth, A.H.: Inflationary universe: A possible solution to the horizon and flatness problems. Physical Review D **23**(2), 347–356 (1981) https://doi.org/10.1103/PhysRevD.23.347

[37] Linde, A.D.: A new inflationary universe scenario: A possible solution of the horizon, flatness, homogeneity, isotropy and primordial monopole problems. Physics Letters B **108**(6), 389–393 (1982) https://doi.org/10.1016/0370-2693(82)91219-9

[38] Riess, A.G., Yuan, W., Macri, L.M., Scolnic, D., Brout, D., Casertano, S., Jones, D.O., Murakami, Y., Peterson, R., Polin, A., *et al.*: A comprehensive measurement of the local value of the hubble constant with 1 km/s/mpc uncertainty from the hubble space telescope and the sh0es team. The Astrophysical Journal Letters **934**(1), 7 (2022) https://doi.org/10.3847/2041-8213/ac5c5b

[39] Gibbons, G.W., Hawking, S.W.: Cosmological event horizons, thermodynamics, and particle creation. Physical Review D **15**(10), 2738–2751 (1977)

[40] Padmanabhan, T.: Thermodynamical aspects of gravity: new insights. Reports on Progress in Physics **73**(4), 046901 (2010)

[41] Verlinde, E.: On the origin of gravity and the laws of newton. Journal of High

Energy Physics **2011**(4), 1–27 (2011)

[42] Li, M.: A model of holographic dark energy. Physics Letters B **603**(1-2), 1–5 (2004)

[43] Collaboration, B.: Improved constraints on primordial gravitational waves from bicep/keck observations to 2018. Physical Review Letters **127**(15), 151301 (2021) https://doi.org/10.1103/PhysRevLett.127.151301 arXiv:2110.00483

[44] Smolin, L.: The Life of the Cosmos. Oxford University Press, New York - Oxford (1997)

[45] Frolov, V., Novikov, I.: Black Hole Physics: Basic Concepts and New Developments vol. 96. Springer, Dordrecht (2012)